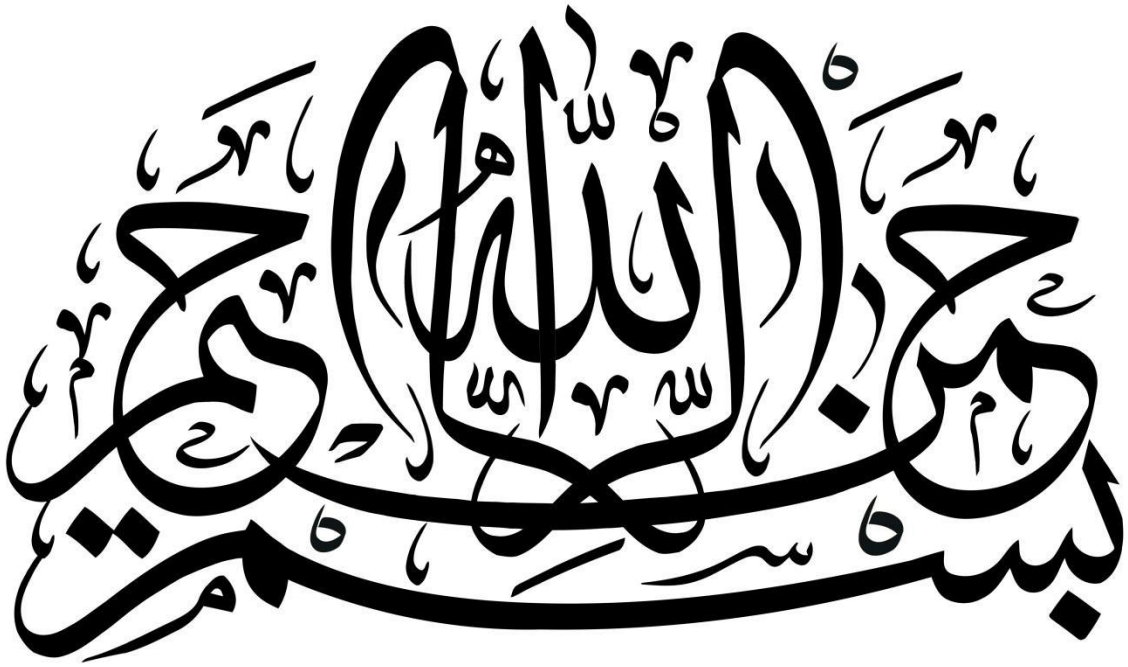
بسم الله الرحمن الرحيم

Republic of Iraq

Ministry of Higher Education & Scientific Research

University of Kerbala

College of Engineering

Mechaincal Engineering Department

Investigation the Factors Affecting the Performance of Heat Exchanger Heat Pipes with High Temperature Difference in Steam Power Plant

A Thesis Submitted to the Council of the Faculty of the College of the Engineering/University of Kerbala in Partial Fulfillment of the Requirements for the Master Degree in Mechanical Engineering

By:

Murtadha Musa Dubaish

Supervisors

Prof Dr. Mohammed Wahhab ALjibory

Asst. Prof. Dr. Mohammed Hassan Abbood

٢٠٢٥/ December

بسم الله الرحمن الرحيم

يَرْفَعِ اللَّهُ الَّذِينَ آمَنُوا مِنكُمْ وَالَّذِينَ أُوتُوا الْعِلْمَ دَرَجَاتٍ

صدق الله العلي العظيم

(سورة المجادلة، آية ١١)

Examination Committee Certification

We certify that we have read the thesis entitled **"Investigation the Factors Affecting the Performance of Heat Exchanger Heat Pipes with High Temperature Difference in Steam Power Plant"** and as an examining committee, we examined the student **"Murtadha Mousa Dubaish"** in its content and in what is connected with it and that, in our opinion, it is adequate as a thesis for the degree of Master in Mechanical Engineering Science.

Supervisor

Signature:
Name: Prof. Dr. Mohammed Wahhab ALjibory
Date: / / 2026

Supervisor

Signature:
Name: Asst. Prof. Dr. Mohammed Hassan Abbood
Date: / / 2026

Member

Signature:
Name: Asst. Prof. Dr. Mohammed Hussein Ahmed Alhwayzee
Date: 4 / 1 / 2026

Member

Signature:
Name: Asst. Prof. Dr. Hayder Noori Mohammed
Date: / / 2026

Chairman

Signature:
Name: Prof. Dr. Audai Hussein Kadhum
Date: / / 2026

Signature:
Name: Prof. Dr. Salah Noori Abbood Alnomani
Head of the Department of Mechanical Engineering
Date: / / 2025

Signature:
Name: Prof. Dr. Haider Nadhim Azziz
Dean of the Engineering College
Date: / / 2025

Supervisor Certificate

We certify that the thesis entitled **"Investigation the Factors Affecting on the Performance of Heat Exchanger Heat Pipes with High Temperature Difference in Steam Power Plant"** was prepared by **Murtadha Mousa Dubaish** under our supervision at the Department of Mechanical Engineering, Faculty of Engineering, University of Kerbala as a partial of fulfilment of the requirements for the Master Degree of Science in the Mechanical Engineering.

Signature:

Prof Dr. Mohammed W. AlJibory

Date: / / 2025

Signature:

Ass. prof. Dr. Mohammed H. Abbood

Date: / / 2025

Linguistic certificate

I certify that the thesis entitled **"Investigation the Factors Affecting the Performance of Heat Exchanger Heat Pipes with High Temperature Difference in Steam Power Plant"** which has been submitted by **Murtadha Mousa Dubaish** has been proofread, and its language has been amended to meet the English style.

Signature:

Name: Asst. Prof. Dr. Husam Jawad Abdulsamad

Date: / / 2025

Undertaking

I certify that this thesis titled "**Investigation the Factors Affecting the Performance of Heat Exchanger Heat Pipes with High Temperature Difference in Steam Power Plant**" is my own work. The work has not been presented elsewhere for assessment. Where material has been used from other sources, it has been properly acknowledged / referred.

Signature:

Murtadha M. Dubaish

Date: / / ٢٠٢٥

Dedication

To All Whom I Love

I Dedicate This Modest Effort

To Imam al-Mahdi (God hastens his fortune), my parents (father & mother), my wife, my children (Zain Al-Abidin and Nouran), my brothers and sisters and all my relatives and friends…

Signature:

Murtadha M. Dubaish

Date: / / ٢٠٢٥

Acknowledgments

Praise and thank for Allah who eased and quadrated us to accomplish this work.

*I would like to express my deepest thanks and sincere gratitude to (**my supervisors: Prof Dr. Mohammed W. AlJibory and Ass. prof. Dr. Mohammed H. Abbood)** who guided me with all his expertise and scientific to accomplish this work correctly.*

I submit my thanks and appreciation to staff of Mechanics Department at the University of Karbala.

I submit my thanks and appreciation to my dear family for providing the support during the period of preparing this work.

I would also like to thank all whom help me to accomplish this work.

Signature:

Murtadha M. Dubaish

Abstract

In many of applications, such as power plants, iron factories, etc., thermal energy may be lost to ambient so, using devices such as heat pipe heat exchangers is necessary to recover this energy. In this study, a thermosiphon heat pipe heat exchanger is constructed for this purpose. The thermal performance of this exchanger is numerically (by using ANSYS-Fluent software) and experimentally investigated. This is at different filling ratios (٣٥٪, ٥٠٪ and ٧٥٪) of a working fluid (DOWTHERM™ A), air velocities of (٠.٥, ١, ١.٥, ٢ and ٢.٥ m/s) at the condenser inlet and wide range of the evaporator inlet air temperature (١٦٠ to ٣٢٠ °C). The exchanger model used in this study includes ٦٠ copper heat pipes with square aluminum fins. The heat pipe (١٠٠ cm total length) consists of three sections namely: evaporation section (٤٠ cm length), adiabatic section (٢٠ cm length) and condensing section (٤٠ cm length). The results show that the filling ratio, air velocity and evaporator air temperature have an important effect on the thermal performance of the heat exchanger. In overall, the optimum values of the filling ratio, air velocity and evaporator inlet air temperature, to obtain the best thermal performance of the exchanger, are ٥٠٪, ٠.٥ m/s and ٣٢٠ °C respectively. Where at these values, the highest condenser air temperature and maximum exchanger effectiveness (٢٤٠ °C and ٧٤٪ numerically and ٢٥٠ °C and ٧٧٪ experimentally) are obtained. Through the comparison between the numerical and experimental results, an excellent agreement is found between them with a maximum deviation percentage does not exceed ٥٪.

Keywords: steam power plant, heat pipe heat exchanger, thermal effectiveness, temperature, filling ratio

Table of Contents

List of Figures

List of Tables

List of Abbreviations

Abbreviation	Full description
AR	The Ratio of the Adiabatic Length to the Evaporator
CFD	Computational Fluid Dynamics
٢D	Two-Dimensional
FR	Filling Ratio
HP	Heat Pipe
HPHE	Heat Pipe Heat Exchanger
HVAC	Heating, Ventilation, and Air Conditioning
LMTD	Log Mean Temperature Difference
NTU	Number of Transfer Units
ARC	America Radio Corporation
THP	Thermosiphon Heat Pipe
TPCT	Two Phase Closed Thermosiphon
VOF	Volume of Fluid
WHP	Wick Heat Pipe
WHR	Waste Heat Recovery

List of Symbols

English Symbols		
Symbol	**Description**	**Units**
A	Surface area	m^2
C	Phase surface curvature	-
C_p	Specific heat capacity	kJ/kg. °C
Cp_c	Heat capacity of cold air	kJ/kg. °C
Cp_h	Heat capacity of hot air	kJ/kg. °C
D	Diameter	mm
E_S	Thermal energy transferred during the phase change process	kJ/s
e	Specific energy	kJ/kg
F□	Surface tension force	N/m^2
g	Gravitational acceleration	m/s^2
h	Specific enthalpy	J/kg
H	Height	mm
k	Thermal conductivity	W/(m·°C)
$\dot{m}_h$	Mass flow rate of hot air	kg/s

$\dot{m}_c$	The mass flow rate of the cold air	kg/s
$\dot{m}_{lv}$	Mass flow rate due to the evaporation	kg s^{-1}. m^{-3}
$\dot{m}_{vl}$	Mass flow rate due to the condensation	kg s^{-1}. m^{-3}
P	Pressure	Pa
Q	Heat transfer rate	W
r	Mass flow time parameter	-
R_h	Heat resistance	°C/W
S□	Energy source term	-
t	Time	Second
T	Temperature	°C
$\vec{u}$	Phase velocity	m/s
U	Overall heat transfer coefficient	W/m^2. °C

Greek symbols

Symbol	Description	Units
α	Volume fraction	-
Ɛ	Effectiveness of heat pipe	-

μ	Dynamic viscosity	Ps. s
ρ	Density	kg/m^{۳}
σ_{lv}	Coefficient of the surface tension	-
τ	Shear stress	N/m^{۲}
Subscripts		
a	Actual	
c. in	Incoming cold air	
c. out	Outgoing cold air	
Con. out	Condenser outlet	
Evap. in	Evaporator inlet	
h. in	Incoming hot air	
h. out	Outgoing hot air	
in	inlet	
L	Liquid	
Max.	Maximum	
out	outlet	
SAT.	Saturation	
v	Vapor	
w	Metal wall of the heat pipe	

Chapter One

Introduction

Chapter One

Introduction

Problems resulted from the use of fossil fuels, such as air pollution and significant increasing in ambient temperatures, have posed a major challenge to humanity in recent years. According to a report published by the International Energy Agency (IEA) in ٢٠٢٢, carbon dioxide emissions reached ٣٦.٨ billion tons annually, an increase of ٠.٩٪ compared to the previous year. This has prompted researchers to search solutions to replace the fossil fuel or reduce the dependence on it. One proposed solution in this area is the recovery of waste heat in different processes, which can be achieved through the use of different heat exchangers [١].

In this chapter, the historical development of heat pipes, their types, working fluid used to carry heat from the hot section to cold one are dialed with. In addition to regenerative air preheater and its principle, components, advantages and disadvantages. The aim of the current study and outlines of this thesis are also shown in the end of this chapter.

١.١ Historical Development of Heat Pipes

Principle of the heat pipe was known since ١٩٤٢ by Gaugler. However, serious interest in its use did not begin until the early ١٩٦٠s by Grover (an American scientist) who demonstrated the effect of high heat transfer efficiency and proved its usefulness in various fields [٢, ٣]. The first commercial organization which interested in heat pipes is the America Radio Corporation (ARC) in ١٩٦٦, the first use of the heat pipe in practical applications began in California [٤]. In ١٩٦٩, a new heat pipe was designed by George P. Gray (a British scientist in the field of energy). This type of heat pipes transports the liquid from the condenser area to the evaporator area by gravity without using a wick [٥]. Abhat and Seban

[٦] in ١٩٧٤ also conducted tests on a stainless steel heat pipe using different types of wicks (steel and bronze mesh, nickel and bronze mesh). They concluded through the tests that the heat transfer rate in the case of using the heat pipe with the wick is greater by about ١٥ $W/cm^{٢}$ than that without the wick. The development of using heat pipes in many industrial and engineering applications is continues until now.

١.٢ Principle and Types of Heat Pipe

A heat pipe is a two-phase heat transfer device that works based on the working fluid's phase change to transmit heat from a one side to another with a minimal temperature difference. A heat pipe typically consists of a sealed container that is partially filled with a working fluid like water. It is divided into three sections: the condenser, adiabatic, and evaporator section.

There are many types of heat pipe (HP), but the most important and widely used are wick HPs, thermosiphon HPs, flat-plate HPs and concentric spherical HPs. The thermal and physical properties of each model and its applications in different industries are discussed below.

١- **Wick heat pipe:** is one of the simplest and most reliable heat pipes that is suitable for heat transfer processes. This model does not require external energy sources. The most important applications of this model include its use in the tea leaf drying industry, nuclear power plant, TOPAZ-II power systems and Heating, Ventilation, and Air Conditioning (HVAC) systems [٧]. In this model of heat pipes, when the hot end of the heat pipe is heated up, the working fluid changes from the liquid state to the gaseous state (vapor). The vapor produced moves through the tube towards the cold end of the heat pipe, loses its energy and turns into the liquid state see Figure (١.١).

٢- **Thermosiphon (wickless) heat pipe:** is a practical model of heat pipes that has many applications in the ceramic industry, nuclear reactors, heat recovery and steel industry [٨]. This model is designed for conditions where the heat transfer process be vertical knowing that it (heat transfer) depends on the earth gravity principle. In this type of heat pipes, the condenser must be located above the evaporator section (see Figure (١.٢)).

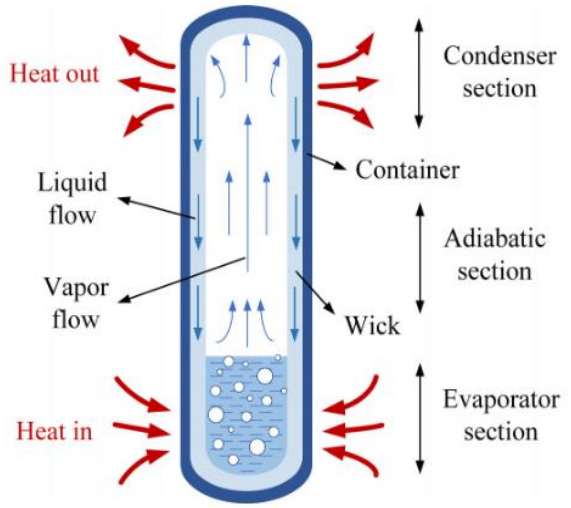

Figure ١. ١: Wick Heat Pipe [١]

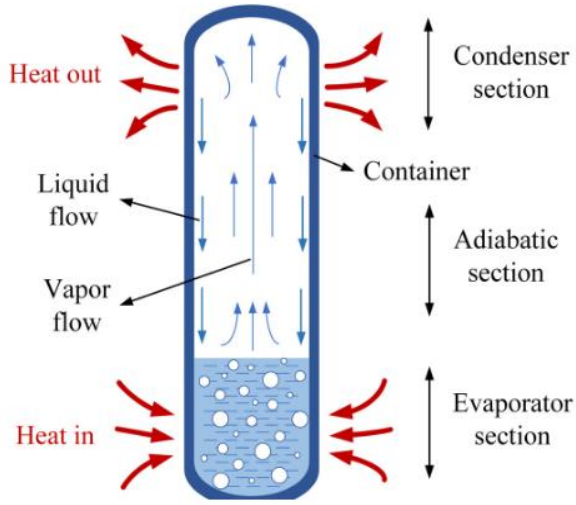

Figure ١. ٢: Thermosiphon Heat Pipe [١]

٣- **Flat-plate heat pipe:** is a one of the suitable heat pipes for heat transfer in limited spaces. This model of heat pipes is made up of flat-plates with very thin sections. The thin structure in this model of heat pipes is the main factor for the heat transfer effectivity. The working principle of this type of heat pipes is applying heat on the surface of heat pipe, a hot fluid separates from cold fluid. Among the most important applications of flat-plate heat pipes, its use in the photovoltaic panels [٩, ١٠] and the steel industry (see Figure ١.٣).

٤- **Concentric tube heat pipe**: is a one of the suitable heat pipes for the use in electronic systems and applications. It is used for heat transfer over long distances because it has relatively high efficiency. It consists of two coaxial tubes, the inner

tube works as an evaporator and the outer tube works as a condenser. The working fluid flows inside the inner tube and facilitates heat transfer [١١] (see Figure (١.٤)).

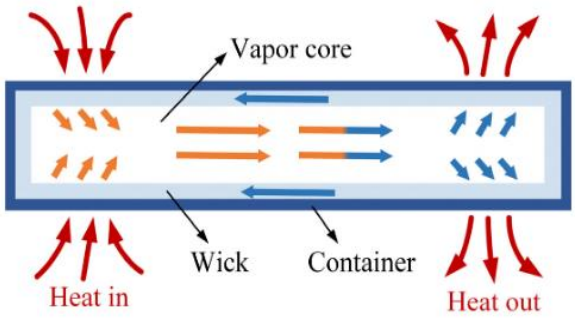

Figure ١.٣: Flat-plate Heat Pipe [١]

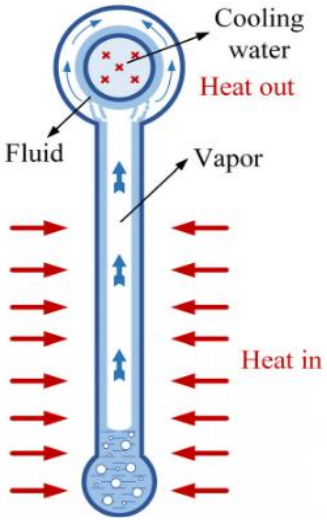

Figure ١.٤: Concentric Tube Heat Pipe [١]

١.٣ Heat Pipe Heat Exchanger

A heat exchanger is a device used to exchange thermal energy between two fluids without mixing them. It is one of the most suitable tools for recovering waste heat in different systems, which consequently improves energy efficiency. The use of heat exchangers for recovering waste energy is reported in various fields, including power plants, textile, refinery, production of building materials, etc. [١٢].

The heat pipe heat exchanger (HPHE) consists of several heat pipes connected in parallel. This design allows for large-scale heat transfer. The HPHE has two ends located in two different environments, one of them located in a cold environment and called the condenser and the other end located in a hot environment and called the evaporator. As shown in Figure (١.٥), when the heat-carrying fluid passes over the evaporator begins to boil and absorbs heat. In other words, along this path, the phase change process from the liquid state to the gas

state occurs without changing in the temperature of the heat pipe reservoir. The vapor produced moves towards the condenser, with a speed about equals the sound speed, as a result, the vapor in contact with the cold environment releases the absorbed heat and turns into the liquid phase [١]. The condensed liquid returns to its original path and this cycle is repeated continuously. In overall of this process, heat is transferred from the hot source to the cold source continuously.

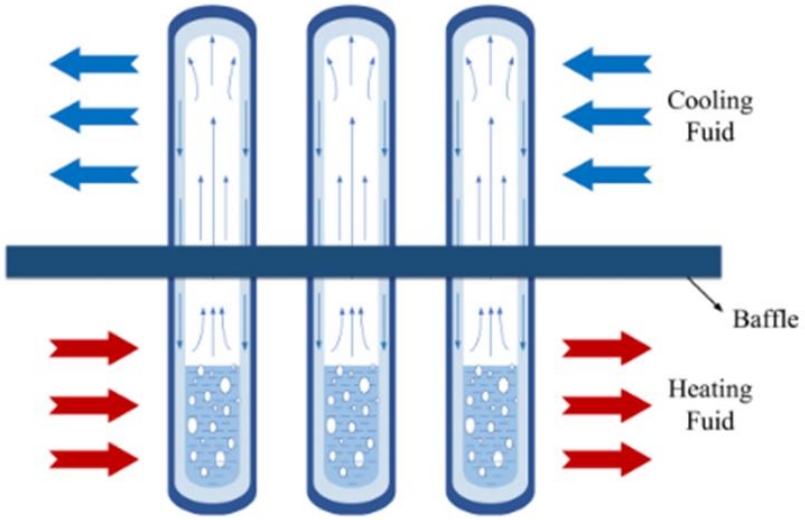

Figure ١.٥: Schematic View of Heat Pipe Heat Exchanger [١]

On the other hand, the heat pipe is also one of the important and practical devices that has high thermal conductivity. This system works according to thermodynamic principles (condensation and evaporation) and is used to build heat exchangers. HPs have the ability to transfer heat over long distances and create a minimum temperature gradient during this heat transfer process. There are different models of HPs that have different structures, configurations, and functions.

١.٤ Working Fluid

The type and quantity of a working fluid required to be used in a heat pipe play a very important role in the operation process of specified heat pipe. The selection of a working fluid depends on the temperatures range of the waste heat stream. The main factors, to select the suitable working fluid, are its liquid boiling temperature and vapor condensation temperature. Figure (١.٦) shows the useful operating temperature ranges for various heat pipe operating fluids, although it was abbreviated by removing the coolants to show the fluids that are most commonly used in waste heat recovery (WHR) [١٣].

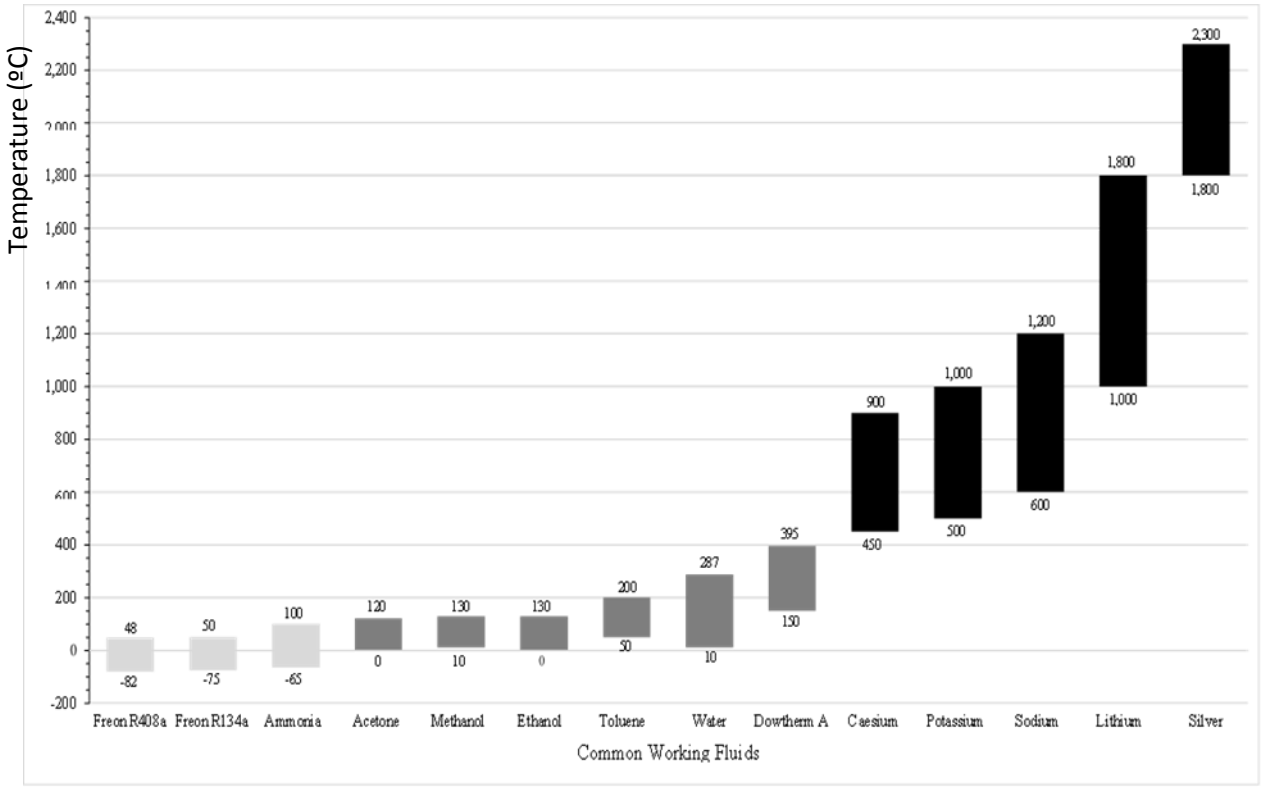

Figure ١.٦: Useful Working Temperature Range of Working Fluids at Normal Pressure and Temperature [١٣]

In addition to temperature ranges, there are other properties and criteria that should also be taken into consideration at selecting a working fluid as following [١٤].

a) Good thermal stability,

b) Good wettability,

c) High thermal conductivity,

d) Good compatibility with wick and container material,

e) Reasonable vapor pressure at operating temperatures,

f) High latent heat of evaporation,

g) Low viscosity of both liquid and vapor phases,

h) High vapor specific heat capacity,

i) High surface tension, if antigravity,

j) Acceptable freezing and pour point,

k) Low toxicity,

l) Low cost and, easily available.

In addition to incorporating nanoparticles into the filament structure, extensive research was conducted on the introduction of nanoparticles into the working fluid, known as Nano fluids. Numerous experiments were conducted by [١٥] on the heat transfer properties of various Nano fluids in different configurations of a heat pipe.

١.٥ Regenerative Air Preheater

The primary function of the regenerative air preheater is to improve the efficiency of the combustion process by recovering waste heat from the flue gases exiting the boiler and using it to preheat the combustion air entering into the furnace.

١.٥.١ Working Principle of Regenerative Air Preheater

An air preheater works as a heat exchanger, transferring heat from the hot flue gases to the cold combustion air. This is typically accomplished by passing the gases and air across metal heat transfer surfaces, such as plates, in an arrangement that allows heat exchange between them without mixing. A rotating heat storage medium (usually in the form of a basket or an array of metal plates) is used. This medium slowly circulates through two separate sectors: one through which the hot flue gas passes, and the other through which the cold combustion air passes. In the flue gas sector, the medium absorbs heat from the gases. As the medium circulates to the combustion air sector, it transfers the stored heat to air. Figures (١.٧) shows a ٣-dimensional schematic diagram of the regenerative air preheater.

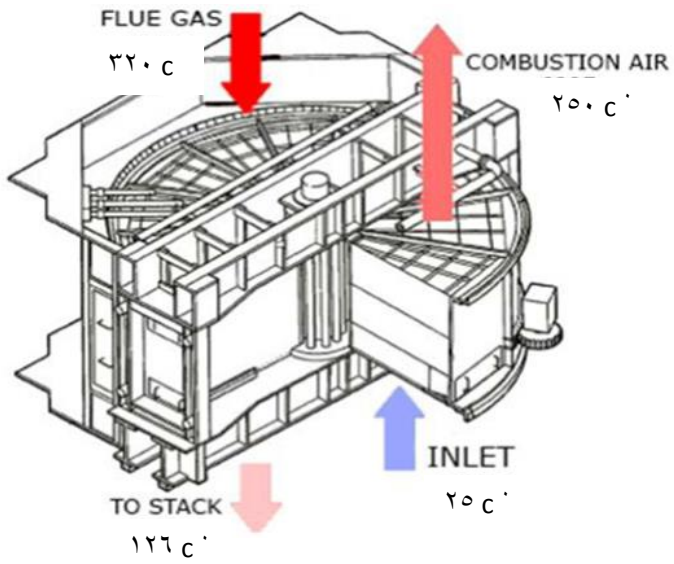

Figure ١.٧: ٣-dimensional Schematic Diagram of Regenerative Air Preheater [١٦]

١.٥.٢ Components of Air Preheater in Thermal Power Plant

The air preheater consists of four main components namely; rotor, heat transfer media, seals and drive mechanism. Figure (١.٨): shows a schematic diagram of components of air preheater.

- Rotor: a structure that holds the heat storage medium and slowly rotates it.

- Heat Transfer Media: metal sheets designed to absorb and store heat efficiently.
- Seals: to prevent gas and air leakage between sections
- Drive mechanism: to move the rotor.

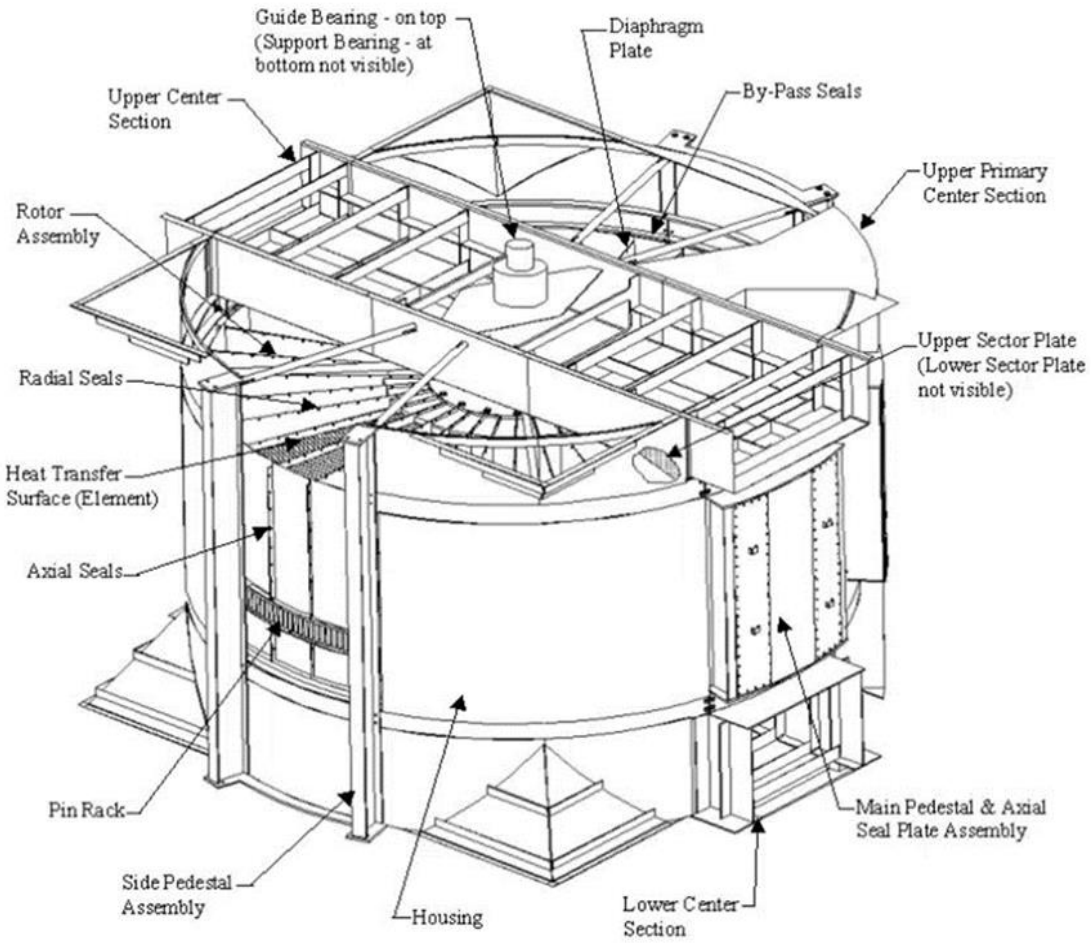

Figure ١.٨: Schematic Diagram of Air Preheater [١٧]

١.٥.٣ Advantages of Air Preheater in Steam Plants

١. It increases the boiler efficiency: By heating the combustion air, the amount of fuel required to achieve the desired combustion temperature is reduced. It is estimated that every ٢٠°C increase in combustion air temperature can result in a ١٪ improvement in the boiler efficiency.

٢. It improves the combustion process: the hot air helps to vaporize the fuel better and speeds up the ignition and complete combustion process, reducing soot and carbon monoxide formation.

٣. It reduces heat losses in flue gases: recovering heat from flue gases results in them exiting at lower temperature, reducing heat energy loss through the chimney and increasing the overall efficiency of the plant.

٤. Fuel Saving: Improving combustion efficiency and reducing heat loss leads to less fuel consumption and therefore, less operating costs.

٥. It reduces harmful emissions: the complete combustion reduces emissions of harmful gases such as carbon monoxide and unburned hydrocarbons.

١.٥.٤ Disadvantages of Air Preheater in Steam Plants

١. Corrosion: Acid condensation in the cold areas of the air heater (especially in ducted air heaters) may cause corrosion. Corrosion-resistant materials should be used or measures should be conducted to prevent the condensation. Figure (١.٩) includes a picture of the Al-Mousayyab thermal power plant with corrosion in the air preheater.

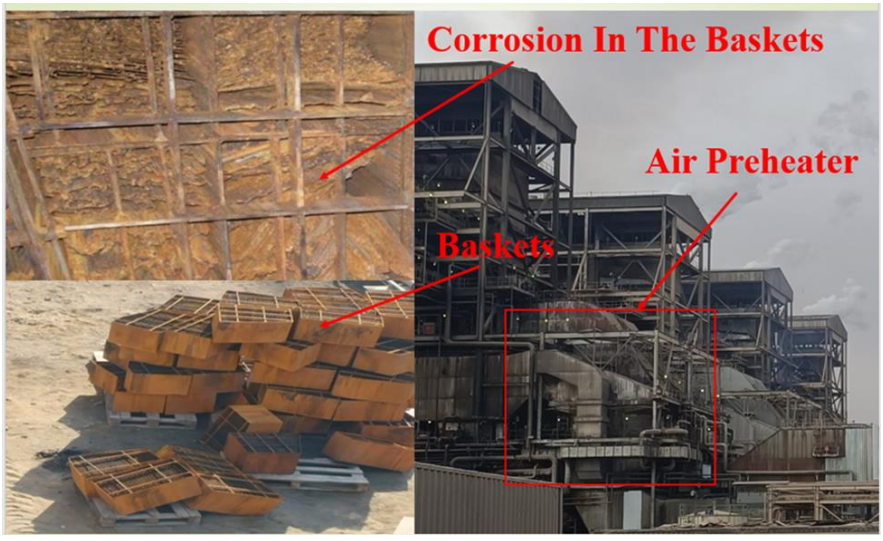

Figure ١.٩: Al-Musayyab Thermal Power Plant with Corrosion in Air Preheater

٢. Fouling: Ash and soot particles may be accumulated on heat transfer surfaces, reducing heat exchange efficiency and increasing resistance to gas and air flow. These buildups require periodic cleaning with soot blowers or water washing.
٣. In regenerative air heaters, a leakage may be occurred between the gas and air sections, reducing the heating efficiency. Seals should be maintained periodically to reduce or avoid this problem.

١.٦ The Aim of This Study

There are two main problems often occur in air preheaters of thermal power plants namely: the blocking and corrosion of baskets of these preheaters as shown in Figure (١.٩). This is due to the moisture coming with the air and exhaust fumes accumulation in these baskets. This will lead to stopping or reducing the air flow to the boiler of the thermal plant. To overcome these problems, the baskets must be replaced between a time duration and another and this requires stopping the plant, which is costly in terms of both time (stopping the plant's production) and finance (the cost of replacing worn baskets). Consequently, it is necessary to consider alternatives to these baskets that perform the same function. One such alternative is a heat pipe which can be a successful alternative.

The aim of this study is: -

١. Conducting a numerical simulation of the thermal performance of a heat pipe heat exchanger (HPHE) based on the volume of fluid (VOF) method by using a computer software (ANSYS-Fluent).
٢. Determining the condenser outlet air temperature and effectiveness of the HPHE through the numerical simulation,
٣. Constructing a test rig of the HPHE consists of eight rows with seven to eight thermosiphons per row,

٤. Conducting experimental tests of the condenser inlet air velocity and filling ratio of the working fluid to measure the condenser outlet air temperature and calculate the effectiveness of the HPHE,

٥. Carrying out comparisons between the experimental and numerical results of the condenser outlet air temperature and effectiveness of the HPHE at different air velocities and filling ratios.

١.٧ Outlines of This Thesis

Chapter ١: It highlights the background of heat pipes, what they are, how they work, what types of heat pipes exist, and finally, what is the purpose of this entire research.

Chapter ٢: This chapter discusses previous literature related to the field of this study. It first provides a summary and introduction to the previous studies, then divides the chapter into numerical studies, experimental studies, and both numerical and experimental studies. In each of these sections, the studies are classified into tables based on the study year, boundary conditions, heat pipe modification way and results and conclusions.

Chapter ٣: This chapter includes two aspects namely: the mathematical model (mathematical equations to calculate the thermal performance of thermosiphon heat pipe heat exchanger (HPHE)) and numerical analysis (simulation of the thermal performance of this HPHE using ANSYS-Fluent software).

Chapter ٤: This chapter describes the testing apparatus and equipment used to conduct tests and experiments, as well as discussing how to calibrate different scales.

Chapter ٥: In this chapter, experimental and numerical results related to the thermal performance of the HPHE under different operating conditions are presented, discussed and compared.

Chapter ٦: In this chapter, the most important conclusions and some recommendations for future work are presented.

Chapter Two

Literature Review

Chapter Two

Literature Review

Introduction

Numerous studies were conducted on heat transfer devices based on natural mass circulation, including both wick and wickless heat pipes. The energy transfer process in both types depends on several factors namely: geometric shape (length, diameter and tilt angle), physical factor (working fluid and filling ratio) and thermal factors (heat flux and temperature). In this chapter, previous different studies related to the subject of the current research would be reviewed, as well as the applications of heat pipes, especially in heat recovery systems that use heat exchangers. This chapter would be divided into three main sections namely: numerical studies, experimental studies, numerical and experimental studies. For each section, there would be a table to summarize previous researches.

٢.١ Numerical Studies

Alammar et al., (٢٠١٦) [١٨] investigated the effect of the filling ratio and tilt angle on the thermal performance of a heat pipe heat exchanger (HPHE) in terms of the temperature distribution and thermal resistance. Using several values of the filling ratio (١٠٠٪, ٨٠٪, ٦٥٪, ٥٠٪, and ٢٥٪) of the working fluid (water) and tilt angle (°٩٠, °٧٠, °٥٠, °٣٠, and °١٠). This is through constructing a numerical model of the HPHE by using ANSYS-Fluent software. The heat pipe used has a total height of ٤٠٠ mm (٢٠٠ mm for each of the evaporator and condenser), outer diameter of ٢٢ mm and inner diameter of ٢٠.٢ mm. The results demonstrated that the optimum values of the filling ratio and tilt angle, at which the thermal resistance be at the lowest level, are ٦٥٪ and ٩٠° respectively.

Fertahi et al., (٢٠١٧) [١٩] numerically (CFD modeling) investigated and analyzed the thermal performance of a wickless HPHE (thermosiphon). This is with and without inclined fins at an angle of °٣٠ with the horizon. These fins were added on the outer surface of the condenser section to improve the thermal performance of the HPHE. Degassed (distilled) water, with a filling ratio of ٢٥٪ of the evaporator condenser size, was used as a heat transfer fluid. The study was done through building a two-dimensional copper model with ٠.٩ mm thickness, ٢٠.٢ mm internal diameter and ٠.٥ m total length (the evaporator length of ٠.٢ m, adiabatic of ٠.١ m and condenser of ٠.٢ m). The results showed that using fins on the condenser surface improves the thermal efficiency of the heat pipe system by approximately ١٦٪ (it increased from ٦٩٪ (without fins) to ٨٥٪ (with fins)).

Al Jubori and Jawad (٢٠٢٠) [٢٠] carried out CFD simulations of a heat pipe (wickless) at changed operation conditions (filling ratio, heat supplied and slope angle of the heat pipe). ANSYS-Fluent software was used to solve the two-phase processes (evaporation and condensation) of a heat transfer fluid (water) in the heat pipe. The heat pipe used has a diameter of ٢٢ mm and total length of ٤٠٠ mm (٢٠٠ mm for each of the condenser and evaporator section). The findings showed that there is a significant reduction (about ٠.١٥ °C/ W) in the heat resistance of the heat pipe at ٢٥٪ water vaporization rate with the increase in heat supplied. In overall, the maximum thermal energy performance was achieved at a filling ratio of ٥٠٪ and slope angle of ٩٠°.

Adrian et al., (٢٠٢١) [٢١] numerically simulated the thermal performance of a HPHE by constructing a two-dimensional geometry using ANSYS-Fluent software. Two copper heat pipes, with two different lengths (١٧٦٩ and ٥٥٠) mm and three heat transfer fluids (R١٣٤a, R٤٠٤a, and R٤٠٧a) with different filling ratios (١٠% to ٧٠٪), were used. The results demonstrated that the highest thermal efficiency of the HPHE (about ٩٠٪) can be achieved by

utilizing R١٣٤a with a filling ratio of ١٠٪ of the overall pipe size. While, using R٤٠٧a produces the least efficiency (approximately ٧٨%) of the HPHE.

Desai et al., (٢٠٢١) [٢٢] numerically studied the thermal performance of a HPHE (thermosiphon) by using three different geometries (circular, square and triangular) of the heat pipe. All the heat pipes used in this study have the same cross-sectional area (٣٥ $mm^{٢}$) and the same length (٢٠٠ mm). The results of the simulation showed that the shape of the heat pipe has a very clear influence on its thermal performance. The circular heat pipe has the best thermal performance compared to the triangular and square heat pipe. The air temperature difference between the outlet and inlet of the condenser section is ٣٥ K in the circular pipe case, ٢٧ K in the triangular pipe case and ٢٦ K in the square pipe case.

Brough et al., (٢٠٢١) [٢٣] numerically studied the heat transfer process in a HPHE using TRNSYS software. This is to optimize the heat recovery conditions and predict the temperature under unstable operation conditions. The method used for heat recovery and temperature prediction is the ε-NTU. In this study, the effect of external fins, with different geometries as shown in Figure (٢.١), on the thermal performance of a heat pipe was investigated to enhance the heat transfer process. The external fins were added on the outer surface of the condenser and evaporator section. The results proved that the presence of these fins on the surface of the heat pipe is very important for recovering waste heat. The results also indicated that, through the process of heat exchange between the incoming cold air and outgoing hot gases, the air temperature increases by ١٥ °C.

Figure ٢.١: Heat Pipes with External Fins Different Shapes [٢٣]

Sadeghi et al., (٢٠٢٢) [٢٤] numerically simulated the thermal behavior of a two-phase copper HPHE (vertical closed thermosiphon) for industrial applications. This is by using a special oil as a working fluid with differing filling ratios (٣٠, ٥٠, ٧٠ and ٩٠٪). The heat pipe used has a total length of ١١٠٠ mm (٥٠٠ mm evaporator length, ٣٠٠ mm condenser length and ٣٠٠ mm adiabatic length), inner diameter of ٢٨ and outer diameter of ٣٢ mm. The results showed that the highest thermal efficiency of the HPHE, which reaches about ٩٦٪, is achieved by using ٣٠٪ filling ratio of the working fluid. Where in this case, the heat resistance of the heat pipe system reaches its lowest value (٠.٥٥ K/W).

Beiginaloo et al., (٢٠٢٢) [٢٥] investigated the thermal performance of a HPHE (wickless) with different lengths of its sections (condenser, evaporator, and adiabatic) using CFD. The variables that were considered in this study are heat load, liquid filling ratio, and condenser-to-evaporator length ratio (AR). Based on momentum, energy and volume transfer equations, the condensation and evaporation processes were simulated. The results of the study showed that the performance of the HPHE can be improved through increasing the heat load and filling ratio and decreasing the AR. In order to

obtain the maximum performance of the HPHE, the values of the AR, heat load, and filling ratio should be equal to ٠.٨٣٢٥, ٢٤٦ W and ٨٥٪, respectively.

Sriwiga et al., (٢٠٢٣) [٢٦] used a HPHE to recover heat of exhaust flue gases from a boiler in a hotel. This is to increase the temperature of water entered into the boiler. This is by simulating the thermal performance of the HPHE using MATLAB program. The working fluid used is R١٣٤a refrigerant with a ٥٠٪ filling ratio. The heat pipe has a total length of ٨٠٠ mm (the evaporator length equals condenser length and equals ٤٠٠ mm) and outer diameter of ١٩ mm. The temperature at the evaporator inlet is ٢٠٠ °C and at the condenser inlet is ٣٠ °C. The study results showed that, under optimization conditions, the thermal energy efficiency of the HPHE is ٢٤٪ and heat recovery rate is ٤.٨٧ kW.

Ali et al., (٢٠٢٣) [٢٧] studied the effect of the filling ratio and tilt angle of a HPHE (wickless) on its thermal performance. This is in terms of the thermal resistance and temperature distribution. ANSYS-Fluent software was used to conduct the numerical simulation of two-phase flow inside the HPHE. The results indicated that the thermal resistance decreases as the heat input is increased in addition, effects of the filling ratio and tilt angle become more significant as the heat input is increased. The lowest total thermal resistance is attained at a tilt angle of ٩٠° and filling ratio of ٦٥٪. The results also indicated that the lowest value of the average temperature of the evaporator walls is obtained by using ٦٥٪ filling ratio while, its highest value is obtained using ٢٥٪ filling ratio.

٢.٢ Experimental Studies

Lukitobudi et al., (١٩٩٥) [٢٨] developed air-to-air heat exchangers using thermosiphon heat pipes under medium temperature conditions. The heat exchangers used are continuous plate finned copper tubes, circular, rectangular,

spirally-finned steel tubes, and bare copper tubes for their heat pipes. The water, with a filling ratio of ٦٠٪ of the evaporator section size, was used as a working fluid. The air velocity range is ١.٥ to ٥ m/s and heat input range is ٤ to ٢٠ kW by using electric heating elements. The results showed that the rectangular plate finned copper thermosiphon heat exchanger has the best thermal performance compared to the other exchangers.

Mozumder et al., (٢٠١٠) [٢٩] experimentally investigated the thermal performance (in terms of the thermal resistance and overall heat transfer coefficient) of a HPHE. This is by using variable filling ratio (٣٥٪ to ١٠٠٪), variable heat input (٢ to ١٠) W, and three working fluids (methanol, acetone and water). The results indicated that the maximum overall heat transfer coefficient of the miniature heat pipe is obtained by using the acetone as a working fluid. The results also indicated that setting the filling ratio of the working fluid at ٨٥٪ of the evaporator volume leads to achieving the best thermal performance of the HPHE. In other words, using this ratio (٨٥٪) leads to increase of the heat transfer coefficient and decrease of the thermal resistance and temperature difference across the evaporator and condenser.

Gedik (٢٠١٦) [٣٠] experimentally studied the effect of a working fluid, heat supplied (input), and cold fluid flow rate on the thermal behavior of a HPHE (thermosiphon). This is by using different working fluids (ethanol, ethylene glycol and water) and two values of the heat supplied (٢٠٠ W and ٦٠٠ W). It was found that the highest thermal performance of the HPHE can be obtained by using ethanol as a working fluid at ١٠ L/h volumetric flow rate and ٦٠٠ W heat supplied.

Mohamed at el., (٢٠١٦) [٣١] experimentally studied the thermal performance of an air-to-air HPHE (wickless). This is by using distilled water as a working fluid with a filling ratio of ٧٥٪ of the evaporator size. The model consists of four rows with twelve copper tubes per row. The tubes were

organized in a staggered pattern with an internal diameter of ٩.٥ mm, outer diameter of ١٠ mm and length of ٩٥٠ mm. To enhance the heat transfer area, aluminum wavy plate fins (with thickness of ٠.١ mm) were placed between tubes. Tests were carried out with different flow rates (the air flow rate through the condenser and evaporator regions). The results showed that the effectiveness of the HPHE increases with the increase in the air temperature at the evaporator inlet.

Ma et al., (٢٠١٦) [٣٢] experimentally studied the thermal performance of a HPHE. The first and second laws of thermodynamics were implemented to analyze the process of recovering wasted thermal energy. The results showed that as the recycled water flow rate is increased, the exergy efficiency increases and effectiveness decreases. Where by increasing the recycled water flow rate from ٠.٨٣ to ١.٨٧ m^3/h, the exergy efficiency increases from ٣٤٪ to ٤١٪ and the effectiveness decreases from ١٩% to ٩%. The results also showed that the optimal flow rates for fresh water and recycled water are ٣ and ١.٢ m^3/h respectively. The results also showed that the HPHE cleaning device plays an effective role in increasing heat transfer. This leaded to increase of the exergy efficiency, heat transfer coefficient, and efficiency by ٤٩.٩٪, ١٩.٧٪, and ١١.٦٪, respectively.

Gedik et al., (٢٠١٦) [٣٣] investigated the effect of a working fluid and its operating characteristics on the performance of a heat recovery system using a gravity heat pipe. This is by using two different working fluids (R٤١٠a and R١٣٤a refrigerants). The parameters that were studied include the coolant flow rate, flue gas velocity, and flue gas temperature. The results showed that the temperature and velocity of the flue gas have a significant effect (positive) on the thermal performance of the system. While, the coolant flow rate has a negative effect (its increasing leads to a decrease in the efficiency of the thermal system). In overall, the results showed that the efficiency of the heat recovery

system by using R٤١٠a is better than using R١٣٤a refrigerant (٥٧.٧٪ for R٤١٠a and ٣٥.٦٪ for R١٣٤a). Figure (٢.٢) shows a schematic view of the gravity heat pipe.

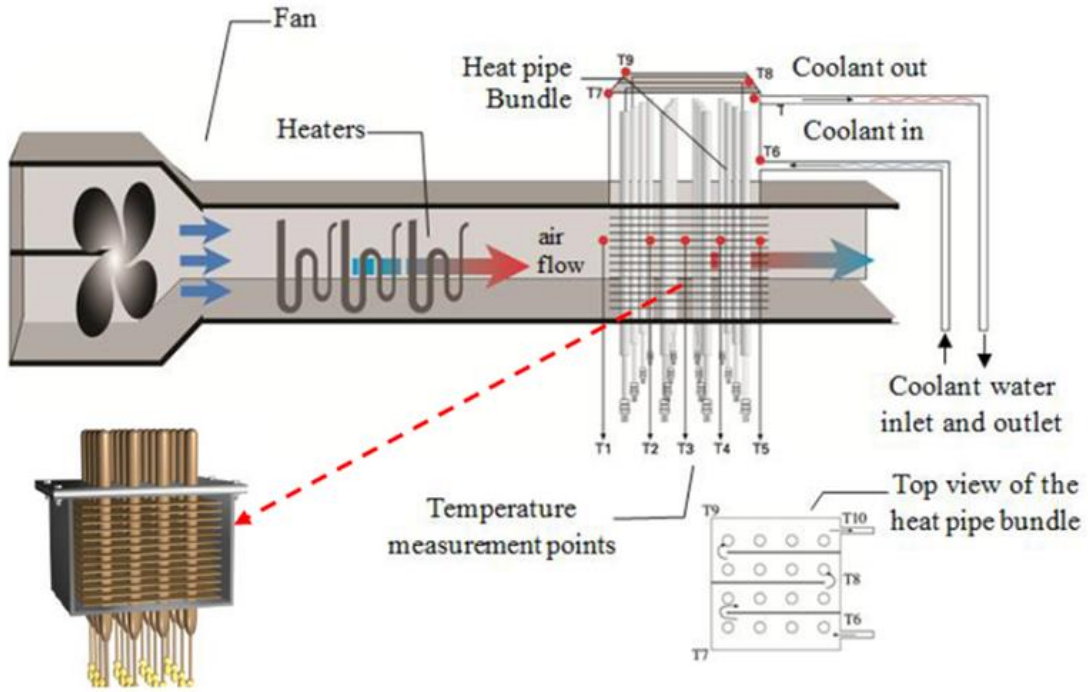

Figure ٢.٢: Schematic View of Gravity Heat Pipe [٣٣]

Naresh and Balaji (٢٠١٧) [٣٤] used (in an experimental study) six rectangular fins (with width of ٥ mm and thickness of ١ mm) inside the condenser of a thermosiphon heat pipe (see Figure (٢.٣)). This is to increase the heat exchange between the working fluid and other fluid. The study was done under wide range of the thermal energy supplied (٥٠ to ٢٧٥) W and by using water and acetone as working fluids with different filling ratios (٨٠٪, ٥٠٪, and ٢٠٪). The thermosiphon has an outer diameter of ٢٦ mm, thickness of ٣ mm and total length of ٥٠٠ mm (٢٠٠ mm evaporator section, ١٠٠ mm adiabatic section, and ٢٠٠ mm condenser section). The results showed that adding fins inside the condenser accelerates the condensation process of the working fluid and thus improves the thermal performance of the heat pipe. In overall, the higher temperature decreased by ١٧٪ and lower heat resistance decreased by ٣٥.٥٪ at the lowest heat supplied.

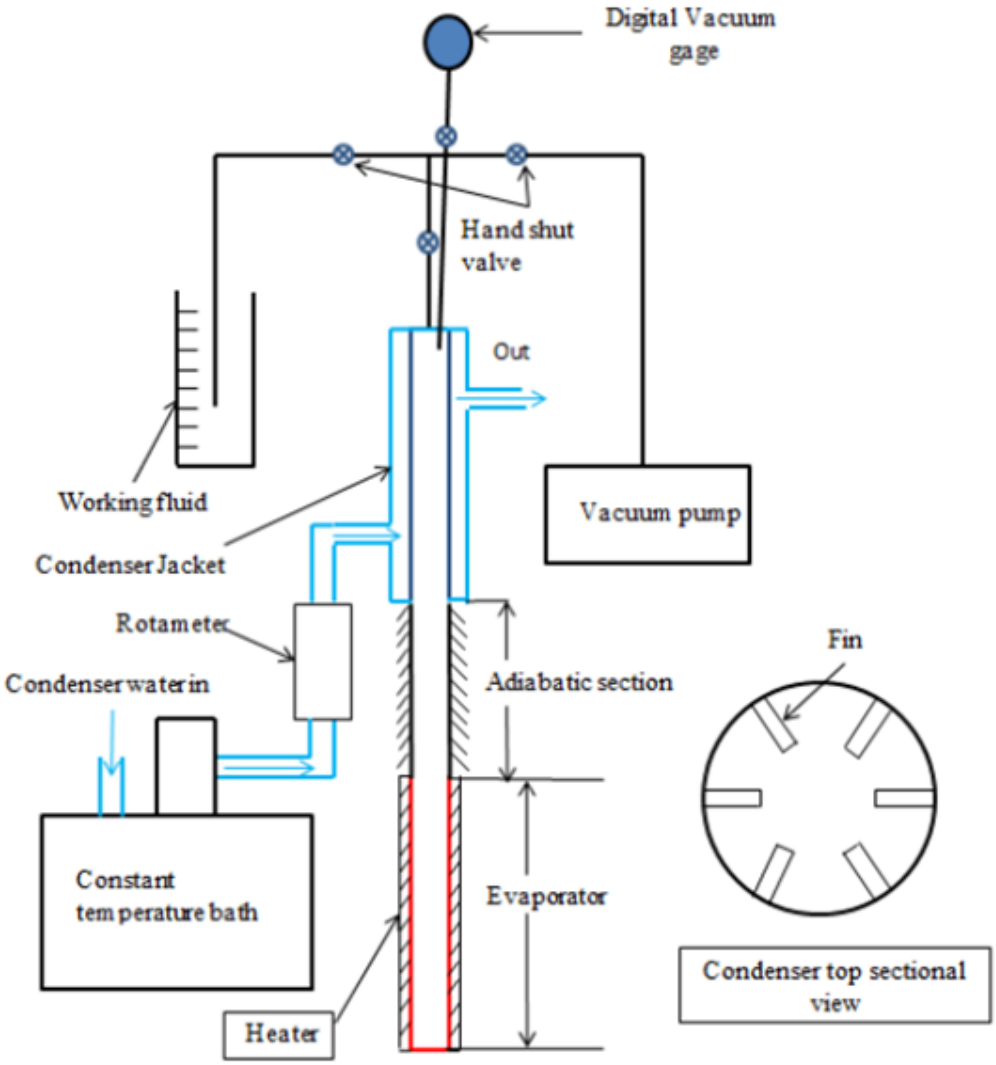

Figure ٢.٣: Experimental Rig of Reference [٣٤]

Muhammad et al., (٢٠١٨) [٣٥] used a HPHE, in an experimental study, with ٤٢ rows of heat pipes and ١٢٠ corrugated fins for heat recovery. The variables of the study include ٣ values of the air velocity and two values of the temperature of air entered into the HPHE. The results of experimental tests showed that the highest thermal efficiency of the HPHE, which equals ٥٤.٤٪, is achieved by using ١ m/s air velocity and ٤٥ ˚C air temperature. The results also showed that the highest heat recovery, which equals ٥.٣٥ kW, is achieved by using ٢ m/s air velocity and ٤٥ ˚C air temperature.

Öztürk et al., (٢٠١٨) [٣٦] experimentally examined the thermal performance of a HPHE for waste heat recovery. This is by using two working fluids (Nanofluid of aluminum oxide particles and distilled water) with a filling ratio of ٣٣٪ of the evaporator volume. The system works based on the gravity flow for the Nanofluid. The heat pipes system has ١٥ copper tubes with a length of ١ m and inner diameter of ١٠ mm. The length of copper tubes in the evaporator, condenser, and adiabatic section are ٤٥٠, ٤٠٠ and ١٥٠ mm respectively. The experimental conditions were controlled by setting the temperature, air mass flow rate, and heat capacity of the exchanger. The parameters studied are the air flow rate (٤٠ to ٨٤ g/s) and heat power of the evaporator unit (٣ and ٦) kW. The results showed that when the Nanofluid is used instead of the distilled water, the thermal efficiency of the HPHE increases. The results also showed that increasing the air velocity in the evaporator section leads to increase of the system efficiency.

Kusumah et al., (٢٠١٩) [٣٧] used, in an experimental study, a U-shaped HPHE, with a stepped arrangement for heat recovery. This is by using different numbers of U-shaped tubes included inside the heat exchanger. The study was carried out under various conditions (different values of velocity and temperature of air). The effect of the number of tubes, air velocity and air temperature on the thermal performance of the HPHE was investigated. The results of the study indicated that the parameter which has the largest and direct impact on the thermal performance of the HPHE is the evaporator inlet air temperature. The results also showed that the highest heat recovery, which equals ٢.١٩ kW is obtained by applying ١.٥ m/s air velocity and ٤٥ °C evaporator inlet air temperature.

Delpech et al. (٢٠١٩) [٣٨] designed and implemented a HPHE for waste heat recovery in ceramic production plants. The heat pipes system implemented consists of ten parallel tubes with a diameter and thickness of ٢٨

mm and ٢ mm respectively. The tubes were connected together via a bottom pipe with a diameter of ٢٨ mm. Each pipe has evaporator section with ٤٣٠ mm length and condenser with ٤٣٠ mm length. The experimental tests were conducted under different operation conditions. The results of the study demonstrated that the proposed system is able to recover ٤ kW of thermal energy.

Hossen et al. (٢٠١٩) [٣٩] experimentally studied the thermal performance of a HPHE under different conditions. The HPHE, which consists of copper heat pipes arranged in stages with using fins (seven in each heat pipe), was evacuated from air and then injected with a working fluid (water). The HPHE was placed between two ducts carrying hot and cold fluids. The cold fluid is atmospheric air and hot fluid is water which its temperature changes between ٥٦ and ٦٦ °C. The performance of the HPHE, in terms of heat transfer coefficient and effectiveness, was evaluated and analyzed. The effect of the filling ratio of water inside the heat pipe was tested at different air flow rates. The results indicated that the performance of the HPHE increases with increasing the air flow rate but this depends on environmental conditions. The results also indicated that the maximum value of this performance is obtained by using a ٤٥٪ filling ratio.

Abdelaziz et al., (٢٠٢١) [٤٠] used a HPHE to reduce energy consumption in air conditioning systems. The study was done under different conditions (evaporator inlet air temperature and air flow rate). The HPHE was charged with R-١٢٣ refrigeration fluid at ٢٥.٨ ˚C as a working fluid. Three models (with outer diameters of ٩.٥, ١٢.٧ and ١٩.٠٥ mm) of wickless horizontal HPHE were used. Each of them made of ٣٢ copper tubes (٠.٥ m length of each tube). The results showed that increasing the air mass flow rate and/or its temperature leads to increase of the HPHE efficiency and at the same time leads to decrease of energy consumption. In overall, the optimal values of the

evaporator inlet air temperature and wickless tube diameter are ٣٥ °C and ١٢.٧ mm respectively. In this case, the energy consumption was reduced to the lowest level (approximately ٣٠٪).

Abedalh et al., (٢٠٢١) [٤١] used, in an experimental study, a HPHE to reduce energy consumption in an air conditioning system. The HPHE used in this study consists of ٤٠ copper tubes arranged in four rows, each row contains ١٠ copper tubes. Each heat pipe has ٧٣ cm total length, ١ cm inner diameter, and ١.٢٣ cm outer diameter. All heat tubes were filled with distilled water with a ratio of ٥٠٪. In this study, the effect of air flow velocity on the temperature difference between the air entered into the evaporator and air leaved the condenser was investigated. The results of the study showed that increasing the air velocity leads to increasing the temperature difference between the evaporator and condenser unit and therefore increase of the efficiency of the HPHE. The maximum efficiency of the HPHE (٦٤.٦٪) was obtained at ١ m/s air velocity and ١٤٠٠ W heat flow rate. The maximum value of heat recovered (٩٢٣.٤ W) was observed at ٢ m/s air velocity and ١٤٠٠ W heat flow rate.

Sukarno et al. (٢٠٢١) [٤٢] developed, in an experimental study, a heat recovery system by using a HPHE in an air conditioning system. The work was conducted under different conditions (air velocity and evaporator inlet temperature). The HPHE, shown in Figure (٢.٤), consists of three, six, and nine rows with four heat pipes in each row arranged in a staggered configuration. The outer diameter of the heat pipe, evaporator length, condenser length, and adiabatic section length are ١٠ mm, ١٦٠ mm, ١٩٠, and ٣٦٠ mm respectively. The HPHE was charged by water as a working fluid with a ٥٠٪ filling ratio. The results showed that increasing the number of rows and air temperature entered into the evaporator section increases the energy recovery rate. In overall, the highest efficiency of the HPHE (which equals about ٦٣%) was

achieved at ٤٥ °C inlet air temperature, ٢ m/s inlet air velocity, and nine rows of heat pipes.

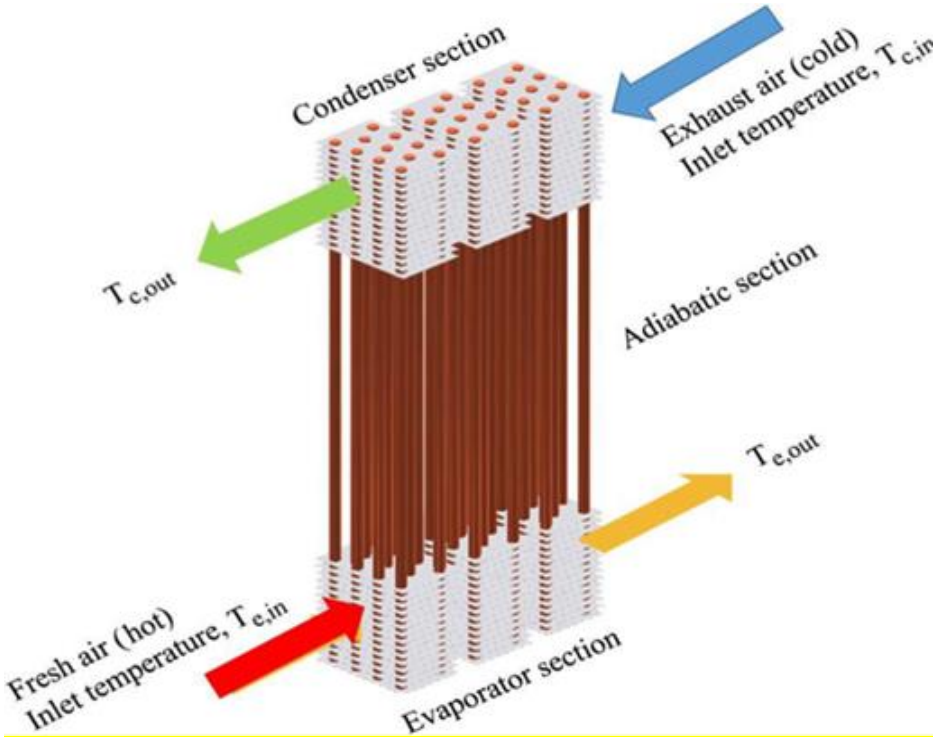

Figure ٢.٤: Wickless Heat Pipe [٤٢]

Sertkaya et al., (٢٠٢٥) [٤٣] experimentally investigated a wicked copper heat pipe (with an outer diameter of ١٥ mm and total length of ٤٥٠ mm) at changed operation conditions. This is by using pure water, methanol, ethanol, acetone, and R١٣٤a, with a filling ratio of ٥٠٪ of the evaporator size, as working fluids. In addition to two heat fluxes (١.١٢ and ٥.٥٨ kW/m^{٢}) and four inclination angles (٠°, ٣٠°, ٦٠°, and ٩٠°). The results indicated that the thermal performance of the heat pipe can be improved by increasing the inclination angle and/or heat flux. The best thermal performance of the heat pipe can be obtained by using R١٣٤a as a working fluid, heat flux of ٥.٥٨ kW/m^{٢} and inclination angle of ٩٠°.

٢.٣ Numerical and Experimental Studies

Noie-Baghban et al., (٢٠٠٠) [٤٤] designed and built, in a numerical and experimental study, an air-to-air HPHE for waste heat recovery. The aim of this study is to reduce air pollution and protect the environment in a hospital. Different models of the HPHE were designed and analyzed by using methanol (with a filling ratio of ٤٥٪) as a working fluid. The heat pipe has an evaporator with a length of ٣٠٠ mm and condenser with the same evaporator length. The air velocity of both streams is the same (٢.٣ m/s). Three electric heaters (١٥٠٠ W total power) were used to heat up air passed across the evaporator. The results showed that increasing the amount of heat entered into the evaporator section leads to increase of the condenser outlet air temperature from ١٧ to ٢١ ˚C. The results also showed that the efficiency of the HPHE obtained is ١٦%.

Noie (٢٠٠٦) [٤٥] numerically and experimentally studied the thermal performance of a thermosiphon HPHE. This is by using the distilled water (with a ٦٠٪ filling ratio) as a working fluid, wide range of the heat supplied (١٨ to ٧٢ kW), various evaporator inlet air flow velocity (٠.٥ to ٥.٥ m/s), and constant condenser inlet air temperature (٢٥ ˚C). The HPHE consists of ٩٠ finned copper tubes arranged with sex rows. The heat pipe has an evaporator and condenser with the same length (٦٠٠ mm) and adiabatic section with ١٠٠ mm length. The results indicated that decreasing the air flow velocity and/or increasing the heat supplied lead to increasing the thermal efficiency of the exchanger. Where by decreasing the air velocity from ٥.٥ to ٠.٥ m/s and increasing the heat supplied from ١٨ to ٧٢ kW, the efficiency increases from ٣٧٪ to ٦٥٪.

Mroue et al. (٢٠١٥) [٤٦] experimentally and analytically modeled and investigated a HPHE. The HPHE contains six carbon steel thermosiphon tubes. Each tube has a length of ٢ m, diameter of ٢٨ mm, and wall thickness of ٢.٥ mm. The installation of tubes was done with a parallel method. In this study, the combined effects of the condenser inlet air temperature and its mass flow

rate on the thermal performance of the heat exchanger were investigated. This is by using multiple air passes at different temperatures (١٠٠ to ٢٥٠ °C) and mass flow rates (٠.٠٥ to ٠.١٤ kg/s). The working fluid used is water. This process was analyzed experimentally and also by a CFD method. The results of the study showed that the effectiveness of the HPHE directly proportional with the evaporator inlet air temperature and inversely with its mass flow rate. Where the maximum value of the effectiveness was obtained by using ٠.٠٥ kg/s mass flow rate and ٢٥٠ °C evaporator inlet air temperature.

Ramos et al., (٢٠١٦) [٤٧] numerically and experimentally studied the thermal performance of a cross-flow HPHE. The HPHE was equipped with six carbon steel thermosiphon heat pipes. The heat pipe has a length of ٢ m, diameter of ٢٨ mm, and thickness of ٢.٥ mm. The study was done by using distilled water (with a filling ratio of ١٠٠٪ of the evaporator size) as a working fluid, variable mass flow rate (٠.٠٥ to ٠.١٧ kg/s), and different evaporator inlet air temperatures (٥٠ to ٣٠٠) °C. The results of the study showed that the thermal effectiveness of the HPHE increases with the increase in the evaporator inlet air temperature and decreases with the increase in the mass flow rate. Where the highest effectiveness of the HPHE, which equals about ١٦٪, is achieved at ٣٠٠ °C inlet air temperature and ٠.٠٥ kg/s mass flow rate. At the same time, the minimum heat resistance of the HPHE (٠.٠٥ K/W) is obtained at these conditions (٠.٠٥ kg/s and ٣٠٠ °C).

Mroue et al., (٢٠١٧) [٤٨] experimentally and numerically investigated the thermal performance of a thermosiphon HPHE. The heat transfer process from air to water was done by using several thermosiphons. The evaporator has different paths for air entry (one, two, and three passes), but in the condenser, two channels were considered for water passage. The study was done under different conditions (different mass flow rates of ٠.٠٥, ٠.٠٨, ٠.١١, and ٠.١٤ kg/s and different air inlet temperatures of ٢٥٠, ٢٠٠, ١٥٠, and

١٠٠ °C). The results demonstrated that the maximum thermal energy transferred by the thermosiphons is achieved at ٠.١٤ kg/s mass flow rate and ٢٥٠ °C evaporator inlet temperature.

Jouhara et al., (٢٠١٧) [٤٩] experimentally and theoretically designed, built, and evaluated a new system for heat recovery in the steel industry by using a flat HPHE. The flat heat pipe system used in this study consists of stainless steel heat pipes. The flat HPHE implemented in the laboratory was evaluated under industrial conditions. The results of experimental tests showed that the heat recovery rate in the proposed system is about ٥ kW. However, in industrial studies of this model, the heat recovery rate is approximately ١٠ kW. The results also showed that considering the initial length of ١ meter for the HPHE and the length of ٧٠ meters for the production line in the steel mill for recovering ٠.٧٥ MW waste heat is possible.

Raghuram et al., (٢٠١٧) [٥٠] experimentally and numerically studied the impact of the tilt angle and type of working fluid on the thermal performance of a thermosiphon HPHE. The heat pipe used in this study is made of copper and has dimensions of ١٢ mm in the diameter, ١ mm in the thickness and ٣٠٠ mm in the length. The study was done by using heat supplied of about ٧.٥ W, two working fluids (acetone and distilled water) and two tilt angles of °٦٠ and °٩٠. The results showed that the best thermal efficiency of the heat pipe is achieved by using acetone as a working fluid and tilt angle of °٦٠.

Xie et al., (٢٠١٩) [٥١] experimentally and numerically investigated the thermal behavior of a HPHE used in a residual heat removal system (RHRS) inside a nuclear power plant. This is by using two diameters of the heat pipe (١٦ and ١٩) mm, condenser length of ١٧٥ mm, adiabatic length of ١٠٠ mm, and evaporator length of ١٧٥ mm. The results showed that the thermal performance of the HPHE by using the diameter of ١٩ mm is better than that using ١٦ mm.

By comparing the numerical results with experimental data, it was found that the deviation percentage between them is less than ١٠٪.

Jouhara et al., (٢٠٢١) [٥٢] experimentally and numerically investigated the thermal performance of a copper HPHE system at variable water flow rate. This is by using different numbers of passes for the evaporator section. The results showed that the increase in the number of passes leads to an improvement of ٢٥٪ in the thermal efficiency of the HPHE. The overall performance of the HPHE and condenser outlet air temperature were predicted by using two theoretical methods: Log Mean Temperature Difference (LMTD) and Effectiveness-Number of Transfer Units (ε-NTU). For the results of the HPHE performance, the error percentage by using the LMTD method is ١٥.٥٪ and using the ε-NTU method is ١٩٪, While for the air temperature, in both methods the error is about ٠.٧ °C.

Ali & Sarsam (٢٠٢٢) [٥٣] numerically and experimentally investigated the thermal performance of a HPHE by using different working fluids (water, R٢٢ and R٤٠٧ refrigerant). The study was carried out under different operation conditions (heat load, filling ratio and evaporator air inlet temperature). In the numerical aspect, MATLAB software was used for modelling of the heat transfer process inside the HPHE. The results indicated that using R٢٢ refrigerant as a working fluid improves the thermal performance of the HPHE by ٣٣٪ while, using R٤٠٧c refrigerant improves it by ٢٢٪ compared to the water. The results also indicated that the heat load, filling ratio and air flow rate have a direct effect on the heat transfer rate. In overall, the optimum operation conditions to obtain the highest performance of the HPHE are ١.٥ kW heat load and ١٠٠٪ filling ratio.

٢.٤ Summary of Literature Review

Tables (٢.١, ٢.٢ and ٢.٣) respectively include summaries of numerical, experimental and numerical and experimental studies.

Table ٢.١: Summary of Numerical Studies

No	Ref. and study year	Boundary conditions and heat pipe modification method	Results and Conclusions
١	Alammar et al., [١٨], ٢٠١٦.	Different filling ratios (١٠٠, ٨٠, ٦٥, ٥٠, and ٢٥) % and Different tilt angles (°٩٠, °٧٠, °٥٠, °٣٠, & °١٠).	The optimum fill ratio and tilt angle, to obtain the HPHE best efficiency, are ٦٥٪ and ٩٠°.
٢	Fertahi et al., [١٩], ٢٠١٧.	Using inclined fins on the outer surface of the condenser of heat pipe.	Using fins improves the thermal efficiency of the heat pipe by about ١٦٪.
٣	Adrian et al., [٢٠], ٢٠٢٠.	Using three HTFs (R١٣٤a, R٤٠٤a, and R٤٠٧a) with various filling ratios (١٠ to ٧٠٪).	The HPHE highest efficiency (about ٩٠٪) is achieved using R١٣٤a with a ١٠٪ fill ratio.
٤	Al Jubori and Jawad [٢١], ٢٠٢١	Using different filling ratios and many slope angles of the WHP). Using water as a heat transfer fluid.	the maximum performance (minimum heat resistance) was achieved at a filling ratio of ٥٠٪ and slope angle of °٩٠.
٥	Desai et al., [٢٢],	Three different geometries (circular, square and triangular of	The square pipe has a thermal performance better than the

	٢٠٢١.	the heat pipe.	triangular and circular pipe.
٦	Brough et al., [٢٣], ٢٠٢١.	Using different designs of external fins inside heat pipes.	The average and maximum errors of modeling method are ٤.٤٪ & ١٥٪.
٧	Sadeghi et al., [٢٤], ٢٠٢٢.	Using differing filling ratios (٣٠, ٥٠, ٧٠ and ٩٠٪).	The highest efficiency (٩٦٪) is achieved at ٣٠٪ filling ratio.
٨	Beiginaloo et al., [٢٥], ٢٠٢٢.	Diverse heat loads, different liquid fill ratios, and different condenser-to-evaporator lengths (AR).	The optimum values of AR, heat load, and filling ratio are ٠.٨٣, ٢٤٦ W and ٨٥٪, respectively.
٩	Sriwiga et al., [٢٦], ٢٠٢٣.	Different inlet air temperatures.	The thermal efficiency is ٢٤٪ and heat recovery rate is ٤.٨٧ kW.
١٠	Ali [٢٧], ٢٠٢٣.	Different working fluid filling ratios and different inclination (tilt) angles.	The optimum values of the fill ratio and tilt angle are ٦٥٪ and ٩٠° respectively.

Table ٢.٢: Summary of Experimental Studies

No.	Ref. and study year	Boundary conditions and heat pipe modification way	Results and Conclusions
١	Lukitobudi et al., [٢٨], ١٩٩٥.	Different designs of heat pipe (circular tubes, rectangular tubes, spirally-finned steel tubes, and bare copper tubes).	The rectangular plate finned copper heat exchanger has the best thermal performance compared to others heat pipes.
٢	Mozumder et al., [٢٩], ٢٠١٠.	Different filling ratios (٣٥٪ to ١٠٠٪), three working fluids (methanol, acetone and water).	The results showed that acetone is the best working fluid compared to others & optimum fill ratio is ٨٥٪.

٣	Gedik [٣٠], ٢٠١٦.	Different working fluids (ethanol, ethylene glycol and water) and two heats supplied (٢٠٠, ٦٠٠) W.	The best thermal efficiency of heat pipe is obtained using ethanol as a working fluid and ٦٠٠ W heat supplied.
٤	Mohamed at el., [٣١], ٢٠١٦.	Using a model consists of four rows with ١٢ copper tubes per row with ٠.٩٥ & ١ cm internal & outer diameter & ٩٥cm length.	The results showed that the effectiveness increases with increasing the temperature at the evaporator inlet.
٥	Ma et al., [٣٢], (٢٠١٦).	Using fresh and recycled water as working fluids with different flow rates.	Using recycled water better than the fresh water and the optimal flow rate is ٣ m^3/h for fresh water and ١.٢ m^3/h for recycled water.
٦	Gedik et al., [٣٣], ٢٠١٦.	Different working fluids (R٤١٠a and R١٣٤a refrigerants).	Using R٤١٠a refrigerant as a working fluid is better than R١٣٤a.
٧	Naresh and Balaji [٣٤], ٢٠١٧.	Using six rectangular fins inside the condenser section, using water and acetone as working fluids.	Using fins in the condenser improves the efficiency of system, using acetone better than water as a working fluid.
٨	M. diyah et al., [٣٥], ٢٠١٨.	Different air velocities and different inlet air temperatures.	The HPHE highest efficiency (٥٤.٤٪), is achieved using ١ m/s air velocity & ٤٥ ˚C air temperature.
٩	Öztürk et al., [٣٦], ٢٠١٨.	Using two working fluids (Nanofluid and distilled water), different flow rates (٤٠ to ٨٤ g/s) and various heat (٣ & ٦)kW.	Using the Nanofluid as a working fluid better than the distilled water, increasing the air velocity improves the system efficiency.

١٠	Kusumah et al., [٣٧], ٢٠١٩.	Using different values of the velocity and temperature of air.	The optimum values of the air velocity and temperature are ١.٥m/s and ٤٥°C respectively.
١١	Delpech et al. [٣٨], ٢٠١٩.	Using a heat pipe system of ten parallel tubes with ٢٨ mm diameter and ٢ mm thickness.	The proposed heat pipe system is able to recover ٤ kW thermal energy.
١٢	Sakil Hossen, [٣٩], ٢٠١٩.	Using different values of filling ratio of the working fluid and air flow rate.	The maximum performance of the heat pipe is obtained by using ٤٥٪ filling ratio.
١٣	Abdelaziz et al., [٤٠], ٢٠٢١.	Using a heat pipe of wickless tubes with different diameters and different air temperatures.	The pipe best efficiency is obtained at ٣٥°C inlet air temperature & ٢.١mm tube diameter.
١٤	Abedalh et al., [٤١], ٢٠٢١.	Using different air velocities and different heat flow rates.	The maximum efficiency of the HP (٦٤.٦٪) is obtained at ١ m/s air velocity and ١.٤ kW heat flow rate.
١٥	Sukarno et al. [٤٢], ٢٠٢١.	Using various inlet air temperature, various air speed and two numbers of rows of heat pipes (٤ and ٩).	The highest efficiency of the heat pipe (٦٢.٦٪) is achieved at ٤٥°C inlet air temperature, ٢m/s air velocity and nine rows of pipes.
١٦	Sertkaya et al., [٤٣], ٢٠٢٥	Using pure water, methanol, ethanol, acetone, and R١٣٤a, with ٥٠٪ fill ratio a, two powers of ١.١٢ and ٥.٥٨ kW/m^{٢} and tilt angles (٠, ٣٠, ٦٠, & ٩٠°).	The best thermal performance of the heat pipe can be obtained by using R١٣٤a as a working fluid, heat flux of ١.١٢ kW/m^{٢} and ٩٠° tilt angle.

Table ٢.٣: Summary of Numerical and Experimental Studies

No.	Ref. and study year	Boundary conditions and heat pipe modification way	Results and Conclusions
١	Noie-Baghban et al., [٤٤], ٢٠٠٠.	Using different models of heat pipe with different tube shapes and different working fluids.	The heat absorbed in the operator for experimental tests is close to the numerical results.
٢	Noie [٤٥], ٢٠٠٦.	Using different inlet air temperatures and various air flow rate. The fill ratio of working fluid is ٦٠٪.	Increasing the air flow rate from ٥ to ٥.٥ m/s increases the efficiency of the heat pipe from ٣٧٪ to ٦٥٪.
٣	Mroue et al. [٤٦], ٢٠١٥.	Using different inlet air temperatures and different air flow rates.	The difference between the numerical and experimental results is less than ١٠٪.
٤	Ramos et al., [٤٧], ٢٠١٦.	Using a heat pipe equipped with six heat pipes.	The temperature difference predicted in the evaporator & condenser with a real sample is ٥٪.
٥	Mroue et al., [٤٨], ٢٠١٧.	Using different inlet air temperatures and different fluid mass flow rates.	The difference ratio between the CFD and experimental results is ١٥٪.
٦	Jouhara et al., [٤٩], ٢٠١٧.	Using a flat HPHE consists of stainless steel heat pipes.	The heat recovery rate in the proposed system is near ٥ kW.
٧	Raghuram et al., [٥٠], ٢٠١٧.	Using heat input of ٧.٢٩ W, two working fluids (acetone and distilled water) and two tilt angles of ٦٠° and ٩٠°.	The best thermal efficiency of the heat pipe is achieved by using acetone as a working fluid and tilt angle of °٦٠.
٨	Xie et al., [٥١], ٢٠١٩.	Using a heat pipe heat exchanger (HPHE) with different diameters.	The thermal performance of the heat pipe is obtained by using the diameter of ١٩ mm.

٩	Jouhara et al., [٥٢], ٢٠٢١.	Using different numbers of passes for the evaporator section of the heat pipe.	Increasing number of passes improves the efficiency of the heat pipe by about ٢٥٪.
١٠	Ali & Sarsam [٥٣], ٢٠٢٢.	Using different working fluids (water, R٢٢ and R٤٠٧c refrigerant), different heat loads, different filling ratios of working fluid.	Using R٢٢ refrigerant as a working fluid better than R٤٠٧c refrigerant and water, The HPHE highest performance is obtained using ١.٥ kW load & ١٠٠٪ fill ratio.

٢.٥ The Novelty of the Current Study

A lot of research, to improve the thermal performance of HPHEs, were conducted by previous researchers. But, few of them have focused on using these HPHEs by connecting them to power plants to recover lost energy. While the use of DOWTHERM™ A as a working fluid (with different filling ratios) in a thermosiphon heat pipe has not been done previously, and this represents a gap in research literature. Thus, this research came to fill this gap through a numerical and experimental study of the thermal performance of a HPHE integrated into the Al-Musayyab steam power plant. This is under the effect of the working fluid filling ratio and condenser inlet air velocity. Then, analyzing and comparing the results obtained to achieve the optimum values of the filling ratio and air velocity that give the best thermal performance of the HPHE.

Chapter Three

Mathematical Model and Numerical Analysis

Chapter Three

Mathematical Model and Numerical Analysis

This chapter is divided into two main sections. The first is the mathematical model of a thermosiphon heat pipe heat exchanger (HPHE) which describes the mathematical equations to evaluate the thermal performance of this HPHE. The second section is the numerical analysis (simulation by using ANSYS-Fluent software) of the thermal performance of this HPHE.

٣.١ Mathematical Model

The most important criteria of the thermal performance of the thermosiphon HPHE is its effectiveness (Ɛ). It (effectiveness of HPHE) is defined as the ratio of the actual heat transfer rate ($Q_{act.}$) to the maximum possible heat transfer rate ($Q_{max.}$) as follows [٥٤]: -

$$\varepsilon = \frac{Q_{act.}}{Q_{max}} \quad \ldots (٣.١)$$

The actual heat transfer rate can be calculated by using one of the following equations [٥٥]:

١. For the cold air side:

$$Q_{act.} = \dot{m}_c \, Cp_c (T_{c.\,out} - T_{c.\,in}) \quad \ldots (٣.٢)$$

٢. For the hot air side:

$$Q_{act.} = \dot{m}_h \, Cp_h (T_{h.\,in} - T_{h.\,out}) \quad \ldots (٣.٣)$$

Where: -

- $\dot{m}_c$ and $\dot{m}_h$ are the mass flow rates of the cold and hot air, respectively,

- Cp_c and Cp_h represent the specific heat capacities of the cold and hot air, respectively,
- $T_{c.\ in}$ and $T_{c.\ out}$ are the inlet and outlet temperatures of the cold air respectively,
- $T_{h.\ in}$ and $T_{h.\ out}$ are the inlet and outlet temperatures of the hot air respectively,

The maximum possible heat transfer rate is given by the next equation [٥٥]: -

$$Q_{max} = C_{min}(T_{h.\ in} - T_{c.\ in}) \quad \ldots (٣.٤)$$

Where: - C_{min} is the minimum heat capacity of a fluid and equals: -

$$C_{min} = (\dot{m}_h Cp_h)_{min} \quad \ldots (٣.٥)$$

Or:

$$C_{min} = (\dot{m}_c Cp_c)_{min} \quad \ldots (٣.٦)$$

The Number of Transfer Units (NTU) method can be applied to find the effectiveness of the HPHE [٥٦]:

$$NTU = UAC_{min} \quad \ldots (٣.٧)$$

Here, U is the overall heat transfer coefficient, and A is the surface area of the HPHE.

The effectiveness of a thermosiphon HPHE can also be found by the following relationship [٥٧]: -

$$\varepsilon = ١ - exp(-NTU) \quad \ldots (٣.٨)$$

The effectiveness of the HPHE can also be calculated in terms of the inlet and outlet temperatures of air streams by using Eq. (٣.٩) or (٣.١٠). This is after

substituting Eq. (٣.٥) or (٣.٦) in Eq. (٣.٤), then substituting Eq. (٣.٤) and Eq. (٣.٢) or (٣.٣) in Eq. (٣.١). This is by depending on the relative heat capacity rates of the hot and cold air streams (Cp_h and Cp_c), as follows [٥٥-٥٧]: -

- $If\ Cp_c < Cp_h$

$$\varepsilon = \frac{(T_{c.\ out} - T_{c.\ in})}{(T_{h.\ in} - T_{c.\ in})} \quad \ldots (٣.٩)$$

- $If\ Cp_c > Cp_h$

$$\varepsilon = \frac{(T_{h.\ in} - T_{h.\ out})}{(T_{h.\ in} - T_{c.\ in})} \quad \ldots (٣.١٠)$$

These expressions provide a mathematical foundation for evaluating the thermal performance of the HPHE based on inlet and outlet temperatures of air streams.

This model facilitates the comparison of effectiveness at different filling ratios (٣٥٪, ٥٠٪ and ٧٥٪), allowing for an assessment of their effects on the overall thermal performance of the thermosiphon HPHE.

٣.٢ Numerical Analysis

This section focuses on describing the numerical methodology employed in this study to simulate the thermal performance of a thermosiphon HPHE using ANSYS-Fluent software. The aim is to establish a robust computational model capable of accurately capturing the change phase processes of the working fluid (DOWTHERM™ A) occurred within the heat pipe. The simulations are designed to assess the system response for different filling ratios of the working fluid (٣٥٪, ٥٠٪, and ٧٥٪) of the evaporator.

The numerical analysis is based on a volume of fluid (VOF) model to track the liquid-vapor interface within the heat pipe. Detailed descriptions of the computational domain geometry, mesh generation, boundary and initial

conditions, selected physical models, material properties, and solution settings are provided. Emphasis is placed on the preparation strategy, convergence criteria, and assumptions made to ensure numerical stability and physical accuracy. This methodological framework serves as the basis for the simulations and ensures consistency and repeatability in evaluating the impact of different operational parameters on the thermal performance of a heat pipe.

٣.٢.١ Assumptions

To facilitate the process of solving equations, there are some assumptions that can be taken into consideration as follows: -

١) Considering hot air instead of exhaust hot gases,

٢) Frictional losses are negligible,

٣) Heat generated by the fans is negligible,

٤) Properties of air, such as the density and specific heat (Cp), are constants with temperature change,

٥) The flow is two-dimensional and transient,

٦) The power input is ٨٠٠٠ W,

٧) The evaporator inlet air velocity is constant and equals ١ m/s,

٨) The condenser inlet air temperature is constant and equals ٢٤ °C,

٩) Evaporator inlet air temperature is variable with the time (١٦٠ to ٣٢٠ °C).

٣.٢.٢ Thermo-physical Properties of the Test Model

DOWTHERM™ A was selected as a working fluid for this study due to its superior thermal stability and favorable thermo-physical properties at elevated temperatures. Therefore, it is particularly suitable for high-temperature heat transfer applications such as those in heat exchangers of steam power

plants. An accurate determination of properties of working fluids is essential for modeling the coupled heat and mass transfer processes in a thermosiphon heat pipe, especially under phase change conditions. The numerical model used in this work incorporates temperature-dependent thermo-physical properties of DOWTHERM™ A in both the liquid and vapor phases. These properties are considered as essential inputs to capture the complex behavior during evaporation and condensation processes. These properties are density (ρ), specific heat capacity (Cp), dynamic viscosity (μ), thermal conductivity (k), and vapor pressure. The simulation environment in ANSYS-Fluent dynamically adjusts these properties according to conditions of the local temperature and pressure to ensure accurate modeling of phase-change behavior. The latent heat of vaporization and saturation temperature are also incorporated to reflect the energy exchanges occurred at the phase boundary.

Tables (٣.١) and (٣.٢) respectively summarize the saturated liquid and vapor properties of DOWTHERM™ A across a range of operating temperatures. For example, the liquid density decreases from ١٠٦٣.٥ kg/m³ at ١٥°C to ٦٧٢.٥ kg/m³ at ٤٠٥°C. While, the dynamic viscosity drops significantly from ٥.٠٠ Pa.s to ٠.١٢ Pa.s over the same range. These variations have a great influence on the fluid dynamics, pressure drop, and heat transfer rates within the heat pipe.

Table ٣.١: Saturated Liquid Properties of DOWTHERM™ A [٥٨]

Temperature (°C)	Specific Heat (kJ/kg·K)	Density (kg/m³)	Thermal Conductivity (W/m·K)	Viscosity (mPa·s)	Vapor Pressure (bar)
١٥	١.٥٥٨	١٠٦٣.٥	٠.١٣٩٥	٥.٠٠	٠.٠٠
٦٥	١.٧٠١	١٠٢٣.٧	٠.١٣١٥	١.٥٨	٠.٠٠
١٠٥	١.٨١٤	٩٩٠.٧	٠.١٢٥١	٠.٩١	٠.٠١

١٥٥	١.٩٥٤	٩٤٧.٨	٠.١١٧١	٠.٥٦	٠.٠٦
٢٠٥	٢.٠٩٣	٩٠٢.٥	٠.١٠٩١	٠.٣٨	٠.٢٨
٢٥٥	٢.٢٣١	٨٥٤.٠	٠.١٠١١	٠.٢٧	٠.٩٧
٣٠٥	٢.٣٧٣	٨٠١.٣	٠.٠٩٣١	٠.٢٠	٢.٦٠
٣٥٥	٢.٥٢٧	٧٤٢.٣	٠.٠٨٥١	٠.١٦	٥.٨٠
٤٠٥	٢.٧٢٥	٦٧٢.٥	٠.٠٧٧١	٠.١٢	١١.٣٢

Table ٣.٢: Vapor Properties of DOWTHERM™ A [٥٨]

Temperature (°C)	Specific Heat (kJ/kg·K)	Density (kg/m³)	Thermal Conductivity (W/m·K)	Viscosity (mPa·s)	Vapor Pressure (bar)
١٥	٠.٧٨٥	٢٩.٩٠	٠.٠٢٤٣	٠.٠٠١٧	٠.٠٠٠
٤٩.٥	١.٢٩٠	٢٤.٩٠	٠.٠٢٦٩	٠.٠٠٤٨	٠.٠٠٠
١٤٨.٩	٢.٠٠٠	١٠.٨٥	٠.٠٣٨٠	٠.٠٣٩٠	٠.٠٦٤
١٨٢.٢	٢.٢٢٩	٩.٠٦	٠.٠٥٦١	٠.١٤١٠	٠.٢١٤
٢١٥.٥	٢.٥٦٦	٨.٠٣	٠.٠٧٩٠	٠.٣٢٠٠	٠.٥٢٧
٢٤٣.٢	٢.٨١٤	٧.١٦	٠.١٠٢٣	٠.٥٦٨٠	٠.٩٧٠
٢٧٠.٠	٣.٠٩٠	٦.٣٩	٠.١٢٦٥	٠.٨٢١٠	١.٦٢٨
٢٩٦.٦	٣.٣٨٩	٥.٦٨	٠.١٥١٤	١.١٠٠٠	٢.٦٥٥
٣٢٣.٢	٣.٧١٢	٥.٠٢	٠.١٧٧١	١.٤١١٠	٤.٥٩٠
٣٥٠.٢	٤.٠٧٠	٤.٤٢	٠.٢٠٣٨	١.٧٨٠٠	٧.٩٣٤
٣٧٧.٥	٤.٤٦٥	٣.٨٧	٠.٢٣١٤	٢.٢١٨٠	١٣.٢٢٨

For modelling of conduction and convection heat transfer from the external environment, the thermal properties of copper (used as a pipe material) and air (as a cooling medium) are also defined in the CFD setup. Table (٣.٣) presents the constant properties of air and copper employed in this simulation.

Table ٣.٣: Properties of Copper and Air [٥٩]

Description	Symbol	Air	Copper	Units
Density	ρ	١.٢٢٥	٨٩٧٨	kg/m³
Dynamic Viscosity	μ	١.٧٨٩٤×١٠□□	–	kg·m□¹·s□¹
Specific Heat	Cp	١٠٠٦.٥	٣٨١	J/kg·K
Thermal Conductivity	k	٠.٠٢٤٢	٣٨٧	W/m·K

The simulation also incorporates the variation in these properties during the phase change process from liquid to vapor and vice versa. For instance, the density and viscosity of DOWTHERM™ A change significantly during phase transition, which can affect the flow dynamics and heat transfer within the heat pipe. The saturation temperature and latent heat of vaporization are defined according to the specific working conditions of the steam power plant, ensuring that the simulation accurately reflects the real-world operation of the heat pipe. The accurate representation of these material properties is essential for predicting of the performance of the heat pipe under different filling ratios.

In summary, the accurate incorporation of these fluids and material properties into the numerical simulation enhances the fidelity of the CFD model in predicting the thermo-hydraulic performance of the heat pipe under different filling ratios and operating conditions.

٣.٢.٣ Partial Differential Equations

The numerical analysis of the thermosiphon heat pipe is based on the fundamental principles of fluid dynamics and heat transfer. These are represented by the conservation equations of mass, momentum, and energy, which can be solved using the volume of fluid (VOF) method in ANSYS-Fluent software. The simulation also includes phase-change processes of a working fluid that are modelled using the same method (VOF) to capture the interface between the liquid and vapor phases accurately. The VOF was selected because

it can track the interface between immiscible phases and since it allows to resolve the partial differential equations together [٦٠].

In a control volume inside a heat pipe, the summation of volume fractions of phases of a fluid equal one. The volume fraction in each cell of the grid is represented by α_v for the vapor phase and α_l for the liquid phase. According to the value of this fraction, a working fluid inside a heat pipe may be totally liquid, totally vapor, or mixture of them. Therefore, properties of this fluid (thermal conductivity (k), density (ρ), and dynamic viscosity (μ) are found as follows [١٩]: -

$$k = \alpha_l k_l + (١ - \alpha_l) k_v \quad \ldots (٣.١١)$$

$$\rho = \alpha_l \rho_l + (١ - \alpha_l) \rho_v \quad \ldots (٣.١٢)$$

$$\mu = \alpha_l \mu_l + (١ - \alpha_l) \mu_v \quad \ldots (٣.١٣)$$

In this simulation, the numerical code treats a working fluid phase inside each cell of the grid as follows: -

If α_l =١ then the phase inside the cell is totally liquid,

If α_l =٠ then the phase inside the cell is totally vapor,

If $٠ < \alpha_l < ١$ then there is mixture of two phases (vapor and liquid) inside the cell.

٣.٢.٣.١ Continuity Equation

The continuity (mass conservation) equation ensures the conservation of mass in the computational domain and is given by [٦١]:

$$\frac{\partial \alpha_v \rho_v}{\partial t} + \nabla(\alpha_v \rho_v \overrightarrow{u_v}) = \dot{m}_{lv} - \dot{m}_{vl} \quad \ldots (٣.١٤)$$

Where: -

- $\dot{m}_{vl}$ and $\dot{m}_{lv}$ are respectively the mass flow rates due to the condensation and evaporation process (kg/s),

- α_v represents the volume fraction of the vapor phase,
- ρ_v represents the vapor density (kg/m³),
- $\overrightarrow{u_v}$ represents the velocity of the vapor phase (m/s),
- t represents time (s).

According to temperature regimes, $\dot{m}_{vl}$ and $\dot{m}_{lv}$ can be represented as follows [٦٢, ٦٣]: -

If $T < T_{SAT}$, then: -

$$\dot{m}_{vl} = r_l \, \alpha_v \rho_v \left[\frac{T - T_{SAT}}{T_{SAT}}\right] \quad \ldots (٣.١٥)$$

If $T > T_{SAT}$, then: -

$$\dot{m}_{lv} = r_v \, \alpha_l \rho_l \left[\frac{T - T_{SAT}}{T_{SAT}}\right] \quad \ldots (٣.١٦)$$

Where: - r_l and r_v represent mass flow time parameters, T and T_{SAT} are temperature and saturation temperature (K).

These equations (٣.١٥ and ٣.١٦) can be used to describe the positive mass flow from the liquid to vapor phase or vice versa for problems of the phase change (evaporation and condensation) processes of a working fluid. This change in the phase of a working fluid takes place at constant pressure and is governed by the saturation temperature (T_{SAT}).

To solve two phase flows that occurred inside a heat pipe, Eq. (٣.١١) is used. While, single phase flows can be solved by the next equation [٦٤].

$$\sum_{L=١}^{n} \propto_L = ١ \quad \ldots (٣.١٧)$$

Where: α_L is the volume fraction of the liquid phase.

٣.٢.٣.٢ Momentum Equation

The momentum (Navier–Stokes) equation governs the transport of momentum and includes effects of pressure, viscous forces, gravity, and surface tension [٦٧]: -

$$\frac{\partial(\rho\vec{u})}{\partial t} + \nabla(\rho\vec{u}\vec{u}) = -\nabla p + \nabla\tau + \rho g + F_{\square} \quad \ldots (٣.١٨)$$

Where: -

- p is the pressure (Pa),
- τ is the Shear stress (Pa)
- g is the gravitational acceleration vector (m/s²) and
- F□ is the surface tension force (N) and is given by the next equation [١٩].

$$F_{\square} = ٢\sigma_{lv}\frac{\alpha_l\rho_l C_v\nabla\alpha_v + \alpha_v\rho_v C_l\nabla\alpha_l}{\rho_l+\rho_v} \quad \ldots (٣.١٩)$$

Where: - **C** represents the surface curvature and σ_{lv} represents the coefficient of the surface tension and is given by the next equation [٦٦].

$$\sigma_{lv} = ٠.٠٩٨٠٥٨٥ - ١.٨٤٥ \times ١٠^{-٥}T - ٢.٣ \times ١٠^{-٧}\,T^{٢} \quad \ldots (٣.٢٠)$$

٣.٢.٣.٣ Energy Equation

The energy conservation equation, that takes into account heat conduction, convection and latent heat transfer due to the phase change, is given by [١٩]: -

$$\frac{\partial(\rho e)}{\partial t} + \nabla(\rho e\vec{u}) = \nabla(k\nabla T) + \nabla(p\vec{u}) + E_S \quad \ldots (٣.٢١)$$

Where: -

- E_S represents the thermal energy transferred into or from the working fluid during the phase change process (KW),

- e is the specific energy (kJ/kg) and is given by the next equation.

$$e = \frac{\alpha_l \rho_l e_l + \alpha_v \rho_v e_v}{\alpha_l \rho_l + \alpha_v \rho_v} \quad \ldots (٣.٢٢)$$

Where: -

$$e_l = C_{p.l}(T - T_{SAT}) \quad \ldots (٣.٢٣)$$

$$e_v = C_{p.v}(T - T_{SAT}) \quad \ldots (٣.٢٤)$$

In the VOF method, the temperature (T) and energy (e) are treated as average variables.

٣.٢.٣.٤ Heat Transfer Through Heat Pipe Metal Wall

The heat flow, through the metal wall of the heat pipe, takes place by conduction. In the case of the two-dimensional heat transfer, the next equation is applied as follows: -

$$\rho_w C_w \frac{\partial T}{\partial t} = k_w \left(\frac{\partial^2 T}{\partial x^2} + \frac{\partial^2 T}{\partial y^2} \right) \quad \ldots (٣.٢٥)$$

C_w, k_w, and ρ_w are properties (specific heat capacity, thermal conductivity and density) of the metal wall material of the heat pipe.

٣.٢.٤ Geometry and Mesh of the Test Model

To accurately simulate the physical configuration of a heat pipe heat exchanger integrated into a steam power plant, the computational geometry of the thermosiphon heat pipe was constructed and developed. The heat pipe was designed as a two-dimensional, axially symmetric, consisting of three main sections: the evaporator zone, adiabatic zone, and condenser zone. Each section exhibits distinct thermodynamic and fluid dynamic behaviors, essential to the operation of the system as a whole.

Evaporator Section: It is located at the lower end of the heat pipe and receives heat from the hot stream. Here, the working fluid (DOWTHERM™ A) undergoes phase change from liquid to vapor due to heat absorption. This section is under a boundary condition of constant heat flux.

Adiabatic Section: It is positioned in the center of the heat pipe between the evaporator and condenser, it works as a transport zone. No heat exchange with the environment occurs in this region. The vapor generated in the evaporator travels through this section with minimal thermal interaction, preserving its energy for release it in the condenser section.

Condenser Section: It is located in the upper end of the heat pipe. It dissipates heat to the surrounding cold air stream. In this section, the vapor condenses into liquid form again, releasing latent heat and completing the thermodynamic cycle of the heat pipe.

The computational domain was discretized using structured meshing techniques to enhance stability and accuracy of the numerical results. A very fine mesh was applied in regions where large gradients in temperature and velocity were expected particularly near the liquid-vapor interface and in the boundary layers within the evaporator and condenser zones. Mesh sensitivity analysis was conducted to ensure mesh-independence of the simulation results, and the final grid provided a very excellent balance between the accuracy of results and computational cost. Corresponding to the geometry of the heat pipe, the computational domain is discretized using a structured or unstructured mesh depending on the complexity of the region. Special attention is paid to the evaporator and condenser sections, where elements of the fine mesh are employed to accurately capture the phase change phenomena. The mesh resolution in these regions is critical for ensuring that the simulation results are accurate and reliable. A balance is maintained between the computational

efficiency and accuracy by optimizing the mesh density across different sections of the heat pipe.

Mesh statistics of the computational domain are listed in Table (٣.٤) including the total number of nodes and elements used in this simulation.

Table ٣.٤: Mesh Statistics of the Computational Domain

Property	Value
Geometry Type	٢D (Space Claim)
Length Unit	Meters
Bounding Box Length (X)	١.٥ × ١٠□² m
Bounding Box Length (Y)	١.٠ m
Bounding Box Length (Z)	٠.٠ m
Surface Area (Approx.)	١.٥ × ١٠□² m²
Number of Nodes	١٦٠,١٦٠
Number of Elements	١٥٠,٠٠٠
Number of Bodies	١
Active Bodies	١
Volume	٠.٠ m³ (٢D model)
٢D Tolerance	١.٠ × ١٠□□

Figure (٣.١) illustrates, on the left side, a schematic diagram of the heat pipe geometry and its three functional sections (evaporator, adiabatic, and condenser), along with the assigned boundary conditions. While on the right side, it shows the mesh of this heat pipe.

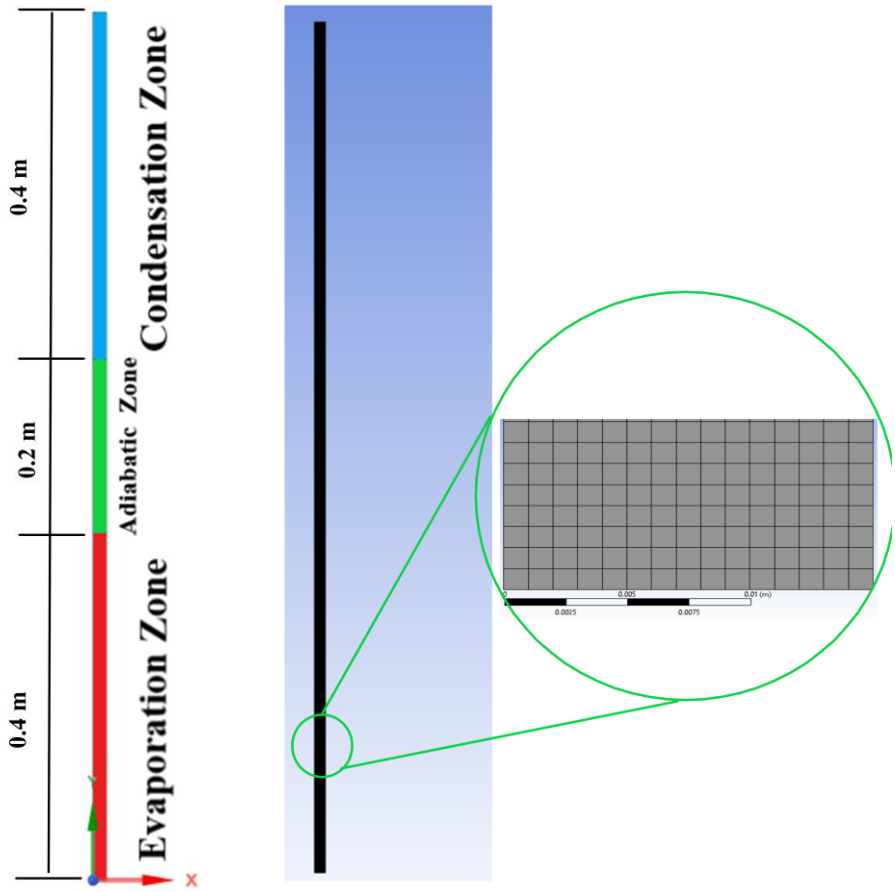

Figure ٣.١: Schematic Diagram of the Geometry and Mesh of the Heat Pipe

٣.٢.٥ Boundary Conditions of the Test Model

The boundary conditions in this numerical part are defined to accurately replicate the operating environment of the heat pipe within a heat recovery system of a steam power plant. These conditions are critical for capturing the fluid flow, heat transfer, and phase change phenomena occurred during the operation of the HPHE.

٣.٢.٥.١ Boundary Conditions Setup

The following major boundaries were defined in ANSYS Fluent: -

Evaporator Section: A constant temperature boundary condition is applied to simulate the heat input from the hot stream. This promotes evaporation of the working fluid (DOWTHERM™ A), initiating the phase change process. The

wall boundary is set to no-slip, ensuring that the fluid velocity at the pipe wall is zero.

Condenser Section: To simulate heat rejection to the cooling air, a convective boundary condition or a constant wall temperature is applied, depending on the case. The no-slip condition is maintained here as well. The airflow velocity at the condenser inlet varies in different cases to analyze its effect on heat transfer effectiveness.

Adiabatic Section: The adiabatic region is thermally insulated by applying an adiabatic (no heat flux) boundary condition to its walls. No-slip conditions are also maintained if the flow of a fluid is involved in this section. This ensures that no thermal energy is exchanged with the surroundings in this region.

Phase Change Interface: The interface between regions of the liquid and vapor is defined using a coupled thermal boundary to capture the phase transition. Parameters such as latent heat of vaporization and saturation temperature are defined to enable accurate modeling of evaporation and condensation.

Table (٣.٥) summarizes the simulation boundary conditions applied in ANSYS-Fluent.

Table ٣.٥: Boundary Conditions for Heat Pipe Simulation

Region	Boundary Condition Type	Momentum Setting	Thermal Setting	Description
Evaporator Section	Wall	No-slip	Constant Temperature	Simulates heat input and fluid evaporation
Condenser	Wall	No-slip	Convective /	Models heat rejection to

Section			Constant Temp	ambient air
Phase Change Surface	Interface	Coupled	Phase Change Enabled	Captures latent heat effects and vapor-liquid dynamics
Adiabatic Section	Wall	No-slip (if applicable)	Adiabatic (no heat flux)	Prevents heat transfer through insulated region

٣.٢.٥.٢ Simulation Operating Scenarios

To evaluate the performance of the HPHE under different conditions, a series of cases were simulated with variations in filling ratio and airflow velocity on the condenser side. The evaporator-side air velocity and heat input were kept constant. These scenarios were designed to investigate the effects of varying the working fluid volume (filling ratio) and external air velocity on the thermal performance and heat transfer characteristics of the heat pipe. The simulation outcomes provide a comprehensive understanding of how operational parameters affect the phase change, pressure drop, and overall thermal effectiveness.

Table (٣.٦) includes the boundary conditions for all cases of this simulation.

Table ٣.٦: Operating Boundary Conditions for Simulation Cases

Case	١			٢			٣			٤			٥		
Filling ratio (%)	٣٥	٥٠	٧٥	٣٥	٥٠	٧٥	٣٥	٥٠	٧٥	٣٥	٥٠	٧٥	٣٥	٥٠	٧٥
Condenser inlet velocity (m/s)	٠.٥			١			١.٥			٢			٢.٥		

٣.٢.٦ Numerical Model Setup in ANSYS Fluent

The numerical analysis was executed using ANSYS-Fluent, a sophisticated CFD software that offers extensive capabilities for simulating multiphase flow and heat transfer. It can be said that the numerical results are accurate and convergent when residuals be equal or less than $١٠^{-٥}$ for the continuity, $١٠^{-٧}$ for the momentum, and $١٠^{-٩}$ for energy. A time step of ٢×١٠^{-٤} s was applied in all numerical tests.

The key settings and models employed in this simulation are shown in Figure (٣.٢).

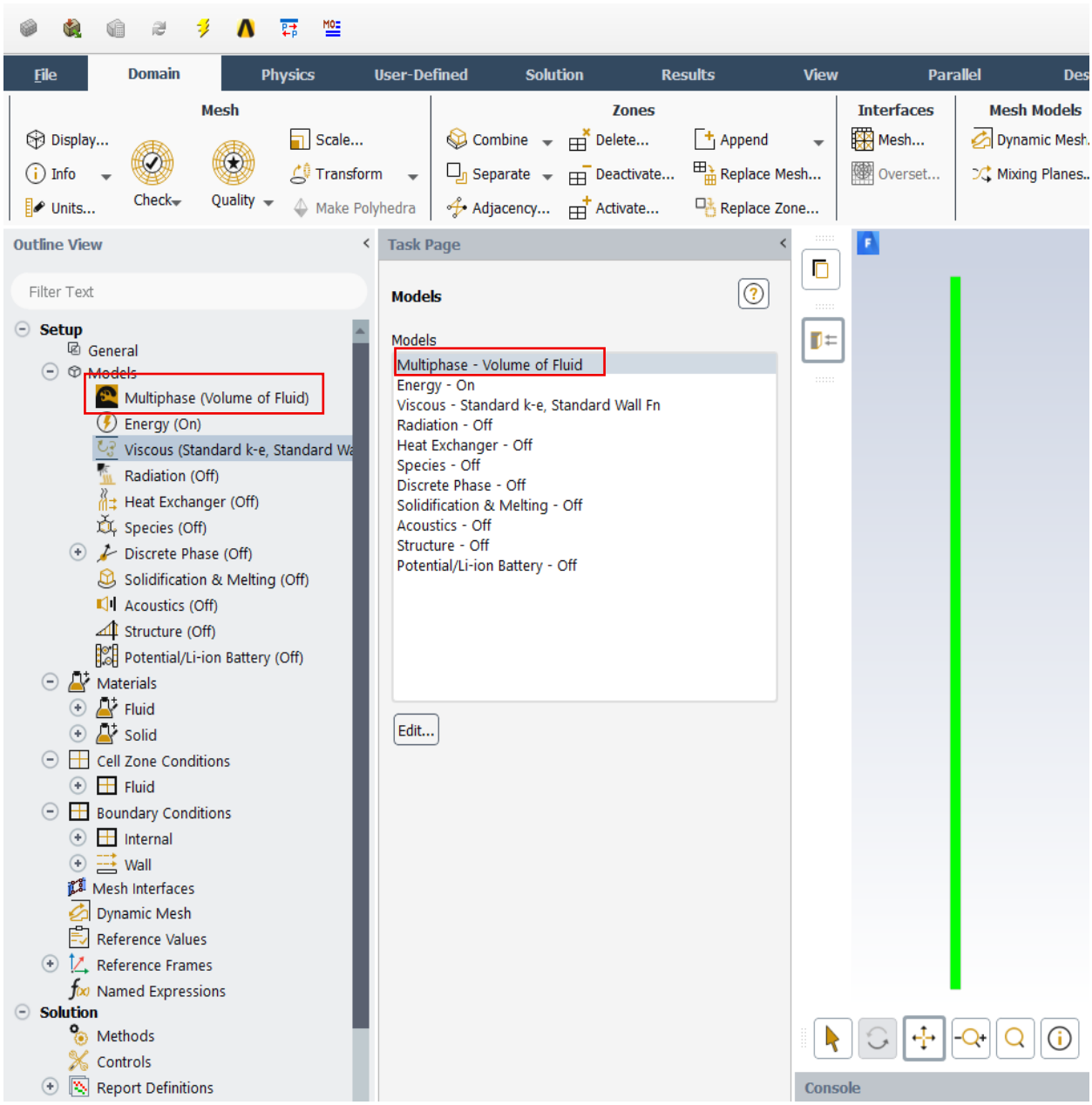

Figure ٣.٢: Volume of Fluid (VOF) Model Setting

- **Multiphase Model:** The Volume of Fluid (VOF) model was utilized to simulate the two-phase flow within the heat pipe. This model is particularly well-suited for tracking the liquid-vapor interface and modeling the complex interactions between the phases. The VOF model allows for the accurate prediction of phase distribution within the heat pipe, which is critical for assessing its performance.
- **Evaporation and Condensation:** The phase change processes (evaporation and condensation) were modeled using the built-in evaporation-condensation model in ANSYS-Fluent. This model calculates the mass transfer between the liquid and vapor phases based on the local temperature and pressure gradients. The accurate modeling of these processes is essential for predicting the thermal behavior of the heat pipe under different operation conditions.
- **Solver Settings:** The simulation was conducted using a pressure-based solver, which was coupled with the SIMPLE (Semi-Implicit Method for Pressure Linked Equations) algorithm for pressure-velocity coupling. These algorithms were chosen for their robustness and efficiency in handling complex flow fields. The second-order upwind scheme was employed for spatial discretization, ensuring the accuracy and stability in the simulation results. This scheme is particularly effective in reducing the numerical diffusion and enhancing the simulation results.

٣.٢.٧ Mesh Independence Test

To ensure the accuracy and reliability of the numerical simulation, a mesh independence test was performed. This test involves generating and testing multiple mesh densities to evaluate their impact on key simulation outputs, such as temperature distribution, heat flux, and fluid velocity within the heat pipe. The goal is to find the best mesh that gives a sufficient accuracy with

minimum computational cost. The final mesh configuration, consists of about ١٦٠١٦٠ nodes and ١٥٠٠٠٠ elements, was selected based on the point at which the further mesh refinement don't lead to important changes in the results. Thus, confirming the mesh-independent behavior.

Figure (٣.٣) illustrates the comparison of simulation outputs at different mesh sizes, showing the convergence trend and justifying the final mesh choice. It's clear that the error in the wall temperature stabilizes as the mesh is refined, demonstrating that the results become independent of mesh size after ~١٥٠,٠٠٠ elements.

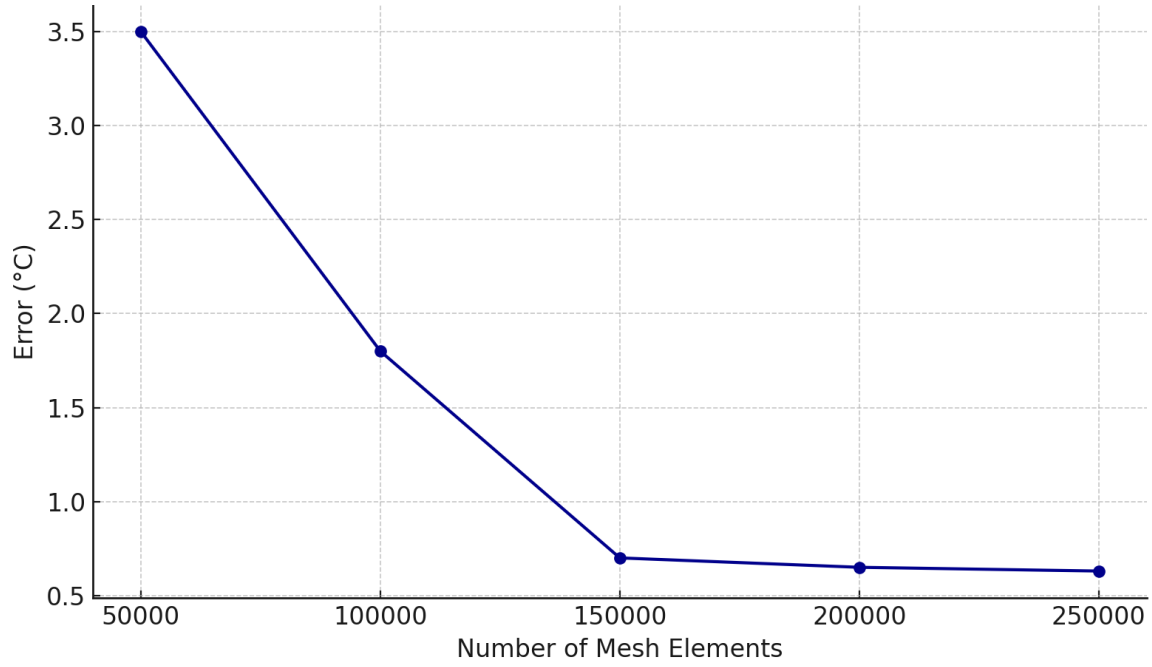

Figure ٣.٣: Simulation Outputs Against Different Mesh Sizes

The verification of grid independence and precise convergence control together enhance the reliability of the CFD results. This provides a solid foundation for analyzing the heat transfer performance of the heat pipe under different operating conditions and filling ratios.

٣.٢.٨ Simulation Scenarios

Figure (٣.٤) presents a comprehensive flowchart of the numerical analysis methodology adopted in this study for simulating of phase-change heat transfer inside the heat pipe. The flowchart systematically outlines the sequential steps required to develop and execute an accurate and reliable CFD model using the Volume of Fluid (VOF) method in ANSYS-Fluent software. The process begins by creating the geometry, where the physical dimensions and structure of the heat pipe including the evaporator, adiabatic, and condenser sections are precisely modeled. This is based on the actual configuration used in the steam power plant. After that, generating the mesh, in which the computational domain is discretized into a finite number of control volumes or elements. A special attention is given to the mesh refinement in critical areas such as the evaporator-condenser interface to ensure the capture of sharp gradients in velocity, temperature, and volume fraction.

Then, the material properties of all fluids and solids involved particularly the working fluid (DOWTHERM™ A), air, and copper are defined. This is in accordance with their thermo-physical properties, including temperature-dependent properties for both liquid and vapor phases. The boundary conditions are then applied to simulate the actual thermal environment of the heat pipe. These conditions include constant heat input at the evaporator, convective cooling at the condenser, and adiabatic conditions along the adiabatic section. The solver setup follows involving the selection of appropriate numerical schemes, time stepping (transient simulation) and phase interaction models (evaporation and condensation). The simulation is then executed, where the flow field and temperature distribution are computed iteratively until convergence is achieved.

Finally, the post-processing stage includes the visualization and analysis of simulation results, such as temperature contours, velocity vectors, phase distribution, and heat transfer performance metrics. These outputs are

essential for understanding of the thermal behavior of the heat pipe under different filling ratios and operating conditions. This well-structured numerical workflow ensures that the complex multiphase flow and phase-change phenomena occurred within the heat pipe are accurately captured and analyzed. This provides valuable insights for the performance of the heat pipe in thermal management applications.

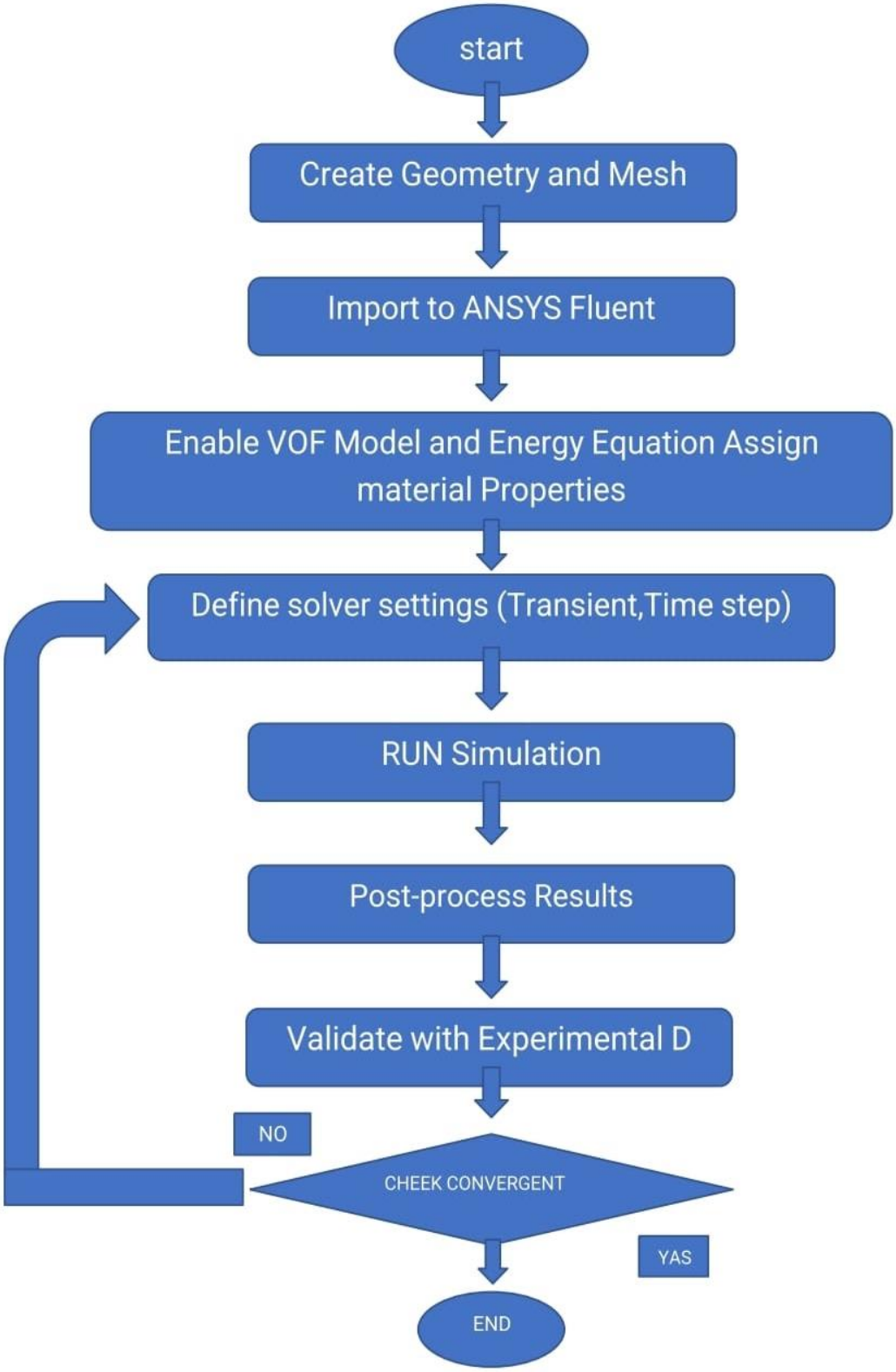

Figure ٣.٤: Flow Chart of Numerical Analysis

٣.٢.٩ Summary

In this chapter, a detailed numerical analysis methodology was presented to simulate the performance of heat pipes under various filling ratios. The simulation was carried out using ANSYS-Fluent by employing the VOF model to capture the complex phase change processes occurred within the heat pipe. The chapter also discussed the governing equations, model geometry, material properties, boundary conditions, and solver settings that are integral to the simulation. A mesh independence study and convergence criteria were established to ensure the reliability of the results. The simulation scenarios analyzed in this chapter provide a basis for understanding the impact of filling ratios on the heat pipe performance, and the results will be discussed in detail in the results chapter.

Chapter Four

Experimental Work

Chapter Four

Experimental Work

This chapter includes the detailed description of the experimental rig (thermosiphon heat pipe heat exchanger) used in this study, measurement devices, and experimental procedure. In addition to the uncertainty analysis of experimental readings and experimental data analysis. The experimental method involves using three filling ratios (٣٥٪, ٥٠٪, and ٧٥٪ of the evaporator size) of a working fluid (DOWTHERM™ A) at different condenser inlet air velocities (٠.٥ to ٢.٥ m/s). Also, the tests were carried out at variable evaporator inlet air temperatures (١٦٠ to ٣٢٠ °C). All experimental tests were carried out at the laboratories of the Mechanic Department, College of Engineering, University of Karbala, Iraq.

٤.١ Experimental Rig

The experimental rig was designed and manufactured locally, then installed at one of laboratories of Mechanical Engineering Department, College of Engineering, University of Karbala. It consists of ٦٠ copper heat pipes with square aluminum fins, air flow ducts, electrical air heater, two air fans, and structural components. The heat pipes were prepared in seven rows; each contains seven or eight tubes. Each heat pipe (١٠٠ cm total length) consists of three sections namely; an evaporation section with a length of ٤٠ cm, adiabatic section with a length of ٢٠ cm, and condensing section with a length of ٤٠ cm.

Figures (٤.١ a and b) respectively shows a schematic diagram and picture of the experimental rig.

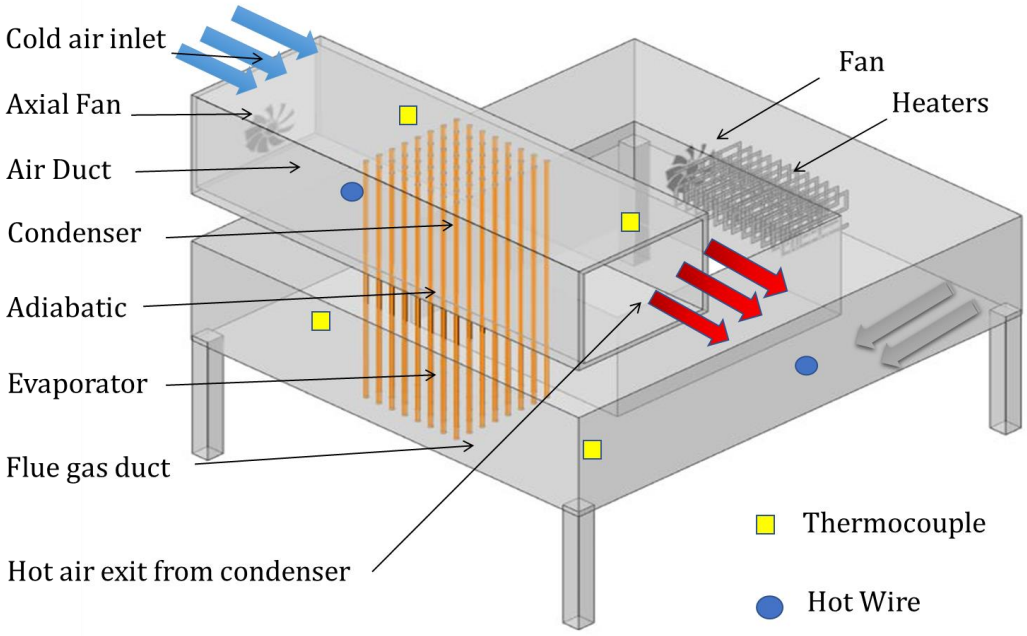

(a)

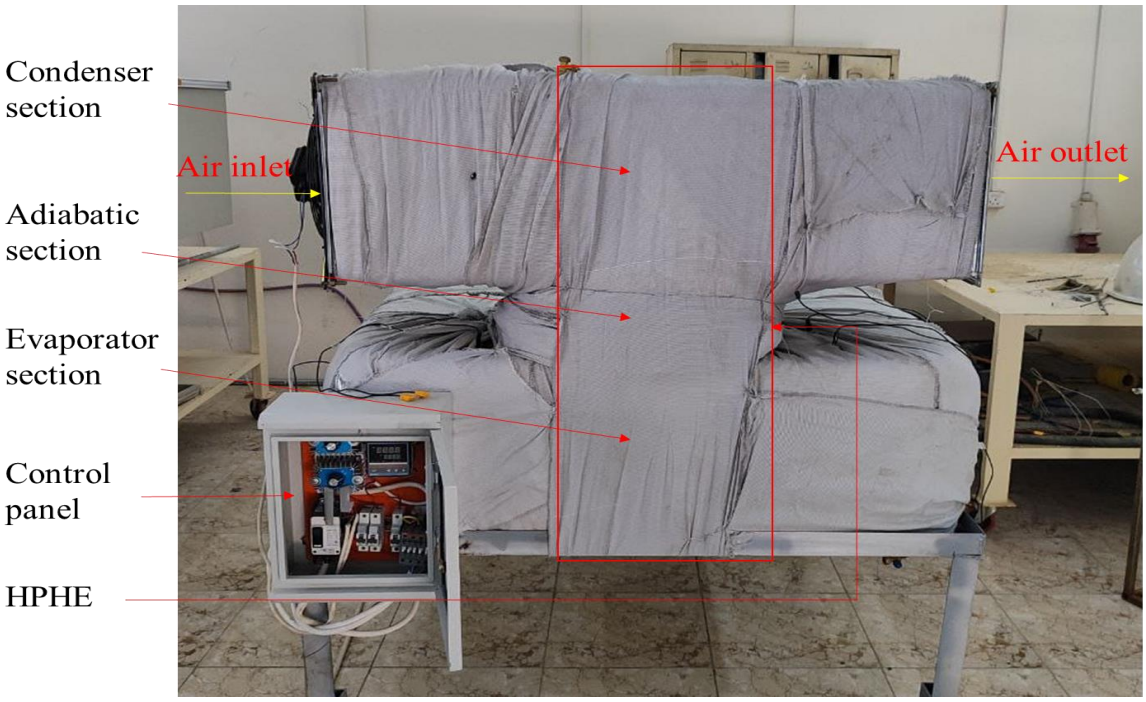

(b)

Figure ٤.١: a: Schematic Diagram of the Experimental Rig and

b: Picture of the Experimental Rig

Materials used in the construction of the rig can withstand high temperatures and work efficiently with the working fluid (DOWTHERM™ A). These materials were selected for their excellent heat transfer properties, heat resistance, and low reactivity with fluids. Additionally, they are durable and corrosion-resistant, ensuring long-lasting platform performance.

Table (٤.١) includes specifications (properties, dimensions, operation temperatures range, and functions) of each component of the rig.

Table ٤.١: Specifications of the Experimental Rig

Component	Dimensions (mm)	Material	K (W/m·K)	Temperatures Range (°C)	Function
Heat pipe	D_{in} =١٥,	Copper	٣٩٠	٢٤ to ٣٢٠	Transfers heat from the evaporator to condenser
	D_{out} =١٦,				
Evaporator	H = ٤٠٠	Copper	٣٩٠	٢٤ to ٣٢٠	Primary location for heat input
Condenser	H = ٤٠٠	Copper	٣٩٠	٢٤ to ٢٥٠	Input air heating
Air heater	Cross section: ٤٠٠×٤٠٠	Tungsten	١٧٤	٠ to ١٠٠٠	Heats up air passed across the evaporator
Thermocouple (K-type)	D = ٣, H =١٠٠٠	Chromel Alumel	٣٠-٣٥	-٢٠٠ to ١٣٧٢	Measures temperatures
Working fluid	Variable (according to the fill ratio)	DOWTHERM ™ A	٠.١٤	١٥ to ٤٠٠	Absorbs and transfers heat within the heat pipe
Insulation material	Thickness = ٥٠	Fiber glass	٠.٠٤	٠ to ١٠٠٠	Minimizes heat loss from heat pipe to surroundings
Fan	Cross section: ٤٠*٤٠	Iron	٨٠.٢	٠ to ١,٥٣٨°C	Circulating airflow
Hot wire	-	Polycarbonate	-	-٢٠ to ٤٥	Measures airflow

Table (٤.٢) shows components of the experimental rig.

Table ٤.٢: Components of the Experimental Rig

Component Number	Component picture
١. Inlet cold air ٢. Outlet hot air ٣. Flue gas duct	 (a)
١. Condenser section ٢. Adiabatic section ٣. Evaporator section ٤. Control board	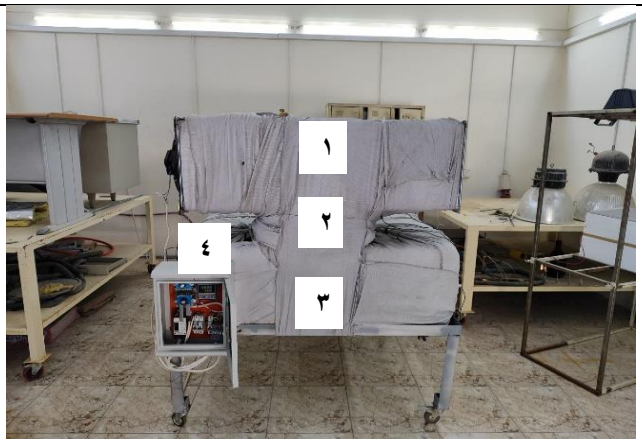 (b)

١. Condenser fan ٢. Evaporator fan	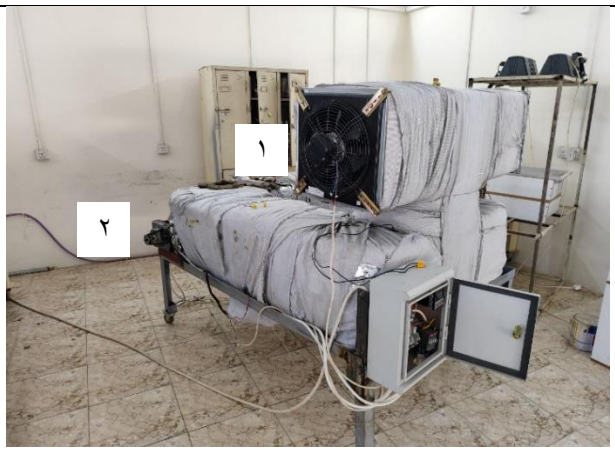 (c)
١. Heater	 (d)
١. Heat pipes and fins	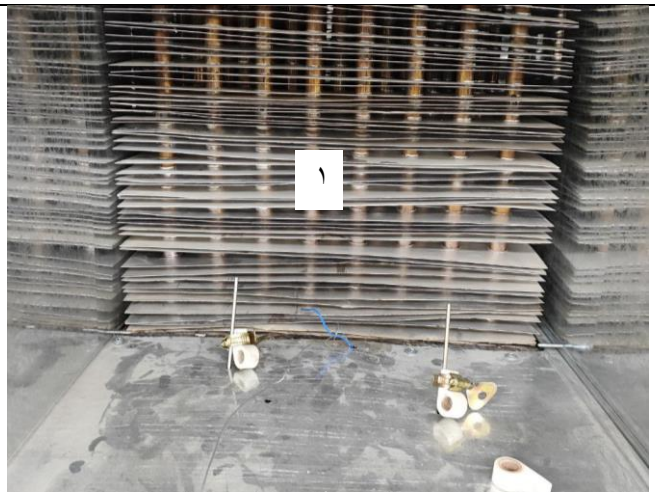 (e)

٤.٢ System Maintenance and Preparation

To ensure the reliability of the devices used in this rig, a systematic maintenance and preparation protocol was implemented. The routine maintenance steps are outlined below:

٤.٢.١ System Inspection

A comprehensive review of all components of the system was conducted to verify compliance with experimental requirements and assess any signs of wear. The first step is to replace the bearing. The P٢٠١ bearing, shown in Figure (٤.٢), is a compact pillow-type bearing unit designed for light-duty applications. It consists of a cast iron or coated aluminum housing and an internal ball bearing (UC٢٠١), allowing smooth shaft rotation. With a bore diameter of ١٢ mm, this bearing is typically used in applications requiring stable compact support. The bearing is mounted with two screws and secured to the shaft with either set screws or an eccentric locking collar. For maintenance, the bearing includes a grease connection, allowing for easy lubrication to ensure long-term performance.

Figure ٤.٢: Fan Shaft Bearing

٤.٢.٢ Air Heater Inspection

Air heaters, which are essential for heat application, should be checked regularly for effectiveness, and any damaged units replaced to ensure even heat distribution. Four ٢٠٠-watt steel air heaters, each ٨ mm in diameter and ١ m long were installed inside the inlet duct of the evaporator section at different temperatures. All heaters are connected directly to the power supply.

٤.٢.٣ Air Fan and Control System

Air fans and control system are inspected for consistent airflow. Necessary repairs or adjustments are made to maintain control over the fan speed and the system airflow. The ILKA VIK-٣٠A٤S industrial blower fan is a powerful and durable fan designed for industrial and commercial use. It has a motor power of ١١٠ W. The fan has a maximum speed of ١٣٧٠ rpm, air capacity of ٢٠٠٠ m^3/h, and frame size of ٤٠ × ٤٠ cm. Figures (٤.٣a and b) respectively show the control system of the experimental rig and air fan.

(a) **(b)**

Figure ٤.٣: a: Control System of the Experimental Rig and b: Air Fan

٤.٢.٤ Heat Pipe Heat Exchanger Preparation

Modifications were made to improve control of fluid levels within the heat pipe, allowing for precise adjustment based on the required filling ratio. A precisely measured hole was drilled in the heat pipe to facilitate installation of the discharge valve. The location was carefully determined, and a suitable drill bit was used to ensure that the hole in the correct size for secure and proper installation, thus preventing damage to the pipe. After that, the pipe was prepared for brazing, as shown in Figure (٤.٤a). A vacuum valve was then installed and tightly welded to the heat pipe to ensure efficient operation. In the welding process, a brazing technique was used to create a durable and leak-proof joint. The pipe ends were first cleaned, flux was applied, and the joint was evenly heated with a torch. Once the proper temperature was reached, the solder was applied, forming a solid and reliable bond. After cooling, any remaining flux was removed, see Figure (٤.٤b).

(a) **(b)**

Figure ٤.٤: a: Perforating the Heat Pipe to Install the Vacuum Valve and b: Vacuum Valve Welding

٤.٢.٥ Leakage Inspection

All connections and valves are thoroughly inspected for any potential leaks to ensure system integrity. This inspection is important to identify any weak points or leakages that may affect the performance and safety of the system. To verify system integrity, the heat pipe is charged with compressed air at ٢٧٥ psi to detect any leakages, see Figure (٤.٥). By ensuring all connections are tightly sealed, the system maintains its efficiency and reliability, preventing fluid loss that may affect the accuracy of experimental results. This meticulous approach ensures stable system operation and the continuity of the experiment throughout its duration.

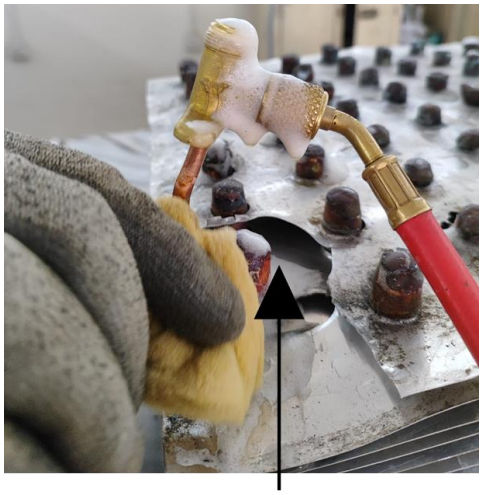

Figure ٤.٥: Leakage Inspection

٤.٢.٦ Insulation Check

The thermal insulator (Figure (٤.٦)) on the outer surface of the adiabatic section and structural components was inspected to prevent any heat loss. It is entirely made of fiberglass wool (with ٥ cm thickness and thermal conductivity coefficient of ٠.٠٣٤ W/m °C) [٥٨].

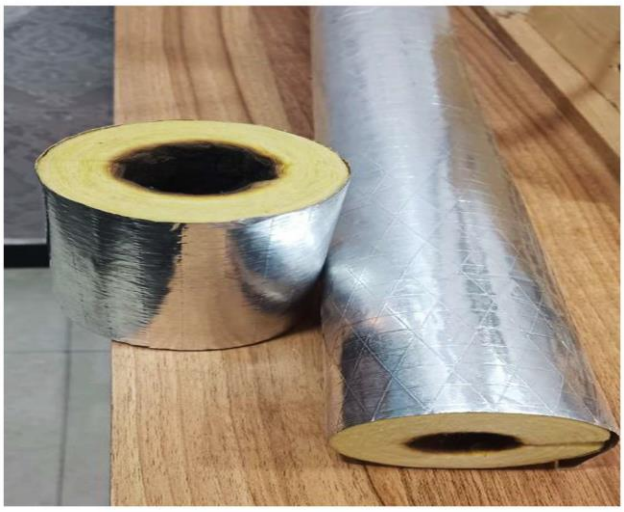

Figure ٤.٦: Thermal Insulator (Fiberglass Wool)

٤.٢.٧ Electrical System and Wiring Inspection

All electrical connections were inspected for wear, proper grounding, and safety compliance. Worn-out wiring was replaced to prevent potential hazards.

٤.٢.٨ Cleaning Deposits

Pipes and heat exchangers were cleaned regularly to prevent sediment build-up, which could impede fluid flow or reduce thermal performance.

٤.٢.٩ Ventilation System Check

Ventilation and exhaust systems were maintained to ensure airflow around heat-sensitive components and to support safe lab conditions. Control and data logging software were updated to ensure compatibility with the latest sensors and accuracy of data output.

٤.٢.١٠ Working Fluid

The working or heat transfer fluid used in this study is DOWTHERM™ A which was obtained from certified suppliers in China. It was selected for this study because it has several important characteristics that make it ideal for use in

heat pipe systems. It has a high thermal conductivity and low viscosity which allow for efficient heat transfer and quick response to changes of temperature. The fluid also has a wide useful temperature range, typically between ١٥ °C to ٤٠٠ °C as mentioned in Table (٤.١), allowing it to function effectively in various environmental conditions and operating temperatures. This wide range of operational temperatures ensures that the fluid remains efficient in a variety of thermal management applications, making it suitable for both high and low temperature environments. DOWTHERM™ A fluid also has well-defined physical properties, such as the density which is approximately ١.٠٦ Kg/m³ at ٢٥ °C [٥٨]. This property helps to ensure a stable flow within the heat pipe system, optimizing heat transfer across different parts of the system. Additionally, its freezing point is typically below ١٢ °C, allowing it to remain in the liquid state under low-temperature conditions, while its boiling point is around ١٥٠ °C, providing a high tolerance for elevated temperatures without vaporizing prematurely. This wide operational range ensures that the fluid can withstand varying temperature extremes without compromising the integrity of the heat pipe system. The detailed specifications of the DOWTHERM™ A fluid, including its chemical composition, thermal properties, density, freezing point, boiling point, and useful temperature range are provided in Appendix (A). In addition to the certification documents that confirm the fluid purity, quality, and compliance with industry standards, verifying that it meets all necessary criteria for high performance applications.

Figure (٤.٧) shows DOWTHERM™ A and its filling method inside the heat pipe.

Figure ٤.٧: DOWTHERM™ A and Its Filling Method

٤.٣ Measurement Devices

٤.٣.١ Thermocouples

The measurement device used to measure temperature is thermocouple of K type shown in Figure (٤.٨). In this study, eight thermocouples were used in different locations of the rig. To ensure accurate data, thermocouples were calibrated regularly as would be shown later (page (٧٢)).

Figure ٤.٨: Thermocouple Device

٤.٣.٢ Data Logger

The device used to record and show readings of temperature in this work is the data logger (BTM-٤٢٠٨SD model, Type of ١٢ CH and ٠-١٣٧٠ °C temperatures range) shown in Figure (٤.٩). The calibration of this device would be shown later (page (٧٢)). The calibration certificate is shown in Appendix (B).

Figure ٤.٩: Data Logger

٤.٣.٣ Hot Wire Anemometer

The hot wire anemometer (shown in Figure (٤.١٠)) was used to measure the airspeed at the condenser section inlet and evaporator inlet.

Figure ٤.١٠: Hot Wire Anemometer

٤.٣.٤ Vacuum Pump and Pressure Gage

To evacuate the heat pipe from air, the vacuum pump (VE٢١٠٠N) shown in Figure (٤.١١a) was used. For measuring the pressure inside the heat pipe, the pressure gage (with a range of temperatures of -٣٠ to ٥٠٠ psi (-١ to ٣٥ bar)) was used as showing in Figure (٤.١١b).

(a) **(b)**

Figure ٤.١١: a: Typical Vacuum Pump (VE٢١٠٠N) and

b: Pressure Gage

٤.٤ Measurement Points Locations

Locations of measurement points (mps) of the temperature and air velocity are shown in Figure (٤.١٢) and Table (٤.٣). Table (٤.٤) summaries the variables required to be measured.

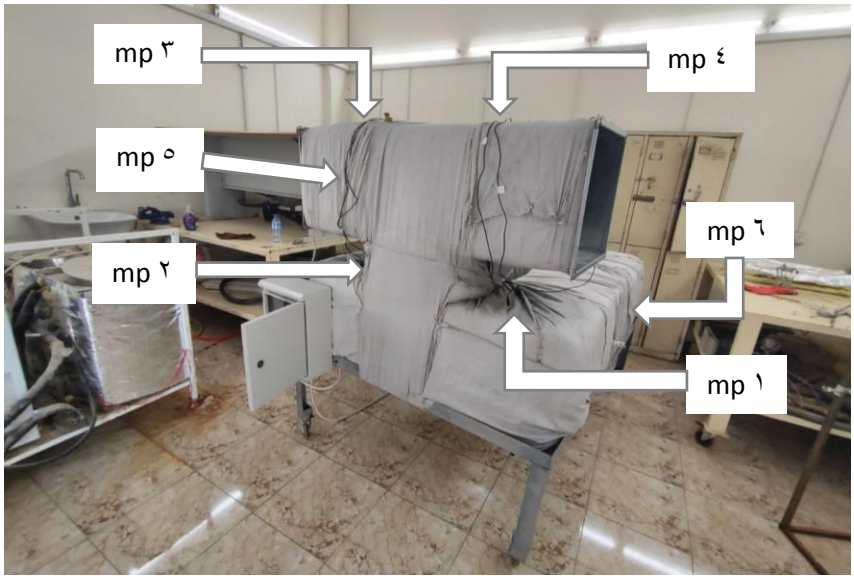

Figure ٤.١٢: Temperature and Air Velocity Measurement Points Locations

Table ٤.٣: Temperature and Air Velocity Measurement Points Locations

Measurement Point	Location	Measured Variable	Instrumentation Used
mp١	Inlet of evaporator	Temperature	K-Type Thermocouple
mp٢	Outlet of evaporator	Temperature	K-Type Thermocouple
mp٣	Inlet of condenser	Temperature	K-Type Thermocouple
mp٤	Outlet of condenser	Temperature	K-Type Thermocouple
mp٥	Inlet of condenser	Air velocity	Hot Wire Anemometer
mp٦	Inlet of evaporator	Air velocity	Hot Wire Anemometer
mp٧	Heater surface	Surface temperature	K-Type Thermocouple

Table ٤.٤: Measured Variables Summary

Variable	Units	Description	Notes
Inlet Temperature	°C	Air temperature at the evaporator inlet	Measured at MP١
Outlet Temperature	°C	Air temperature at the evaporator outlet	Measured at MP٢
Air Velocity	m/s	Air velocity at the evaporator inlet	Measured at MP٣
Heater surface temperature	°C	Surface temperature of the heating element	Measured at MP٧

٤.٥ Calibration of Measuring Devices

To obtain the required accuracy of experimental readings, the data logger, thermocouple, and hot-wire anemometer were calibrated.

٤.٥.١ Data Logger Calibration

The data logger was sent to a calibration and standardization center in Baghdad city (central organization standardization and Quality Calibration) for the purpose of the calibration. Results of the calibration are shown in the certificate presented in Appendix (B).

٤.٥.٢ Thermocouple Calibration

The steps of the thermocouple calibration are as follows: -

١. Check at Zero (Ice Point):

- ❖ Prepare an ice bath (water + crushed ice in an insulated container).
- ❖ Place the thermocouple in the container of the water and ice.
- ❖ Wait until the reading stabilizes.

- ❖ Compare the reading to ٠ °C, if there is a difference, record it.

٢. Check at ١٠٠ °C (Boiling Point):

- ❖ Heat up pure water to the boiling Point (١٠٠ °C).
- ❖ Then place the thermocouple in the boiling water and wait.
- ❖ Compare the reading with ١٠٠ °C, if there is a difference, record it.

٤.٥.٣ Hot-Wire Anemometer Calibration

The Hot-Wire Anemometer depends on the principle of thermal cooling of a thin wire as it passes through an air stream. Therefore, it requires a calibration to correlate the electrical signal with the actual air speed.

The calibration steps are as following: -

١. Setting up a stable testing environment:

Use a duct provided with a fan contains a speed regulator. The goal is to ensure the airflow is stable and of known speed.

٢. Reference device:

Set up a UNI-T Anemometer (shown in Figure (٤.١٣)) as the reference speed device.

This device is calibrated by the company and provides direct air speed.

٣. Install the sensors:

Place the hot wire sensor next to the UNI-T at the same point in the air stream. They should be a very small distance apart (in order to both of them at the same air velocity).

٤. Take readings:

Start the fan at a low speed first. Then, record the hot wire signal along with the UNI-T reading (m/s).

Repeat the process for several different speeds (at least ٥–١٠ points across the operating range). If there is a deviation, record it.

Figure ٤.١٣: Reference Device (UNI-T Anemometer)

٤.٦ Experimental Procedure

In this study, three filling ratios (٣٥٪, ٥٠٪, and ٧٥٪ of the evaporator size) of the working fluid are applied at five condenser inlet air velocities (٠.٥, ١, ١.٥, ٢ and ٢.٥ m/s). This means that there are fifteen experimental test cases due to multiplying three cases of the filling ratio by five cases of the condenser inlet air velocity. At the beginning of tests and to achieve a vacuum pressure of ٣٠ psi, the air presented inside heat pipes is entirely exited by using the vacuum pump. This step is very important because the air acts as a thermal resistance delaying the evaporation process of the working fluid and thus will reduce the system efficiency. So that eliminating it from heat pipes, makes the system operates more effectively.

The following points represent the experimental steps of this study:

١. After eliminating the air from heat pipes, they are charged with the working fluid (DOWTHERM™ A) at the required filling ratio (٣٥٪ as a first test case).
٢. The air fan installed on the condenser side is operated and set at the required speed (which it gives ٠.٥ m/s air velocity at the condenser inlet).
٣. Air heaters (total power of ٨٠٠٠ W) and fan installed on the evaporator side are operated with waiting until the evaporator inlet air temperature reaches ١٦٠ °C,
٤. The condenser outlet air temperature is measured and recorded for each ١٠ minutes until achieving the maximum value of the evaporator inlet air temperature (٣٢٠ C) and this takes about ١٠٠ minutes,
٥. Turn off all devices with waiting until the system becomes at the room temperature,
٦. Steps (٢, ٣ and ٤) are repeated with increasing the air fan speed (on condition that gives ١ m/s air velocity at the condenser inlet as a second test case) for step (٢),
٧. Step (٦) is repeated for three times with changing the air fan speed in each time (on condition that gives the condenser inlet air velocity of ١.٥ m/s as a third test case, ٢ m/s as a fourth test case and ٢.٥ m/s as a fifth test case),
٨. All steps in above are repeated for two times with changing the filling ratio to ٥٠٪ in the first time and ٧٥٪ in the second time,

Figure (٤.١٤) shows recording experimental data.

Figure ٤.١٤: Recording Experimental Data

٤.٧ Uncertainty Analysis

Analyzing the uncertainty or error percentage in experimental studies is important and necessary to ensure the reliability of experimental data. Many factors, such as the imprecise calibration, nature of the test environment (static vs. dynamic), measurement method, etc. may contribute to create an uncertainty in experimental results. The total uncertainty is the sum of errors associated with each variable under the test. In overall, uncertainties (that may be occurred in any experimental study) can be classified to two types of errors namely: systematic uncertainties (U_s) and random uncertainties (U_r). Therefore, the total uncertainty (U_t) can be represented by the following equation [٦٧]: -

$$U_t = \pm\sqrt[٢]{U_s^٢ + U_r^٢} \quad \ldots (٤.١)$$

Usually, random uncertainties are very little compared to systematic uncertainties. Therefore, it can be said that the total uncertainty is about equal to systematic uncertainties as follows: -

$$U_t \approx \sqrt{\Sigma U_s^٢} \quad \ldots (٤.٢)$$

Some systematic uncertainties are found in the information given by the manufacturer and the other some can be found through tests of calibration. In this study, there are four systematic uncertainties namely: the pressure gage uncertainty that equals ±٢٪, hot wire uncertainty that equals ±٣٪, data logger uncertainty that equals ±٠.٧٪, and thermocouple uncertainty that equals ±١.٥٪. All these uncertainties are given by the manufacturer except the thermocouple and data logger are found by the calibration. Then the total uncertainty by using Eq. (٤.٢) will be [٦٧].

$$U_t \approx \sqrt{[(\pm ٠.٠٢)^٢ + (\pm ٠.٠٣)^٢] + (\pm ٠.٠٠٧)^٢ + (\pm ٠.٠١٥)^٢} \approx ٠.٠٤ = ٤٪$$

٤.٨ Experimental Data Analysis

To analyze effect of some important factors, such as the filling ratio of a working fluid, heat supplied (Q) and others on the thermal performance of heat pipe, the heat resistance (R_h) of this pipe can be used. It (R_h) can be determined by using the next equation [٦٨]: -

$$R_h = \frac{T_{Evap.\ avg.} - T_{Con.\ avg.}}{Q} \quad \ldots (٤.٣)$$

Where: - $T_{Evap.\ avg.}$ and $T_{Con.\ avg.}$ are the average temperatures of the evaporator and condenser respectively that can be determined as follows : -

$$T_{Evap.\ avg.} = \frac{T١ + T٢ + T٣}{٣} \quad \ldots (٤.٤)$$

$$T_{Con.\ avg.} = \frac{T٥ + T٦ + T٧}{٣} \quad \ldots (٤.٥)$$

In the evaporator section, the heat supplied (Q) can be found using the next equation [٦٨].

$$Q = V \times I \times \theta \quad \ldots (٤.٦)$$

Where: - Q is electrical power (W) and θ is the heat efficiency correction factor and equals ٠.٨٠.

The cooling capacity ($Q_{Con.}$) can be determined by the next equation [٦٨].

$$Q_{Con.} = \dot{m}_c \, Cp_c (T_{Con.\ out} - T_{Con.\ in}) \quad \ldots (٤.٧)$$

Chapter Five

Results and

Discussion

Chapter Five

Results and Discussion

In this chapter, the numerical and experimental results of the condenser outlet air temperature are presented, discussed and compared. In addition to the results of the temperature of the heat pipe surface and heat pipe effectiveness. This is done at three filling ratios of the working fluid, five condenser inlet air velocities, and wide range of the evaporator inlet air temperatures (١٦٠ to ٣٢٠ °C). While, the evaporator inlet air velocity, condenser inlet air temperature, and heat supplied are constants of ١ m/s, ٢٤ °C and ٨٠٠٠ W respectively.

٥.١ Numerical Results

٥.١.١ Effect of Air Velocity

٥.١.١.١ Condenser Outlet Air Temperature

Figure (٥.١) displays the numerical results of the condenser outlet air temperature ($T_{Con.\ out}$) at a filling ratio of ٥٠٪ and five different condenser inlet air velocities (٠.٥, ١, ١.٥, ٢ and ٢.٥ m/s). This is from beginning to end of the simulation and which takes ١٠٠ minutes. The simulation was done at constant evaporator inlet air velocity. As shown in this Figure, the outlet air temperature increases with the progress in the evaporation process of the working fluid due to the heat exchanging process between the working fluid and air. At the same time, it can be seen the effect of the air velocity on its temperature which decreases as the air velocity is increased. This is because when the air velocity is increased, the time duration of the air contact with the heat pipe surface will decrease leading to decreasing of the quantity of thermal energy absorbed by the air and thus decreasing its temperature. In addition to increasing the mass air flow rate ($\dot{m}$) due to increasing of its velocity and this means that the air quantity passed across the

heat pipe will be larger. Therefore, heat will be distributed on more air molecules leading to decreasing its temperature. In overall, the $T_{Con.\ out}$, at the velocity of ٠.٥ m/s, increased from ٢٥ to ٢٤٠ °C through ١٠٠ minutes while, at ٢.٥ m/s it increased from ٢٥ to ١١٢ °C during the same time. In other words, the increase in the $T_{Con.\ out}$ for the case of ٠.٥ m/s is greater by two times than its increase in the case of ٢.٥ m/s and this large difference indicates that the air velocity has a large effect on the $T_{Con.\ out}$.

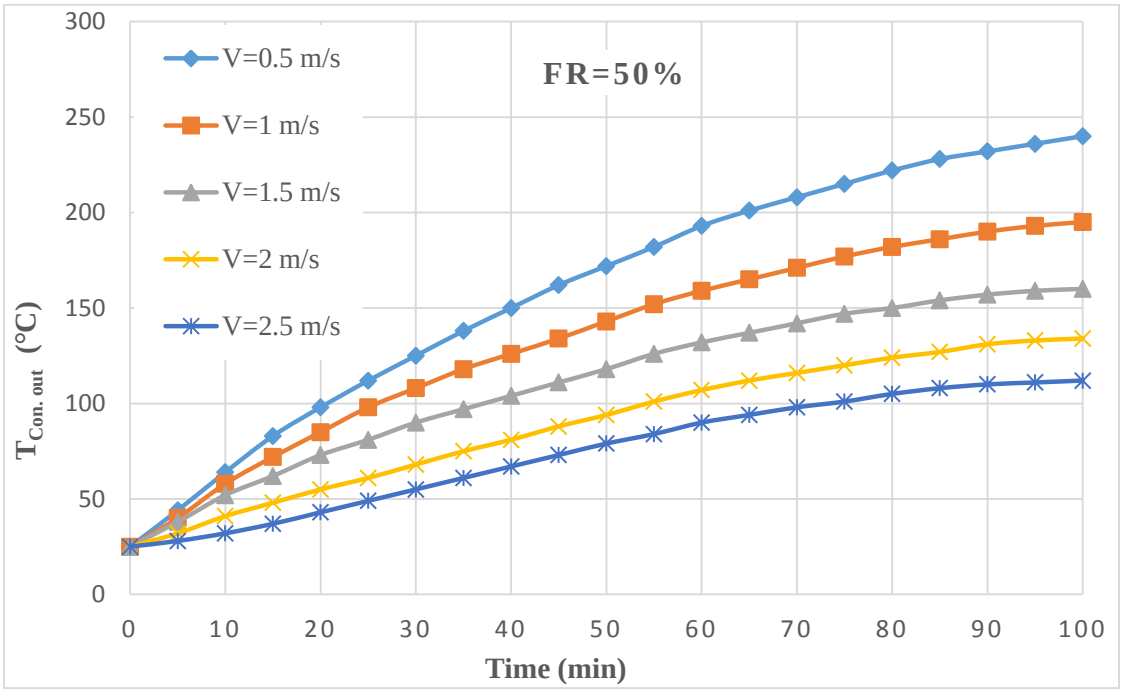

Figure ٥.١: Condenser Outlet Air Temperature with the Time at Different Air Velocities

٥.١.١.٢ Temperature Contours of Heat Pipe Surface

The results of temperature contours of the heat pipe surface at a filling ratio of ٥٠٪ and five condenser inlet air velocities (٠.٥, ١, ١.٥, ٢, and ٢.٥) m/s are shown in Figure (٥.٢). This is to show the influence of the air velocity on the thermal performance of the heat pipe. It is shown, through this Figure, that increasing of the condenser inlet air velocity leads to large reduction in the temperature of the heat pipe surface. This means that the heat pipe performance

greatly affected by the velocity of air passed through it. The explanation for this is that increasing the air flow (because of the increase of its velocity) across the heat pipe leads to absorbing larger heat. This is due to the heat exchanging between the working fluid and air which increases with increasing the air velocity.

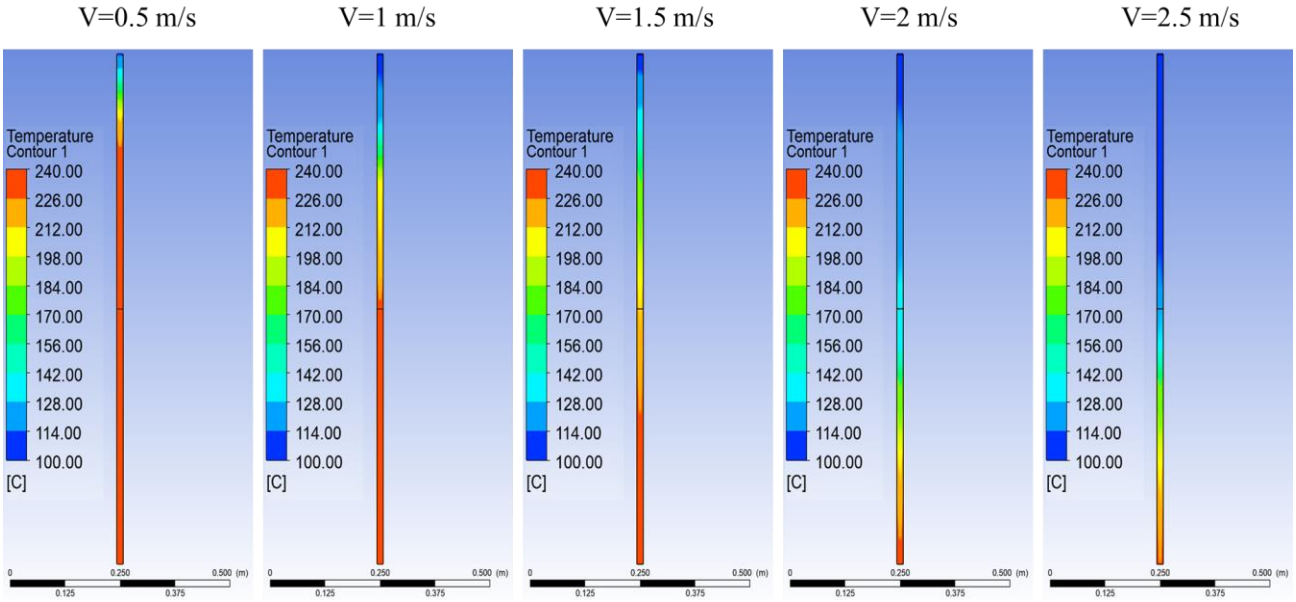

Figure ٥.٢: Temperature Contours of the Heat Pipe Surface at Different Air Velocities and Filling Ratio of ٥٠٪

٥.١.١.٣ Numerical Effectiveness of Heat Pipe Heat Exchanger

Figure (٥.٣) shows the numerical results of the thermal effectiveness of the heat pipe at a filling ratio of ٥٠٪ and five different air velocities (٠.٥, ١, ١.٥, ٢, and ٢.٥) m/s. The effect of the air velocity on the heat pipe effectiveness is significant in this Figure where the effectiveness decreased by about ٥٨% (from ٧٣٪ to ٣١٪) with increasing the air velocity from ٠.٥ to ٢.٥ m/s. This is because increasing the air velocity leads to decreasing its temperature as mention in Section (٥.١.١.١). This backs to the same reasons mentioned previously (increasing the air velocity leads to decreasing the time duration of the air contact with the heat pipe and distributing heat on more air molecules decreasing its temperature). Therefore,

decreasing the effectiveness of the heat pipe because of the direct relationship between it and air temperature according to Eq. (٣.٩).

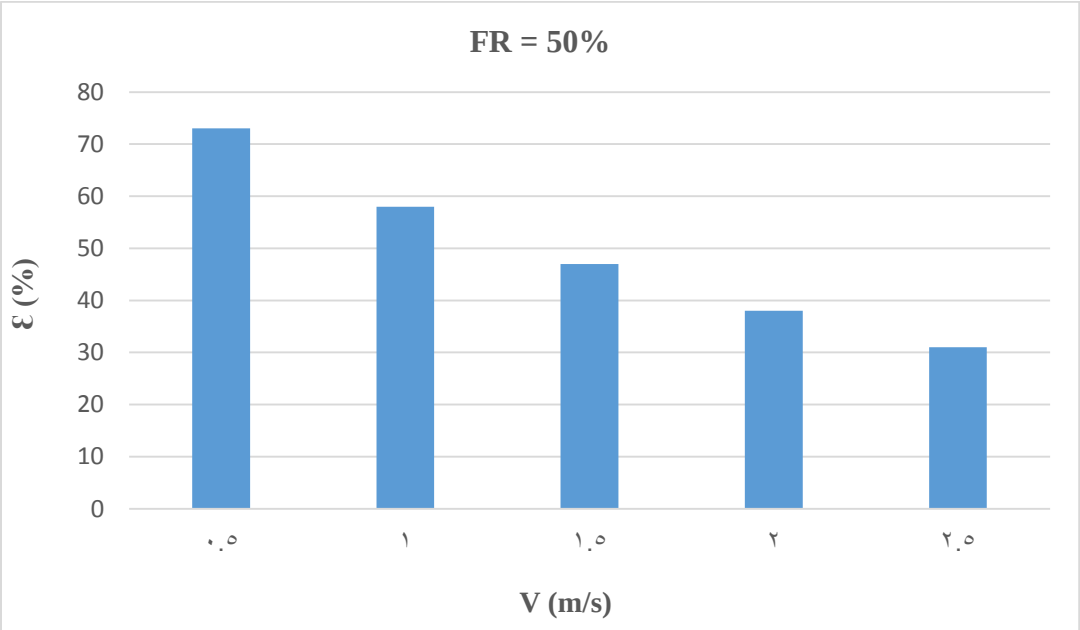

Figure ٥.٣: Numerical Effectiveness of the HPHE at Different Air Velocities

٥.١.٢ Effect of Filling Ratio of Working Fluid

٥.١.٢.١ Condenser Outlet Air Temperature

Figure (٥.٤) displays the numerical results of the condenser outlet air temperature ($T_{Con.\ out}$) at three condenser inlet air velocities of ٠.٥, ١.٥, and ٢.٥ m/s. The simulation was done at different filling ratios (٣٥٪, ٥٠٪, and ٧٥٪ of the evaporator size) of the working fluid and constant evaporator inlet air velocity. This is to show the effect of the filling ratio on the $T_{Con.\ out}$. The results indicate that the $T_{Con.\ out}$ is greatly affected by the filling ratio where its highest value (٢٤٠ °C) is obtained at ٥٠٪ filling ratio. While, the lowest value of the $T_{Con.\ out}$ (١٦٢ °C) is gotten at ٧٥٪ filling ratio (the difference between the two cases is very large (٧٨ °C)). The air velocity in both cases is same (٠.٥ m/s). This means that the optimum

filling ratio of the working fluid inside the heat pipe in this study is ٥٠٪ where the working fluid (DOWTHERM™ A) at this ratio works perfectly.

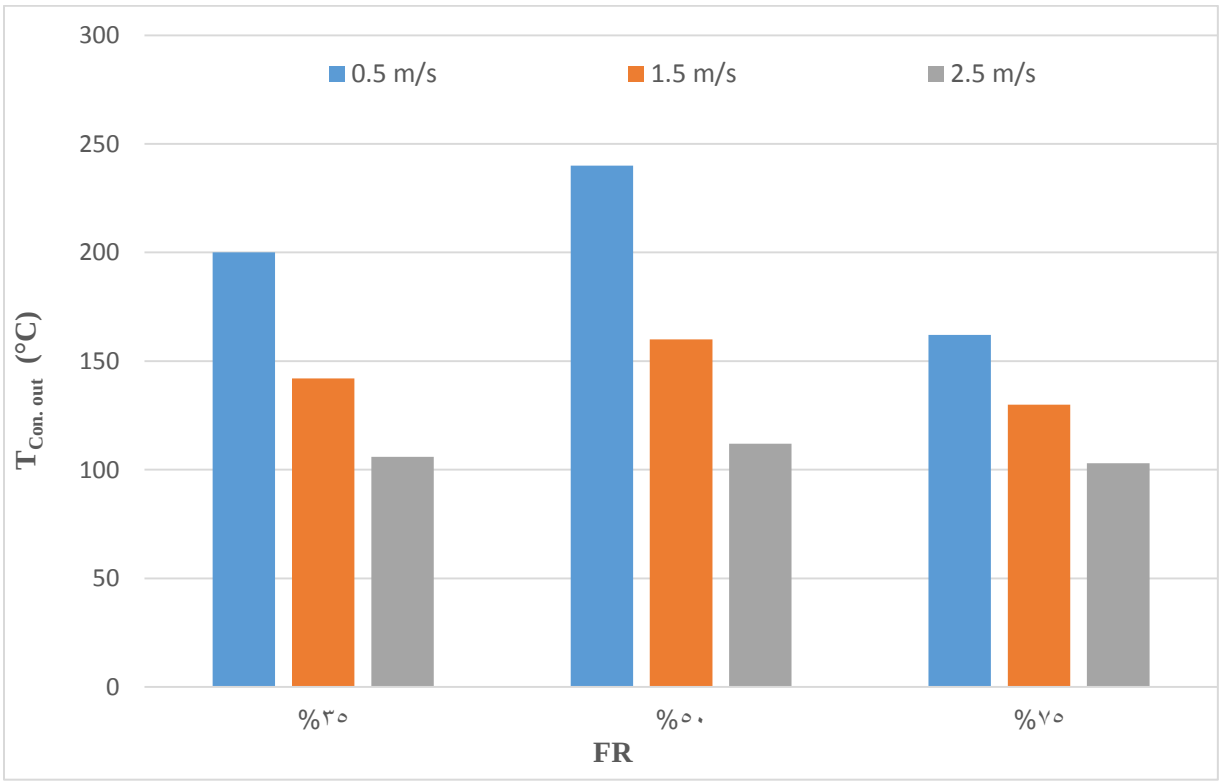

Figure ٥.٤: Numerical Condenser Outlet Air Temperature Versus the Filling Ratio at Different Air Velocities

٥.١.٢.٢ Temperature Contours of Heat Pipe Surface

The results of contours of the temperature of the heat pipe surface at condenser inlet air velocities of ٠.٥, ١, ١.٥, ٢, and ٢.٥ m/s are respectively shown in Figures (٥.٥a, b, c, d, and e). This is to show the effect of the filling ratio on the thermal performance of the heat pipe system where the simulation was carried out at different filling ratios (٣٥٪, ٥٠٪, and ٧٥٪) of the evaporator size. As seen in these Figures, the best filling ratio is ٥٠٪ where at this ratio and at ٠.٥ m/s air velocity (Figure (٥.٥a)), the heat pipe has the largest red (highest temperature) area compared to the filling ratios of ٣٥٪ and ٧٥٪. This is because of using a filling ratio greater than ٥٠٪ leads to greater thermal resistance and higher pressure of the

working fluid. On the other side, using the working fluid with a filling ratio less than ٥٠٪ will lead to drying of the evaporation zone inside the heat pipe and thus a thermal failure of the working fluid.

FR=35% FR=50% FR=75%

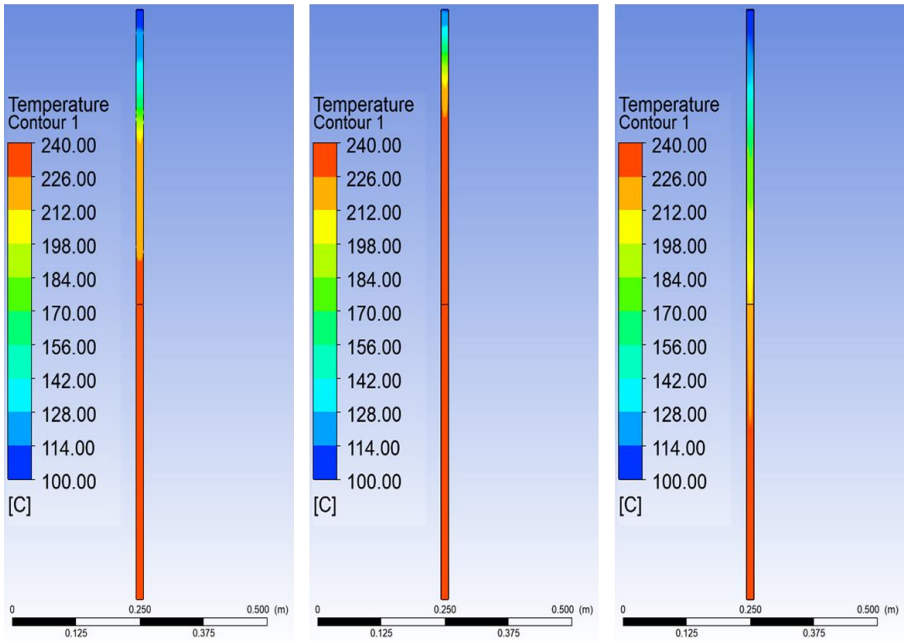

(a)

FR=35% FR=50% FR=75%

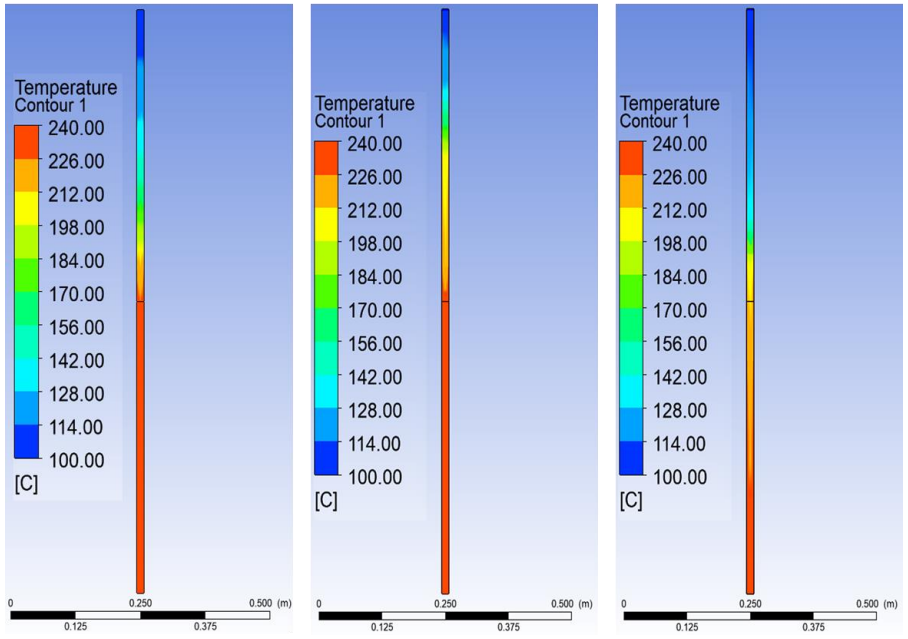

(b)

FR=35% FR=50% FR=75%

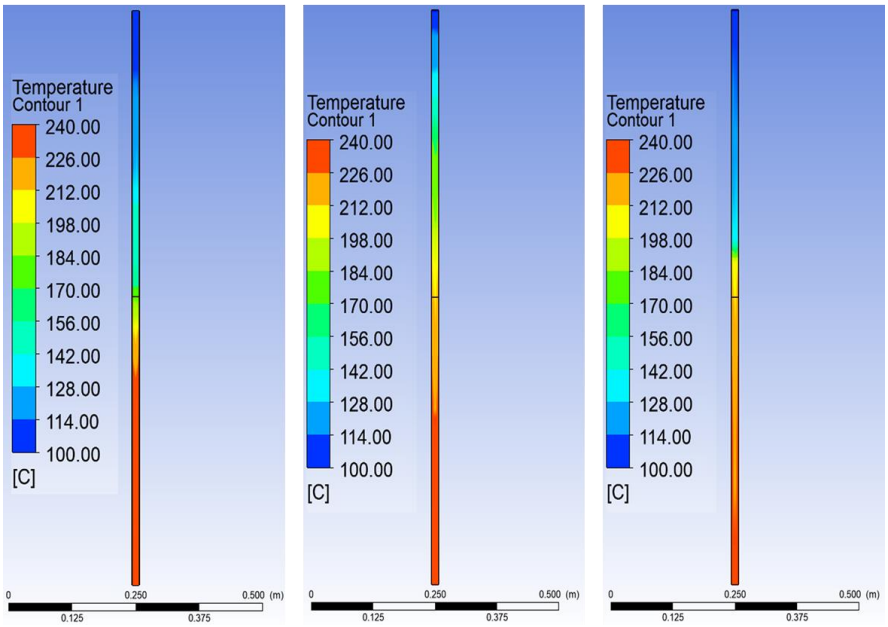

(c)

FR=35% FR=50% FR=75%

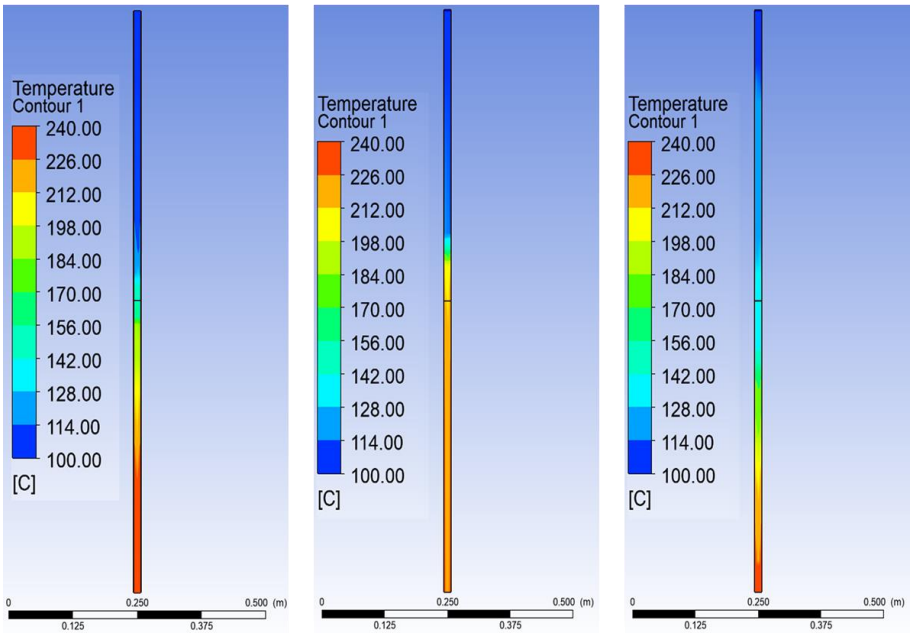

(d)

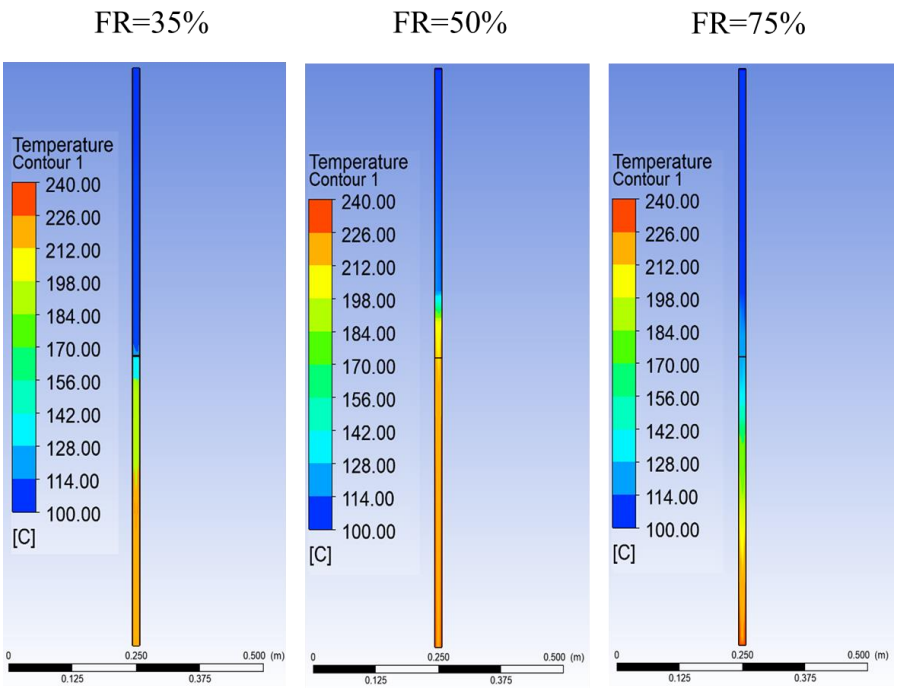

(e)

Figure ٥.٥: Temperature Contours of the Heat Pipe Surface Against the Filling Ratio at Different Air Velocities (a): ٠.٥ m/s, (b): ١ m/s, (c): ١.٥ m/s, (d): ٢ m/s and (e): ٢.٥ m/s

٥.١.٢.٣ Numerical Effectiveness of Heat Pipe Heat Exchanger

To show the influence of the filling ratio of the working liquid on the effectiveness of the heat pipe, three different filling ratios (٣٥٪, ٥٠٪ and ٧٥٪) were used in this study. Figure (٥.٦) demonstrates the numerical results of the effectiveness of the heat pipe at three condenser inlet air velocities of ٠.٥, ١.٥, and ٢.٥ m/s. As shown in this Figure, the best filling ratio of the working fluid is ٥٠٪. Where at this ratio with air velocity of ٠.٥ m/s, the highest effectiveness of the heat pipe (٧٣٪) is achieved. Whereas, using the working liquid with ٧٥٪ filling ratio and the same air velocity (٠.٥ m/s) gives the lowest value (٤٧٪) of the effectiveness of the heat pipe. This because using the working fluid with a filling ratio greater or less than ٥٠٪ does not make it works correctly and therefore a thermal failure of the heat pipe).

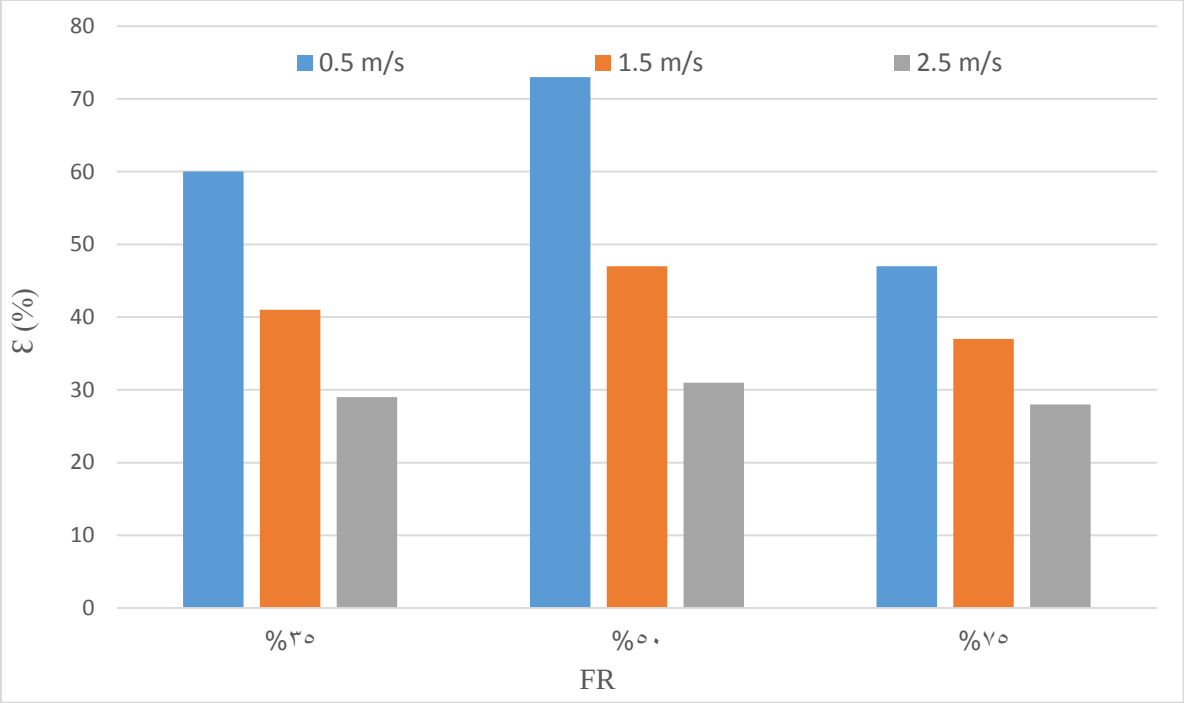

Figure ٥.٦: Numerical Effectiveness of the HPHE Against the Filling Ratio at Different Air Velocities

٥.٢ Experimental Results

٥.٢.١ Influence of Air Velocity

٥.٢.١.١ Condenser Outlet Air Temperature

Figure (٥.٧) shows the experimental results of the condenser outlet air temperature ($T_{Con.\ out}$) from beginning to end of the experiment, which takes ١٠٠ minutes at the filling ratio of ٥٠%. This is at five different velocities of air (٠.٥, ١, ١.٥, ٢ and ٢.٥) m/s at the condenser inlet and constant evaporator inlet air velocity. As shown in this Figure, with the progress in the evaporation process of the working fluid, the air temperature increases due to the heat exchanging process between the working fluid and air. At the same time, increasing the air velocity leads to decreasing its temperature. This retains to the same causes previously mentioned in the numerical aspect (Section (٥.١.١.١)). In general, the $T_{Con.\ out}$, at the

velocity of ٠.٥ m/s, increased from ٢٥ to ٢٥٠ °C through ١٠٠ minutes while, at ٢.٥ m/s it increased from ٢٥ to ١٢٤ °C during the same time.

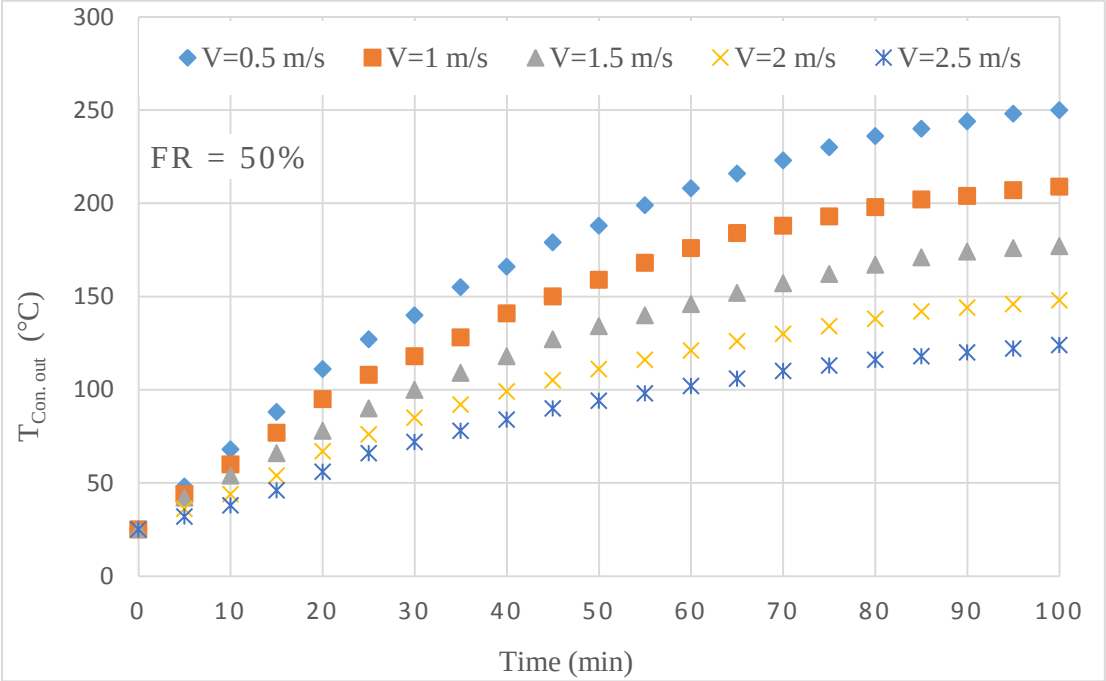

Figure ٥.٧: Condenser Outlet Air Temperature with the Time at Different Air Velocities

٥.٢.١.٢ Heat Pipe Heat Exchanger Effectiveness

To show the effect of the air velocity on the thermal effectiveness of the HPHE, five condenser inlet air velocities (٠.٥, ١, ١.٥, ٢, and ٢.٥) m/s were used. Figure (٥.٨) shows the experimental results of this effect at the filling ratio of ٥٠٪. This is at constant air velocity of the evaporator inlet. As shown numerically in Section (٥.١.١.٣), the effectiveness decreases by ٤٢% (from ٧٧٪ to ٣٥٪) with increasing of the air velocity from ٠.٥ to ٢.٥ m/s. This relates to the same reasons shown previously (increasing the air velocity causes decreasing the air contact time with the heat pipe surface in addition to distributing heat on further air molecules reducing its temperature). Consequently, reduction of the effectiveness of the HPHE due to the direct relationship between them (Eff. and air temperature) based on Eq. (٣.٩).

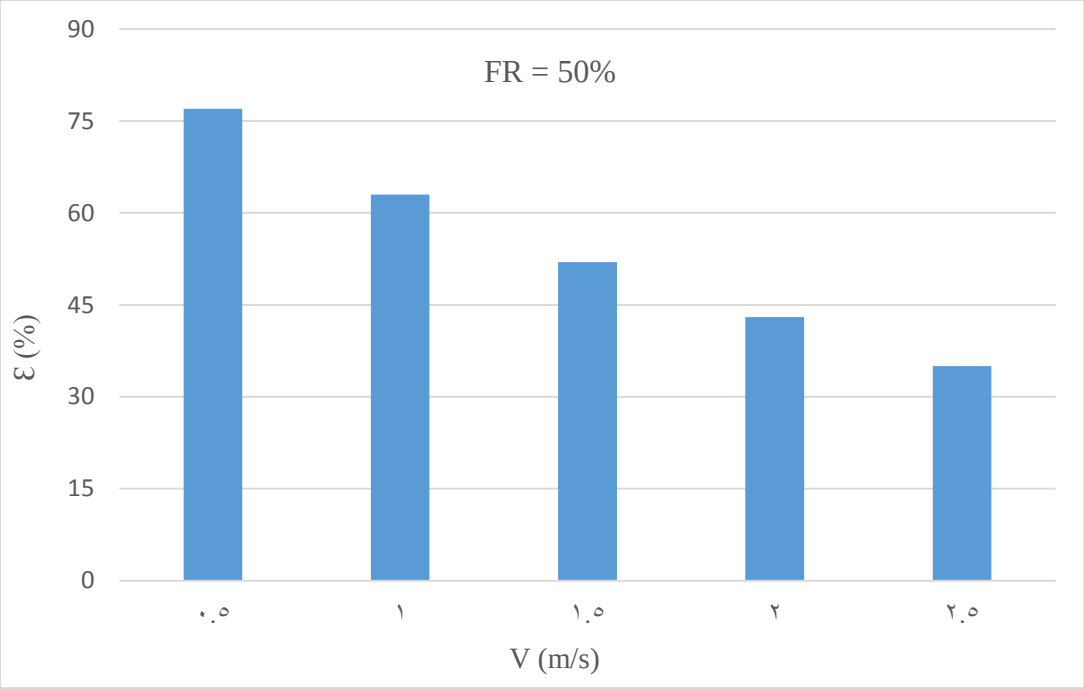

Figure ٥.٨: Experimental Effectiveness of the HPHE at Different Air Velocities

٥.٢.٢ Influence of Filling Ratio of Working Fluid

٥.٢.٢.١ Condenser Outlet Air Temperature

Figure (٥.٩) demonstrates the experimental results of the air temperature at the condenser outlet ($T_{Con.\ out}$) at three air velocities of ٠.٥, ١.٥, and ٢.٥ m/s. This is at different filling ratios of the working fluid (٣٥٪, ٥٠٪, and ٧٥٪). As it was explained in the numerical aspect (Section (٥.١.٢.١)), that the thermal performance of the HPHE in terms of the air temperature largely affects with the filling ratio. Experimentally, it was found that the best filling ratio of the working fluid is ٥٠٪. Where at this ratio, the maximum air temperature (٢٥٠ °C) is achieved. While, using the filling ratio of ٧٥٪ gives the minimum air temperature (which equals ١٧٤ °C). The difference between the two cases is ٧٦ °C (by reducing the velocity, the air temperature decreased by approximately ٣٠٪). This is at the same air velocity, which equals ٠.٥ m/s. The causes for this are same mentioned previously in the numerical aspect (Section (٥.١.٣)).

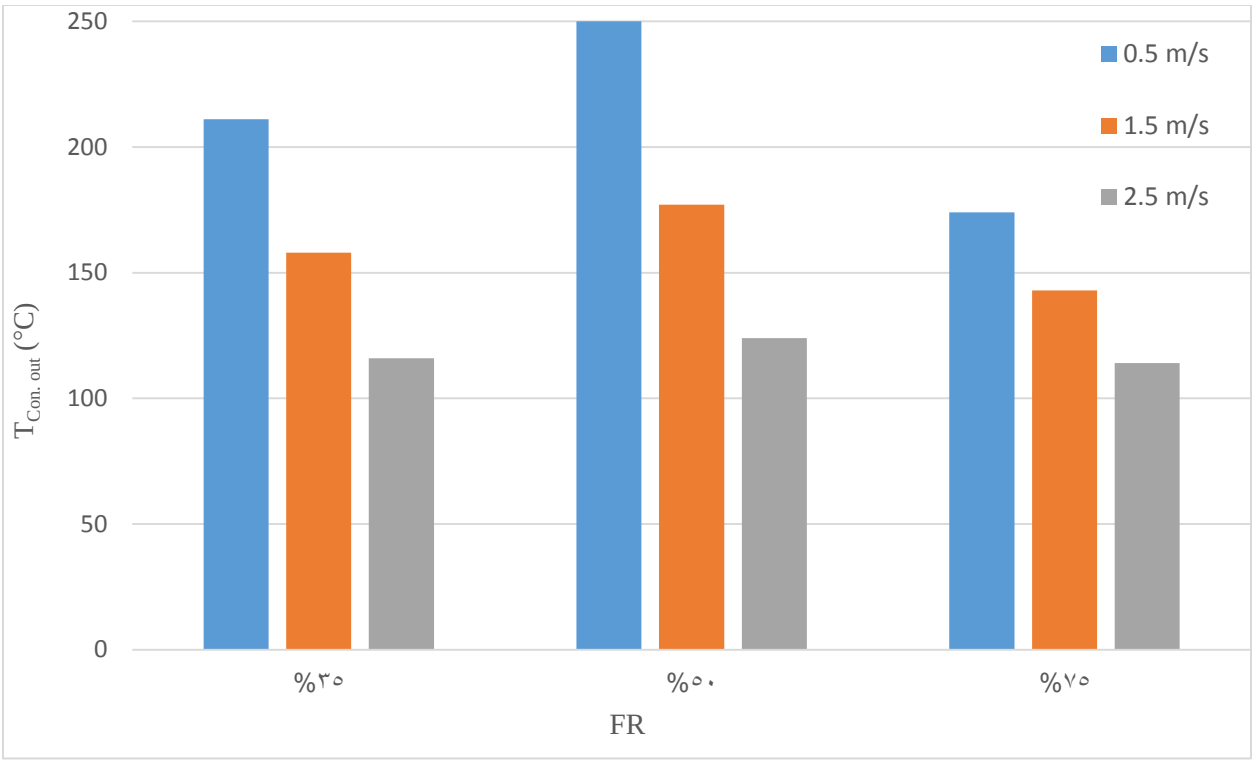

Figure ٥.٩: Experimental Condenser Outlet Air Temperature Versus the Filling Ratio at Different Air Velocities

٥.٢.٢.٢ Heat Pipe Heat Exchanger Effectiveness

To show the filling ratio effect on the thermal effectiveness of the HPHE experimentally, different filling ratios of the working fluid (٣٥%, ٥٠%, and ٧٥٪) were applied in this study. This is at different condenser inlet air velocities of ٠.٥, ١.٥, and ٢.٥ m/s as shown in Figure (٥.١٠). Numerically (as explained in Section (٥.١.٢.٣)), the maximum and minimum value of the effectiveness (٧٣٪ and ٤٧٪) are respectively achieved at filling ratios of ٥٠٪, and ٧٥٪. This is also achieved experimentally but with different values (the maximum and minimum values of the effectiveness are ٧٧٪ and ٥١٪ at filling ratios of ٥٠٪ and ٧٥% respectively). This is at the same air velocity which equals ٠.٥ m/s. This relates to the same reasons explained numerically (shortly, using a filling ratio less or greater than ٥٠٪ don't make the working fluid operates properly and thus a thermal failure of the HPHE).

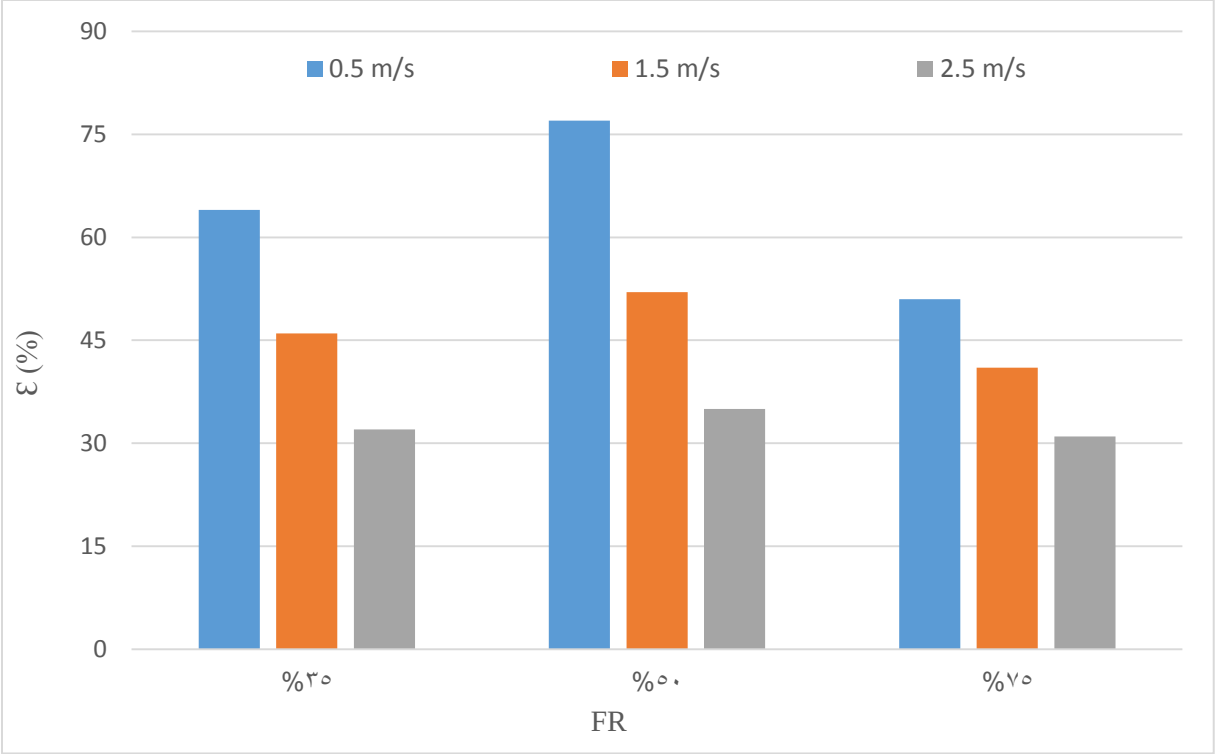

Figure ٥.١٠: Experimental Effectiveness of the HPHE versus the Filling Ratio at Different Air Velocities

٥.٢.٣ Effect of Evaporator Inlet Air Temperature

The experimental results of the condenser outlet air temperature versus the evaporator inlet air temperature at three condenser inlet air velocities of (٠.٥, ١.٥, and ٢.٥ m/s) are respectively shown in Figures (٥.١١a, b, and c). It is noted that there is a strong effect of the evaporator inlet air temperature ($T_{Evap.\ in}$) on the condenser outlet air temperature ($T_{Con.\ out}$). Where the $T_{Con.\ out}$ increased from ٢٥ to ٢٥٠ °C with the increase of the $T_{Evap.\ in}$ from ١٦٠ to ٣٢٠ °C. This is at ٥٠٪ filling ratio and ٠.٥ m/s air velocity (Figure (٥.١١a)). This is because the increasing of the $T_{Evap.\ in}$ leads to increasing of heat transfer rate to the working fluid, which in turn transfers this heat to the air passed across the condenser section.

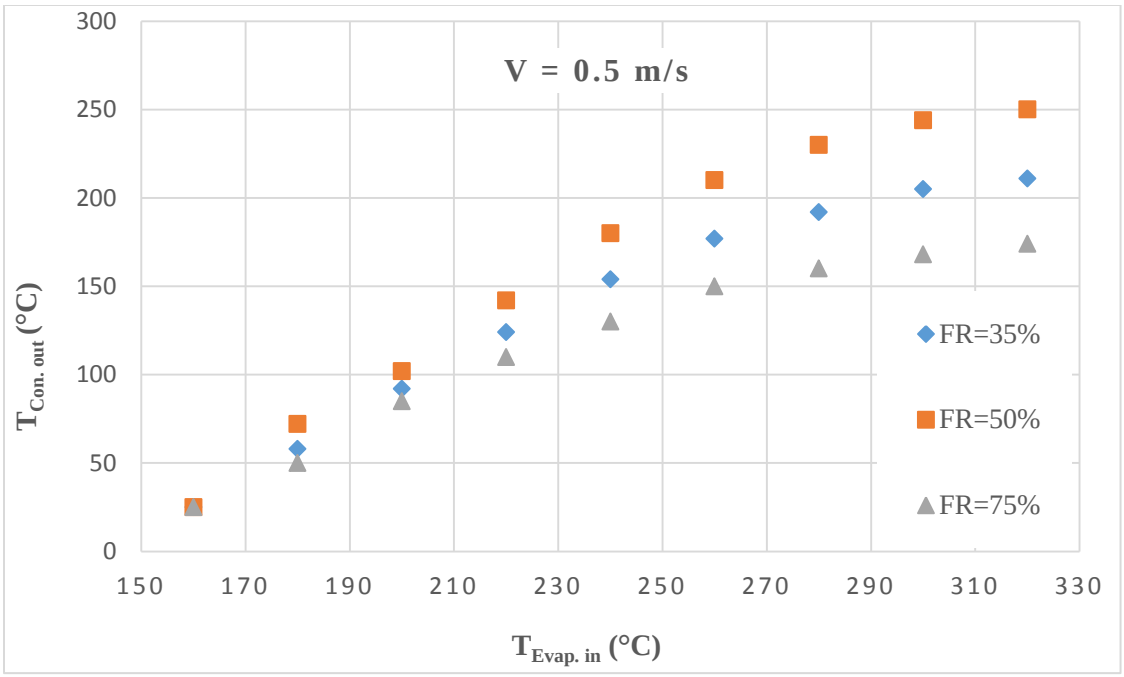
V = 0.5 m/s
300
250
200
150
100
50
0
150 170 190 210 230 250 270 290 310 330
T Con. out (°C)
T Evap. in (°C)
FR=35%
FR=50%
FR=75%

(a)

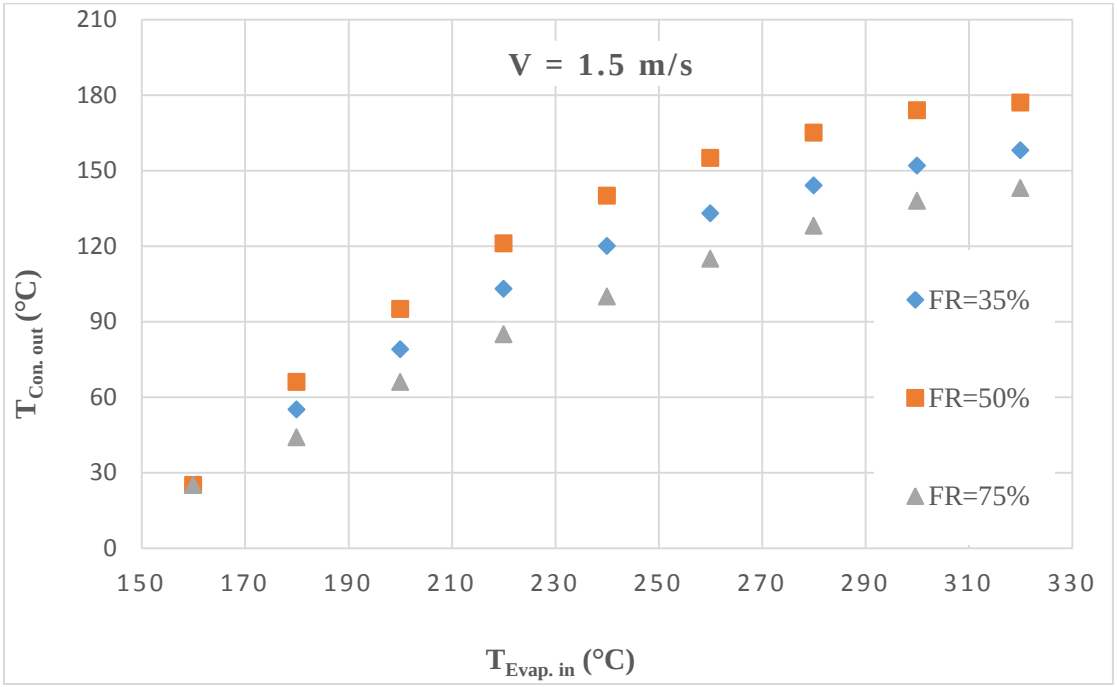
V = 1.5 m/s
210
180
150
120
90
60
30
0
150 170 190 210 230 250 270 290 310 330
T Con. out (°C)
T Evap. in (°C)
FR=35%
FR=50%
FR=75%

(b)

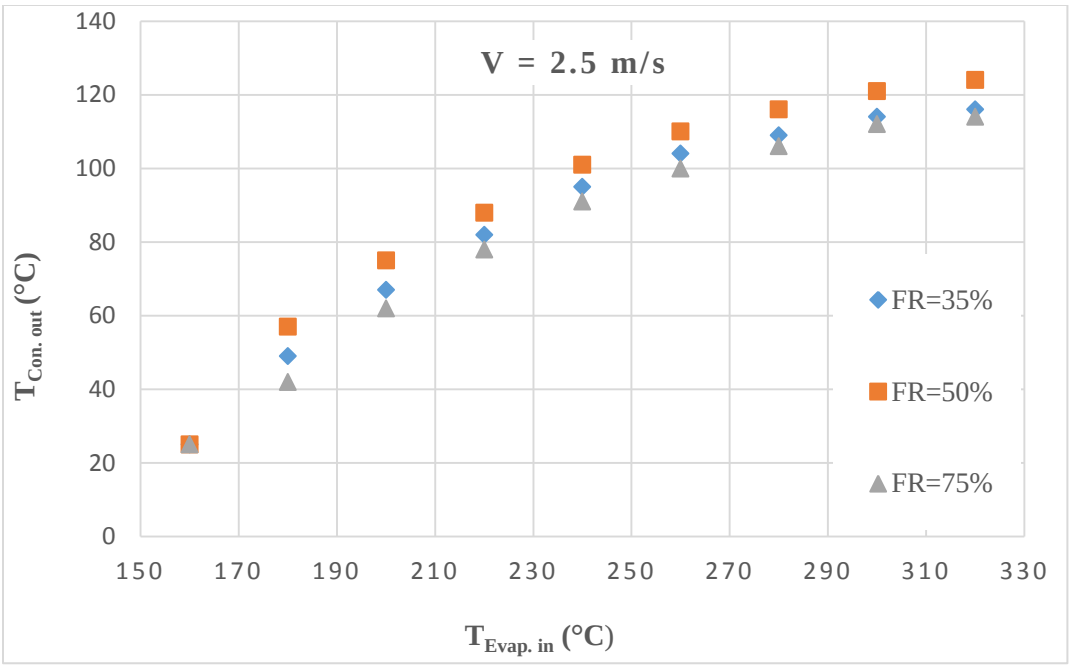

(c)

Figure ٥.١١: Experimental Condenser Outlet Air Temperature versus the Evaporator Inlet Air Temperature at Air Velocity of, (a): ٠.٥ m/s, (b): ١.٥ m/s and (c): ٢.٥ m/s

٥.٣ Results Comparison

To show the deviation percentage between the experimental and numerical results, comparisons between them at different filling ratios and air velocities are carried out. Figures (٥.١٢a, b, and c) show comparisons between the experimental and numerical results of the condenser outlet air temperature ($T_{Con. out}$) at air velocities of ٠.٥, ١.٥, and ٢.٥ m/s respectively. This is at three different filling ratios (٣٥%, ٥٠%, and ٧٥%). Figures (٥.١٣a, b, and c) show comparisons between the experimental and numerical results of the effectiveness of the HPHE at filling ratios of ٣٥٪, ٥٠٪, and ٧٥٪ respectively. This is at different air velocities. The maximum difference percentage between the experimental and numerical results for ($T_{Con. out}$) is less than ٩.٥٪ and for the effectiveness is about ١١٪. This is at ٢.٥ m/s air velocity and ٣٥٪ filling ratio. This is due to some assumptions that

were applied numerically and which cannot be avoided experimentally. In addition to some errors which may occur in the experimental aspect.

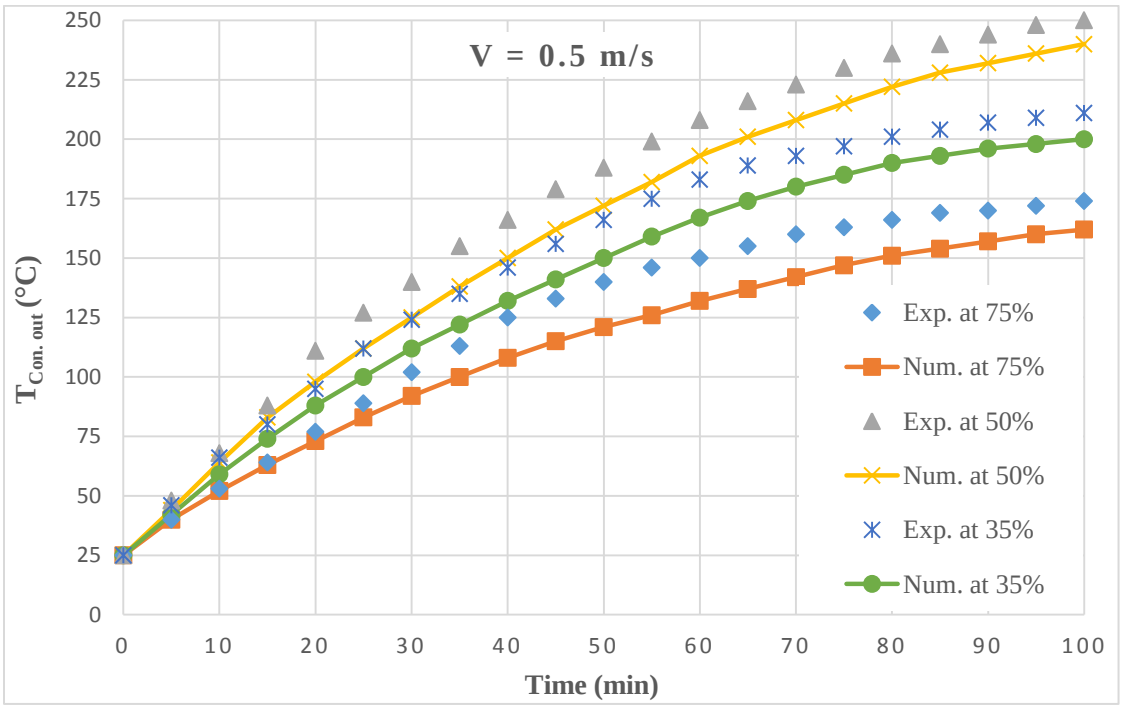

(a)

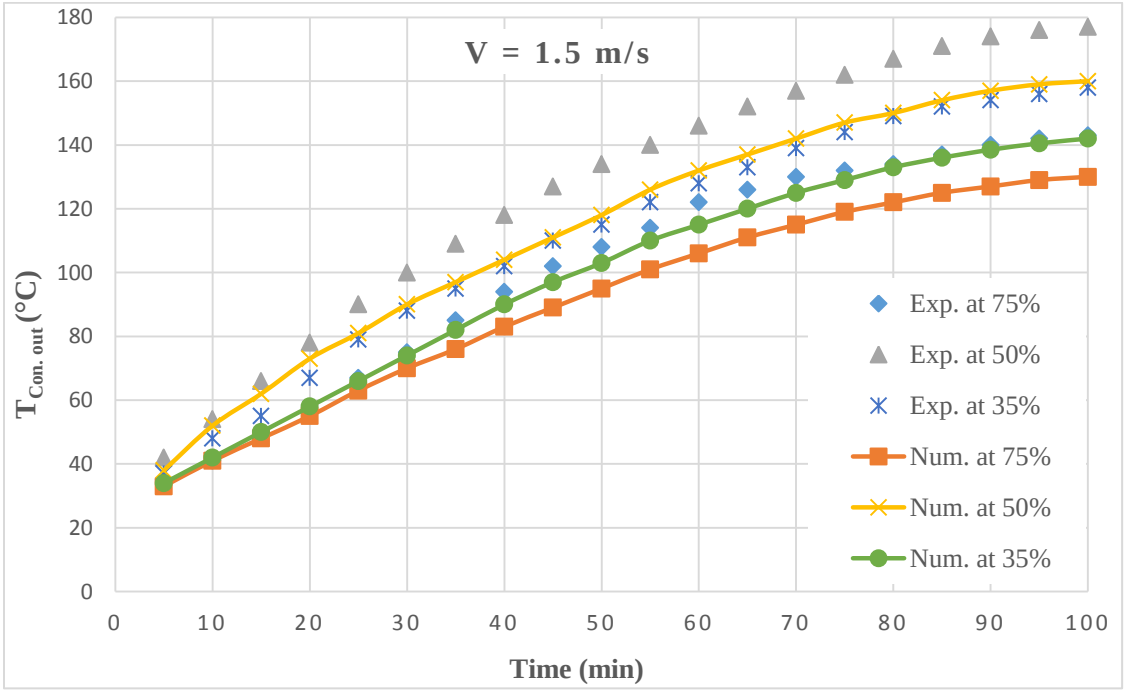

(b)

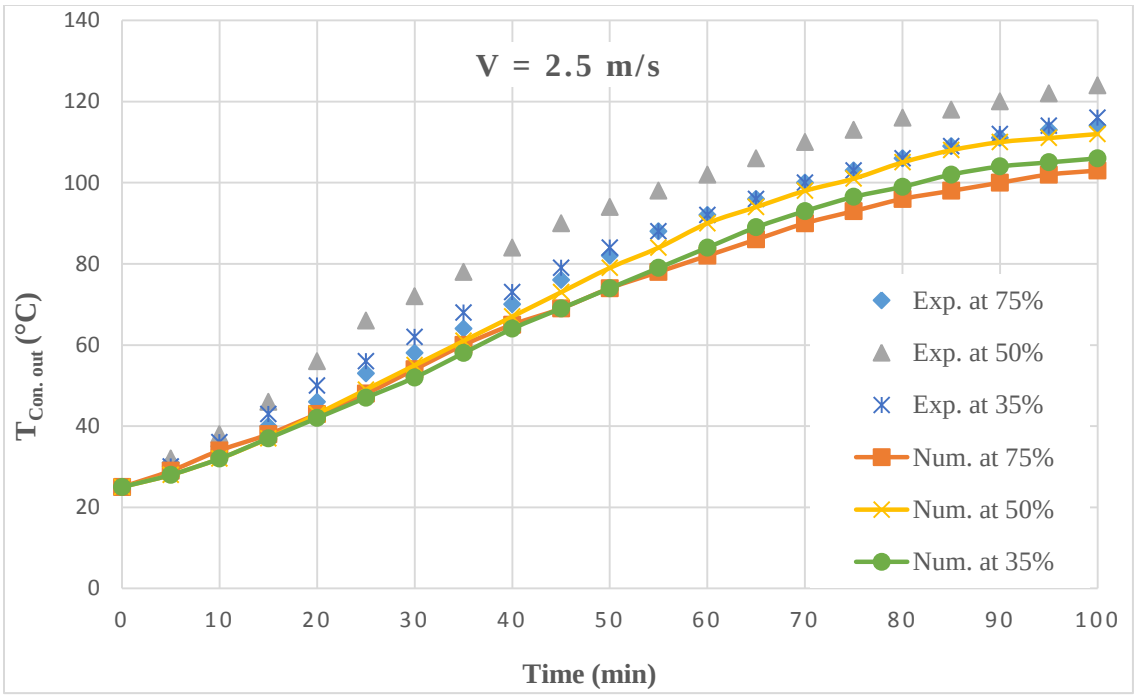

(c)

Figure ٥.١٢: Results Comparison of the Condenser Outlet Air Temperature at Different Filling Ratios at Air Velocity of, (a): ٠.٥ m/s, (b): ١.٥ m/s and (c): ٢.٥ m/s

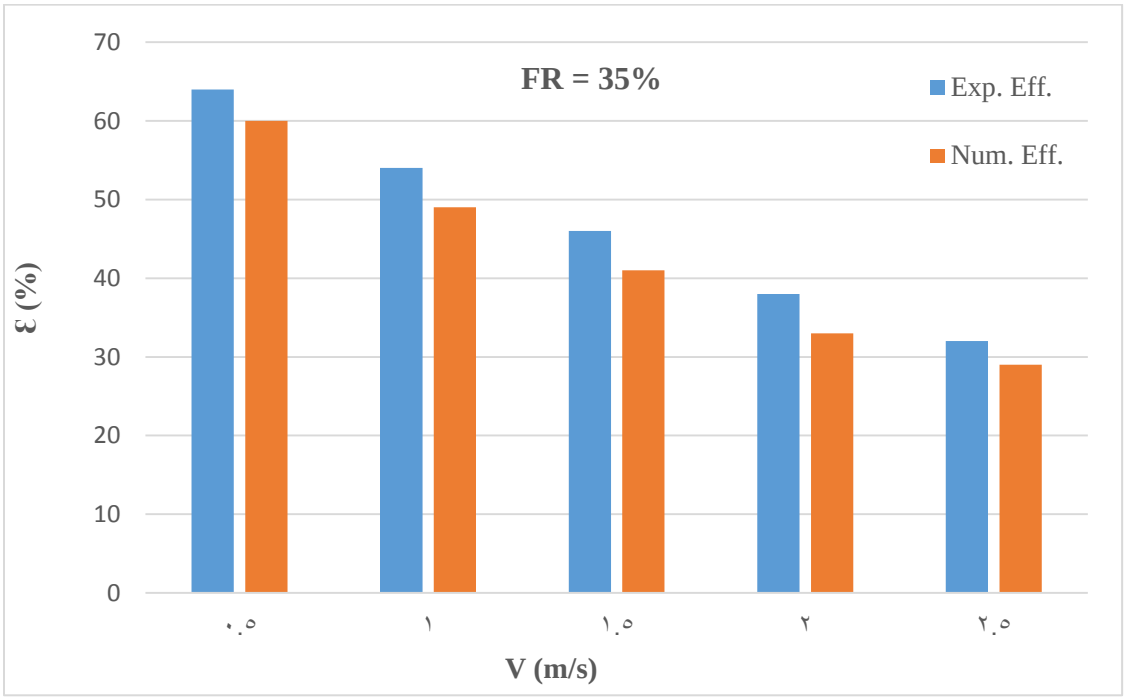

(a)

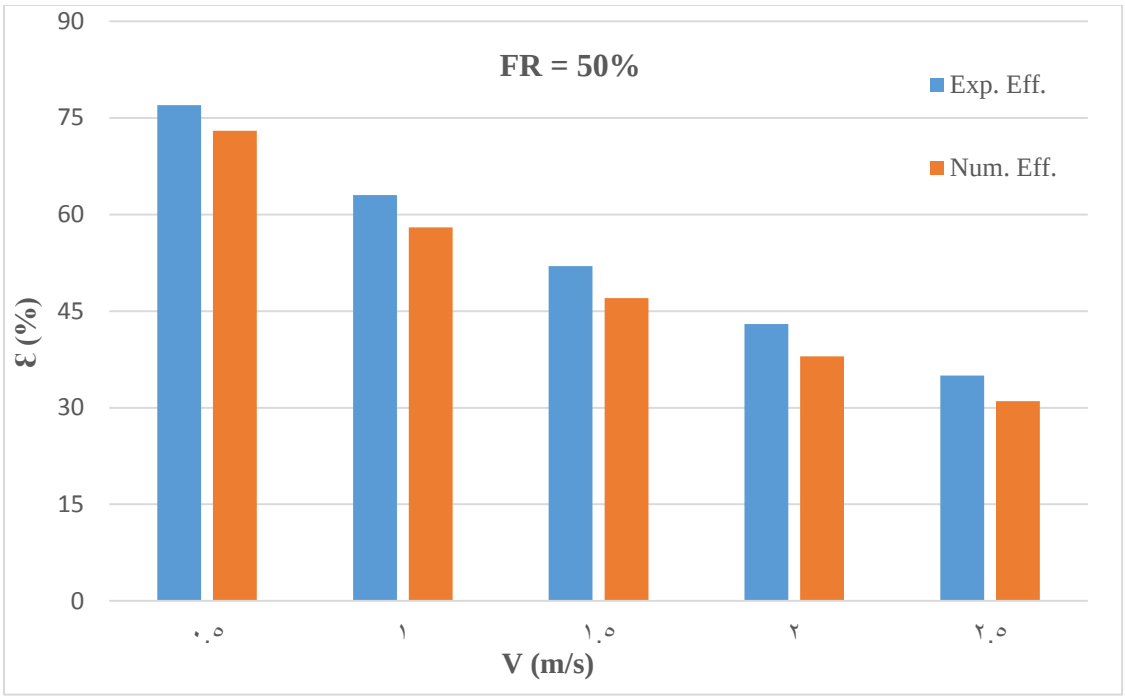

(b)

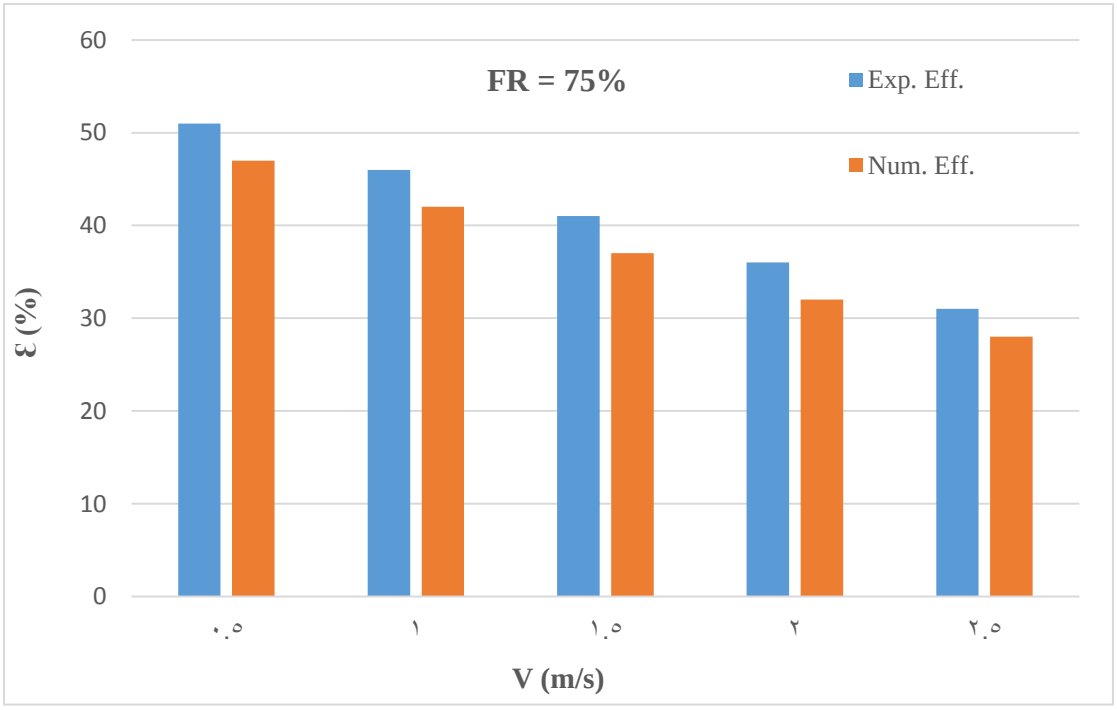

(c)

Figure ٥.١٣: Results Comparison of the HPHE Effectiveness Versus the Air Velocity at Filling Ratio of, (a): ٣٥٪, (b): ٥٠٪ and (c): ٧٥٪

٥.٤ Optimum Inputs and Outputs of HPHE

Table (٥.١) includes the optimum values of inputs (air velocity, filling ratio, and evaporator inlet air temperature) and outputs (condenser outlet air temperature and effectiveness of the HPHE). This is for both aspects (numerical and experimental).

Table ٥.١: Optimum Values of the Inputs and Outputs (Numerical and Experimental Results)

Inputs		Outputs		
Parameter Description	Value	Parameter Description	Num.	Exp.
Condenser inlet air velocity	٠.٥ m/s	Condenser outlet air temperature	٢٤٠ °C	٢٥٠ °C
Filling ratio	٥٠٪	HPHE effectiveness	٧٣٪	٧٧٪
Evaporator inlet air temperature	٣٢٠ °C			

Chapter Six

Conclusions

and

Recommendations

Chapter Six

Conclusions and Recommendations

٦.١ Conclusions

This study includes two aspects namely; experimental and numerical (constructing a numerical model of a heat pipe heat exchanger (HPHE) using ANSYS-Fluent software). In both aspects, the effect of the condenser inlet air velocity and the filling ratio of a working fluid (DOWTHERM™ A) on the thermal performance of the HPHE was investigated. This is through using different values of the air velocity (٠.٥, ١, ١.٥, ٢, and ٢.٥) m/s and filling ratios of ٣٥٪, ٥٠٪, and ٧٥٪). In addition to the tests were done at a wide range of the evaporator inlet air temperature ($T_{Evap.\ in}$ of ١٦٠ to ٣٢٠°C). Through the numerical and experimental results, it was concluded the following points: -

١. There is a large effect of the FR, air velocity and $T_{Evap.\ in}$ on the condenser outlet air temperature ($T_{Con.\ out}$). and thermal effectiveness (Ɛ) of the heat pipe.
٢. Increasing the FR from ٥٠٪ to ٧٥٪ leads to decreasing the $T_{Con.\ out}$ from ٢٥٠ to ١٧٤°C experimentally and from ٢٤٠ to ١٦٢°C numerically, and the Ɛ from ٧٧٪ to ٥١٪ experimentally and from ٧٣٪ to ٤٧٪ numerically. This is at the same air velocity (٠.٥ m/s).
٣. Increasing the air velocity from ٠.٥ m/s to ٢.٥ m/s leads to decreasing of the $T_{Con.\ out}$ from ٢٥٠ to ١٢٤ °C experimentally and from ٢٤٠ to ١١٢ °C numerically, and the Ɛ from ٧٧٪ to ٣٥٪ experimentally and from ٧٣٪ to ٣١٪ numerically. This is for the same FR (٥٠٪).
٤. Generally, the optimum conditions to obtain the best thermal performance of the heat pipe, are ٥٠٪ for the FR, ٠.٥ m/s for the air velocity, and ٣٢٠ °C for the $T_{Evap.\ in}$.

٦.٢ Recommendations

In the current study, the effect of the condenser inlet air velocity and the filling ratio of a working fluid (DOWTHERM™ A) on the thermal performance of the heat pipe heat exchanger was experimentally and numerically studied. In the future, using a hybrid working fluid with different fill ratios or/and installing copper fin inside the heat pipe may be studied. Increasing the evaporator size at the expense of the condenser section may be also studied.

References

[١]- Ding Y., Guo Q., Guo W., Chu W. & Wang Q. ΄Review of Recent Applications of Heat Pipe Heat Exchanger Use for Waste Heat Recovery΅, Journal of Energies, ٢٠٢٤, ١٧(١١), ٢٥٠٤.

[٢]- Gunawan Y., Putra N., Hakim I. I., Agustina D., & Mahlia T. M. I. ΄Withering of Tea Leaves Using Heat Pipe Heat Exchanger by Utilizing Low-Temperature Geothermal Energy΅, International Journal of Low-Carbon Technologies, ٢٠٢١, ١٦(١), ١٤٦-١٥٥.

[٣]- G. Grover, T. Cotter, and G. Erickson, ΄Structures of Very High Thermal Conductance΅, Journal of Applied Physics, ١٩٦٤, vol. ٣٥, no. ٦, pp. ١٩٩٠-١٩٩١.

[٤]- Sukarno, R., Putra, N., Hakim, I. I., Rachman, F. F., & Mahlia T. M. I., ΄Utilizing heat pipe heat exchanger to Reduce the Energy Consumption of Airborne Infection Isolation Hospital Room HVAC System΅, Journal of Building Engineering, ٢٠٢١, ٣٥, ١٠٢١١٦.

[٥]- Delpech, B., B. Axcell, and H. Jouhara, ΄Experimental Investigation Of A Radiative Heat Pipe For Waste Heat Recovery In A Ceramics Kiln΅ Energy, ٢٠١٩, ١٧٠: p. ٦٣٦-٦٥١.

[٦]- Abhat, A., & Seban, ΄΄ Boiling and evaporation from heat pipe wicks with water and acetone΅ R. A. (١٩٧٤).

[٧]- Zhang, W., Wang, C., Chen, R., Tian, W., Qiu, S., & Su, G. H. ΄Preliminary Design and Thermal Analysis of A Liquid Metal Heat Pipe Radiator for TOPAZ-II power system΅, Annals of Nuclear Energy, ٢٠١٦, ٩٧, ٢٠٨-٢٢٠.

[٨]- Ma, H. Ma, H., Du, N., Zhang, Z., Lyu, F., Deng, N., Li, C., & Yu, S.″Assessment of the Optimum Operation Conditions on A Heat Pipe Heat Exchanger for Waste Heat Recovery in Steel Industry̋, Renewable and Sustainable Energy Reviews, ٢٠١٧, ٧٩: p. ٥٠-٦٠.

[٩]- Aamir Al-Mabsali, S. Candido, J. P. Chaudhry H. N., & Gul, M. S. ″Investigation of an Inclined Heat Pipe Heat Exchanger as A Passive Cooling Mechanism on A Photovoltaic Panel, Journal of Energies, ٢٠٢١, ١٤(٢٣), ٧٨٢٨.

[١٠]- Sukarno R., Putra, N., Hakim, I. I., Rachman, F. F., & Mahlia T. M. I.″Utilizing Heat Pipe Heat Exchanger to Reduce the Energy Consumption of Airborne Infection Isolation Hospital Room HVAC System̋, Journal of Building Engineering, ٢٠٢١, ٣٥, ١٠٢١١٦.

[١١]- Ramkumar P., Vivek C. M., Ramasamy S., Kajavali A., & Sivasubramanian M., ″Experimental and Numerical Study Using ANFIS-Neuro Fuzzy Model on Heat Pipe Heat Exchanger̋, Materials Today: Proceedings, ٦٢, ٢١٥٢-٢١٦٢..

[١٢]- Than, S.T.M., K.A. Lin, and M.S. Mon,″Heat Exchanger Design̋, World Academy of Science, Engineering and Technology, ٢٠٠٨. ٤٦: p. ٦٠٤-٦١١.

[١٣]- Brough Daniel J.,″Transient Modelling of Heat Pipe Heat Exchangers With Vertical Thermosyphons For the Purpose of Waste Heat Recovery From Industrial Exhaust Gases̋, Diss. Brunel University London, ٢٠٢٢.

[١٤]- Reay DA, Kew PA, McGlen RJ. Heat Pipes. Theory, Design and Applications. SixthEdit. Oxford: Butterworth-Heinemann; ٢٠١٣.

[١٥]- Kiseev, V., and O. Sazhin. "Heat transfer enhancement in a loop thermosyphon using nanoparticles/water nanofluid." International Journal of Heat and Mass Transfer ١٣٢ (٢٠١٩): ٥٥٧-٥٦٤.

[١٦]- Modi A. K., Haque A., Pratap, B., Bansal, I. K., Kumar, P., Saravanan, S., ... & Kumar, C. R. (٢٠١٧). A Review on Air Preheater Elements Design and Testing. Mechanics, Materials Science & Engineering Journal.

[١٧]- http://coalhandlingplants.com/air-preheater-in-thermal-power-plant.

[١٨]- A. A. Alammar, R. K. Al-Dadah, and S. M. Mahmoud, "Numerical investigation of effect of fill ratio and inclination angle on a thermosiphon heat pipe thermal performance," Applied Thermal Engineering, vol. ١٠٨, pp. ١٠٥٥-١٠٦٥, ٢٠١٦, doi: ١٠.١٠١٦/j.applthermaleng.٢٠١٦.٠٧.١٦٣.

[١٩]- S. Fertahi, T. Bouhal, Y. Agrouaz, T. Kousksou, T. El Rhafiki, Y. Zeraouli, ″Performance optimization of a two-phase closed thermosyphon through CFD numerical simulations̋, Applied Thermal Engineering (٢٠١٧), http://dx.doi.org/١٠.١٠١٦/j.applthermaleng.٢٠١٧.٠٩.٠٤٩.

[٢٠]- Al Jubori, A. M., & Jawad, Q. A. "Computational evaluation of thermal behavior of a wickless heat pipe under various conditions". Case Studies in Thermal Engineering, ٢٢, ١٠٠٧٦٧. (٢٠٢٠).

[٢١]- Adrian, Ł., Szufa, S., Piersa, P., & Mikołajczyk, F.″Numerical model of heat pipes as an optimization method of heat exchangers" , Energies, (٢٠٢١). ١٤(٢٢), ٧٦٤٧.

[٢٢]- K. Desai, G. Lakra, R. Rajesh, and S. Senthur Prabu, "Investigation on the effect of thermal properties by changing geometry of a heat pipe using simulation," Materials Today: Proceedings, vol. ٤٦, pp. ٨٤٧٣-٨٤٧٩, ٢٠٢١.

[٢٣]- Brough, D., Ramos, J., Delpech, B., & Jouhara, H. (٢٠٢١). Development and validation of a TRNSYS type to simulate heat pipe heat exchangers in transient applications of waste heat recovery. International Journal of Thermofluids, ٩, ١٠٠٠٥٦.

[٢٤]- K. Sadeghi, M. Kahani, Mohammad H. Ahmadi, and M. Zamen, "CFD Modelling and Visual Analysis of Heat Transfer and Flow Pattern in a Vertical Two-Phase Closed Thermosyphon for Moderate-Temperature Application", Energies ٢٠٢٢, ١٥, ٨٩٥٥. https://doi.org/١٠.٣٣٩٠/en١٥٢٣٨٩٥٥.

[٢٥]- Beiginaloo, G., A. Mohebbi, and M.M. Afsahi, Combination of CFD and DOE for optimization of thermosyphon heat pipe. Heat and Mass Transfer, ٢٠٢٢. ٥٨(٤): p. ٥٦١-٥٧٤.

[٢٦]- Sriwiga, S., Munsin, R., Watcharadumrongsak, T., Wongpanich, S., Kraitong, K., Lapirattanakun, A., ... & Yeunyongkul, P. (٢٠٢٣). Design of the Optimum Heat Pipe Heat Exchanger to Recover Heat From Flue Gas of Boiler in case of Chiang Mai Orchid Hotel, Thailand. Journal of Technical Education Science, ١٨(٤), ٥٢-٥٩.

[٢٧]- Ali Hakim Mathry, Fadhel N. Al-Mousawi, Nabeel S. Dhidan, Ahmed A Alammar "Numerical simulation of the heat transfer characteristics of a thermosyphon heat pipe with different tilt angles and filling ratios"KJES (٢٠٢٣)

[٢٨]- Lukitobudi, A. R., Akbarzadeh, A., Johnson, P. W., & Hendy, P. (١٩٩٥). Design, construction and testing of a thermosyphon heat exchanger for medium temperature heat recovery in bakeries. Heat Recovery Systems and CHP, ١٥(٥), ٤٨١-٤٩١.

[٢٩]- A. K. Mozumder, A. F. Akon, M. Chowdhury, and S. C. Banik, "Performance of heat pipe for different working fluids and fill ratios," Journal of Mechanical Engineering, vol. ٤١, no. ٢, pp. ٩٦-١٠٢, ٢٠١٠.

[٣٠]- E. Gedik, "Experimental investigation of the thermal performance of a two-phase closed thermosyphon at different operating conditions", Energy and Buildings, vol. ١٢٧, pp. ١٠٩٦-١١٠٧, ٢٠١٦.

[٣١]- Mohamed Abdulsalam D., Aamer M. Al-Dabagh, and Duaa A. Diab. "Experimental Study of Thermal Performance of Heat Pipe Heat Exchanger" International Journal of Computer Applications, ٩٧٥ (٢٠١٦): ٨٨٨٧.

[٣٢]- Ma, H., Yin, L., Shen, X., Lu, W., Sun, Y., Zhang, Y., & Deng, N. ´Experimental study on heat pipe assisted heat exchanger used for industrial waste heat recovery¨, ٢٠١٦, Applied energy, ١٦٩, ١٧٧-١٨٦.

[٣٣]- Gedik, E., M. Yılmaz, and H. Kurt,´Experimental investigation on the thermal performance of heat recovery system with gravity assisted heat pipe charged with R١٣٤a and R٤١٠Ä, Applied Thermal Engineering, ٢٠١٦, ٩٩: p. ٣٣٤-٣٤٢.

[٣٤]- Y. Naresh and C. Balaji, "Experimental investigations of heat transfer from an internally finned two phase closed thermosyphon", Applied Thermal Engineering, vol. ١١٢, pp. ١٦٥٨-١٦٦٦, ٢٠١٧.

[٣٥]- Muhammad D., S. A. Winarta, and N.S.D. Putra,´Experimental Study of Heat Pipe Heat Exchanger Multi Fin for Energy Efficiency Effort in Operating Room Air System¨, International Journal of Technology, ٢٠١٨. ٩(٢): p. ٤٢٢-٤٢٩.

[٣٦]- Öztürk, A., M. Özalp, and A. Sözen, "Experimental investigation of an Al٢O٣/distilled water nanofluid used in the heat pipes of heat exchangers", Gazi University Journal of Science, ٢٠١٨. ٣١(٢): p. ٦١٦-٦٢٦.

[٣٧]- Kusumah, A. S., Hakim, I. I., Sukarno, R., Rachman, F. F., & Putra, N. (٢٠١٩). The application of U-shape heat pipe heat exchanger to reduce relative humidity for energy conservation in heating, ventilation, and air conditioning (HVAC) systems. International Journal of Technology, ١٠(٦), ١٢٠٢-١٢١٠.

[٣٨]- Delpech, B., B. Axcell, and H. Jouhara, "Experimental investigation of a radiative heat pipe for waste heat recovery in a ceramics kiln", Energy, ٢٠١٩. ١٧٠: p. ٦٣٦-٦٥١.

[٣٩]- Hossen, S., Morshed, A. M., Tikadar, A., Salman, A. S., & Paul, T. C. (٢٠١٩). Experimental Investigation of Heat Pipe Heat Exchanger (HPHE) For Waste Heat Recovery Application. In ASTFE Digital Library. Begel House Inc.

[٤٠]- Abdelaziz, G. B., Abdelbaky, M. A., Halim, M. A., Omara, M. E., Elkhaldy, I. A., Abdullah, A. S., ... & Kabeel, A. E. (٢٠٢١). Energy saving via Heat Pipe Heat Exchanger in air conditioning applications "experimental study and economic analysis". Journal of Building Engineering, ٣٥, ١٠٢٠٥٣.

[٤١]- Abedalh, A.S., N.J. Yasin, and H.A. Ameen, "Thermal performance of HAVC system using heat pipe heat exchanger" Journal of Mechanical Engineering Research and Developments, ٢٠٢١. ٤٤(٢): p. ١-٩.

[٤٢]- Sukarno, R., Putra, N., Hakim, I. I., Rachman, F. F., & Mahlia, T. M. I. (٢٠٢١). Multi-stage heat-pipe heat exchanger for improving energy

efficiency of the HVAC system in a hospital operating room. International Journal of Low-Carbon Technologies, ١٦(٢), ٢٥٩-٢٦٧.

[٤٣]- Sertkaya, Ahmet Ali, Yusuf Akyar, and Ahmet Ozsoy. "Experimental Investigation of Low Heat Flux Wicked Heat Pipes Performance with Different Working Fluids and Tilt Angles." Heat Transfer Research ٥٦ (٢٠٢٥).

[٤٤]- Noie-Baghban, S.H. and G. Majideian, "Waste heat recovery using heat pipe heat exchanger (HPHE) for surgery rooms in hospitals", Applied thermal engineering, ٢٠٠٠. ٢٠(١٤): p. ١٢٧١-١٢٨٢.

[٤٥]- Noie, S., "Investigation of thermal performance of an air-to-air thermosyphon heat exchanger using ε-NTU method", Applied Thermal Engineering, ٢٠٠٦. ٢٦(٥-٦): p. ٥٥٩-٥٦٧.

[٤٦]- Mroue, H., Ramos, J. B., Wrobel, L. C., & Jouhara, H. (٢٠١٥). Experimental and numerical investigation of an air-to-water heat pipe-based heat exchanger. Applied Thermal Engineering, ٧٨, ٣٣٩-٣٥٠.

[٤٧]- Ramos, J., A. Chong, and H. Jouhara, "Experimental and numerical investigation of a cross flow air-to-water heat pipe-based heat exchanger used in waste heat recovery", International Journal of Heat and Mass Transfer, ٢٠١٦. ١٠٢: p. ١٢٦٧-١٢٨١.

[٤٨]- Mroue, H., Ramos, J. B., Wrobel, L. C., & Jouhara, H. (٢٠١٧). Performance evaluation of a multi-pass air-to-water thermosyphon-based heat exchanger. Energy, ١٣٩, ١٢٤٣-١٢٦٠

[٤٩]- Jouhara, H., Almahmoud, S., Chauhan, A., Delpech, B., Bianchi, G., Tassou, S. A., ... & Arribas, J. J. (٢٠١٧). Experimental and theoretical investigation

of a flat heat pipe heat exchanger for waste heat recovery in the steel industry. Energy, ١٤١, ١٩٢٨-١٩٣٩.

[٥٠]- J. Raghuram, K. P. Kumar, G. Khiran, K. Snehith, and S. B. Prakash, "Thermal performance of a selected heat pipe at different tilt angles," in IOP Conference Series: Materials Science and Engineering, vol. ٢٢٥, no. ١: IOP Publishing, p. ٠١٢٠٤٣, ٢٠١٧.

[٥١]- Xie, C. Y., Tao, H. Z., Li, W., & Cheng, J. J. (٢٠١٩). Numerical simulation and experimental investigation of heat pipe heat exchanger applied in residual heat removal system. Annals of Nuclear Energy, ١٣٣, ٥٦٨-٥٧٩.

[٥٢]- Jouhara, H., Almahmoud, S., Brough, D., Guichet, V., Delpech, B., Chauhan, A. & Serey, N. (٢٠٢١). Experimental and theoretical investigation of the performance of an air to water multi-pass heat pipe-based heat exchanger. Energy, ٢١٩, ١١٩٦٢٤.

[٥٣]- Ali S. and W. Sarsam, Theoretical and experimental investigation of a heat pipe heat exchanger for energy recovery of exhaust air. Heat Transfer, ٢٠٢٢. ٥١(٤): p. ٣٦٠٠-٣٦١٩.

[٥٤]- Y. A. Çengel, Heat Transfer: A Practical Approach, ٢nd ed. McGraw-Hill, ٢٠٠٣, ISBN: ٠٠٧٢٤٥٨٩٣٣ / ٩٧٨-٠٠٧٢٤٥٨٩٣٠.

[٥٥]- Noie, S. H. (٢٠٠٦). Investigation of thermal performance of an air-to-air thermosyphon heat exchanger using ε-NTU method. Applied Thermal Engineering, ٢٦(٥-٦), ٥٥٩-٥٦٧.

[٥٦]- Gunawan, Y., Putra, N., Hakim, I. I., Agustina, D., & Mahlia, T. M. I. (٢٠٢١). Withering of tea leaves using heat pipe heat exchanger by utilizing

low-temperature geothermal energy. International Journal of Low-Carbon Technologies, ١٦(١), ١٤٦-١٥٥.

[٥٧]- Ramos, J., Chong, A., & Jouhara, H. (٢٠١٦). Experimental and numerical investigation of a cross flow air-to-water heat pipe-based heat exchanger used in waste heat recovery. International Journal of Heat and Mass Transfer, ١٠٢, ١٢٦٧-١٢٨١.

[٥٨]- Moore, Richard L. Implementation of DOWTHERM a Properties into RELAP٥-٣D/ATHENA. No. INL/EXT-١٠-١٨٦٥١. Idaho National Lab.(INL), Idaho Falls, ID (United States), ٢٠١٠.

[٥٩]- White Mary Anne, Physical properties of materials, CRC press, ٢٠١٨.

[٦٠]- C. Hirt, B. Nichols, Volume of fluid (vof) method for the dynamics of free boundaries, Journal of Computational Physics ٣٩ (١) (١٩٨١) ٢٠١ {٢٢٥. doi:http://dx.doi.org/١٠.١٠١٦/٠٠٢١-٩٩٩١(٨١)٩٠١٤٥-٥. URL http://www.sciencedirect.com/science/article/pii/٠٠٢١٩٩٩١٨١٩٠١٤٥٥.

[٦١]- W. Lee, A pressure iteration scheme for two-phase ow modelling (technical paper no. la-ur-٧٩-٩٧٥), Los Alamos, New Mexico, USA: Los Alamos National Laboratory.

[٦٢]- J. Legierski, B. Wie, G. De Mey, et al., Measurements and simulations of transient characteristics of heat pipes, ٤٤٥ Microelectronics reliability ٤٦ (١) (٢٠٠٦) ١٠٩{١١٥.

[٦٣]- N. Z. Aung, S. Li, Numerical investigation on e_ect of riser diameter and inclination on system parameters in a two-phase closed loop thermosyphon solar water heater, Energy Conversion and Management ٧٥ (٢٠١٣) ٢٥ {٣٥. doi:http://dx.doi.org/١٠.١٠١٦/j.enconman.٢٠١٣.٠٦.٠٠١.

[٦٤]- M. Zhang, ٤٥٠ Y. Lai, J. Zhang, Z. Sun, Numerical study on cooling characteristics of two-phase closed thermosiphon embankment in permafrost regions, Cold Regions Science and Technology ٦٥ (٢) (٢٠١١) ٢٠٣ {٢١٠. doi:http: //dx.doi.org/١٠.١٠١٦/j.coldregions.٢٠١٠.٠٨.٠٠١.

[٦٥]- J. Brackbill, D. B. Kothe, C. Zemach, A continuum method for modeling surface tension, Journal of computa- ٤٨٥ tional physics ١٠٠ (٢) (١٩٩٢) ٣٣٥{٣٥٤.

[٦٦]- B. Fadhl, L. C. Wrobel, H. Jouhara, Numerical modelling of the temperature distribution in a two-phase closed ٤٥٥ thermosyphon, Applied Thermal Engineering ٦٠ (١{٢) (٢٠١٣) ١٢٢ {١٣١}. doi:http://dx.doi.org/١٠.١٠١٦/j.applthermaleng.٢٠١٣.٠٦.٠٤٤.

[٦٧]- A. M. Elsayed, "Heat transfer in helically coiled small diameter tubes for miniature cooling systems," University of Birmingham, ٢٠١١.

[٦٨]- Sadeghinezhad, E., Mehrali, M., Rosen, M. A., Akhiani, A. R., Latibari, S. T., Mehrali, M., & Metselaar, H. S. C. (٢٠١٦). Experimental investigation of the effect of graphene nanofluids on heat pipe thermal performance. Applied Thermal Engineering, ١٠٠, ٧٧٥-٧٨٧.

Appendix A

DOWTHERM A with its Certificate

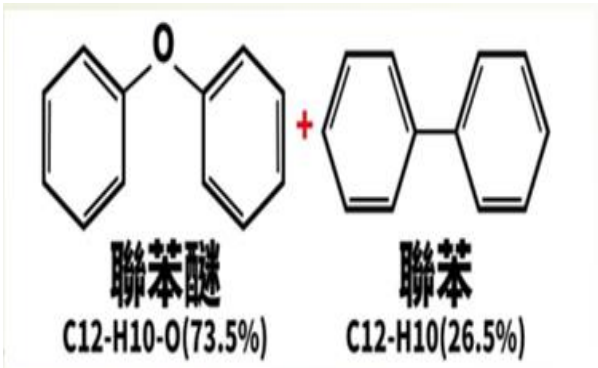

Product Information

DOWTHERM A

Synthetic Organic Heat Transfer Fluid — Liquid and Vapor Phase Data

DOWTHERM* A heat transfer fluid is a eutectic mixture of two very stable compounds, biphenyl ($C_{12}H_{10}$) and diphenyl oxide ($C_{12}H_{10}O$). These compounds have practically the same vapor pressures, so the mixture can be handled as if it were a single compound. DOWTHERM A fluid may be used in systems employing either liquid phase or vapor phase heating.

Recommended use temperature range:
Liquid phase: 15°C (60°F) to 400°C (750°F)
Vapor phase: 257°C (495°F) to 400°C (750°F)

Suitable applications: Indirect heat transfer

For health and safety information for this product, contact your Dow sales representative or call the number for your area on the second page of this sheet for a Material Safety Data Sheet (MSDS).

Typical Properties of DOWTHERM A Fluid†

Composition: Diphenyl Oxide/Biphenyl Blend

Color: Clear to Light Yellow

Property	SI Units	English Units
Freeze Point	12.0°C	53.6°F
Atmospheric Boiling Point	257.1°C	494.8°F
Flash Point[1]	113°C	236°F
Fire Point[2]	118°C	245°F
Autoignition Temperature[3]	599°C	1110°F
Density @ 25°C (75°F)	1056 kg/m³	66.0 lb/ft³
Surface Tension in Air @		
20°C (68°F)	40.1 Dynes/cm	40.1 Dynes/cm
40°C (104°F)	37.6 Dynes/cm	37.6 Dynes/cm
60°C (140°F)	35.7 Dynes/cm	35.7 Dynes/cm
Estimated Critical Temperature	497°C	927°F
Estimated Critical Pressure	31.34 bar	30.93 atm
Estimated Critical Volume	3.17 l/kg	0.0508 ft³/lb
Average Molecular Weight		166.0
Heat of Combustion	36,053 kJ/kg	15,500 Btu/lb

† Not to be construed as specifications
[1] SETA
[2] C.O.C.
[3] ASTM E659-78

Saturated Liquid Properties of DOWTHERM A Fluid (SI units)

Temp. °C	Vapor Pressure bar	Viscosity mPa sec	Specific Heat kJ/kg K	Thermal Cond. W/mK	Density kg/m³
15	0.00	5.00	1.558	0.1395	1063.5
65	0.00	1.58	1.701	0.1315	1023.7
105	0.01	0.91	1.814	0.1251	990.7
155	0.06	0.56	1.954	0.1171	947.8
205	0.28	0.38	2.093	0.1091	902.5
255	0.97	0.27	2.231	0.1011	854.0
305	2.60	0.20	2.373	0.0931	801.3
355	5.80	0.16	2.527	0.0851	742.3
405	11.32	0.12	2.725	0.0771	672.5

Saturated Liquid Properties of DOWTHERM A Fluid (English units)

Temp. °F	Vapor Pressure psia	Viscosity cP	Specific Heat Btu/lb °F	Thermal Cond. Btu/hr ft²(°F/ft)	Density lb/ft³
60	0.000	4.91	0.373	0.0805	66.37
120	0.003	2.12	0.396	0.0775	64.72
180	0.028	1.22	0.418	0.0744	63.03
240	0.16	0.81	0.441	0.0713	61.30
300	0.64	0.59	0.463	0.0682	59.51
360	2.03	0.45	0.485	0.0651	57.65
420	5.38	0.35	0.507	0.0620	55.72
480	12.25	0.28	0.529	0.0590	53.70
540	24.72	0.23	0.552	0.0559	51.57
600	45.31	0.19	0.575	0.0528	49.29
660	76.89	0.16	0.599	0.0497	46.82
720	122.7	0.14	0.627	0.0466	44.08
780	186.4	0.12	0.665	0.0436	40.93

DOWTHERM A
Synthetic Organic
Heat Transfer Fluid

Saturated Vapor Properties of DOWTHERM A Fluid (SI Units)

Temp. °C	Vapor Pressure bar	Liquid Enthalpy kJ/kg	Latent Heat kJ/kg	Vapor Enthalpy kJ/kg	Vapor Density kg/m³	Vapor Viscosity mPa•s	Vapor Thermal Cond. W/mK	Z_{vapor}	Specific Heat (c_p) kJ/kg K	Ratio of Specific Heats c_p/c_v
15	0.00	4.9	407.2	412.1		0.0054	0.0075	1.000	1.044	1.050
65	0.00	88.1	380.9	469.1	0.0040	0.0063	0.0104	1.000	1.227	1.043
105	0.01	158.1	362.7	520.9	0.0341	0.0071	0.0129	0.999	1.366	1.038
155	0.06	251.2	341.5	592.7	0.2583	0.0080	0.0163	0.995	1.528	1.035
205	0.28	351.2	320.2	671.5	1.179	0.0090	0.0200	0.982	1.681	1.034
255	0.97	458.2	297.4	755.6	3.831	0.0100	0.0238	0.954	1.829	1.036
305	2.60	572.2	271.5	843.6	9.896	0.0110	0.0279	0.908	1.976	1.042
355	5.80	693.1	240.6	933.8	22.03	0.0122	0.0322	0.838	2.133	1.057
405	11.32	822.0	201.7	1023.7	45.17	0.0138	0.0368	0.740	2.333	1.094

Saturated Vapor Properties of DOWTHERM A Fluid (English Units)

Temp. °F	Vapor Pressure psia	Liquid Enthalpy Btu/lb	Latent Heat Btu/lb	Vapor Enthalpy Btu/lb	Vapor Density lb/ft³	Vapor Viscosity cP	Vapor Thermal Cond. Btu/hr ft²(°F/ft)	Z_{vapor}	Specific Heat (c_p) Btu/lb °F	Ratio of Specific Heats c_p/c_v
60	0.000	2.5	175.1	177.6		0.0054	0.0044	1.000	0.250	1.050
120	0.003	26.2	167.3	193.5		0.0060	0.0055	1.000	0.279	1.045
300	0.64	103.0	148.0	251.1	0.0130	0.0079	0.0092	0.996	0.361	1.035
360	2.03	131.1	142.0	273.1	0.0388	0.0086	0.0106	0.989	0.385	1.034
420	5.38	160.6	135.8	296.3	0.0967	0.0092	0.0120	0.977	0.409	1.034
480	12.25	191.4	129.2	320.5	0.2100	0.0098	0.0135	0.959	0.433	1.035
540	24.72	223.5	122.1	345.5	0.4102	0.0105	0.0150	0.932	0.456	1.039
600	45.31	256.9	114.2	371.1	0.7389	0.0113	0.0166	0.895	0.480	1.045
660	76.89	291.7	105.3	397.0	1.254	0.0121	0.0183	0.848	0.505	1.055
720	122.7	327.9	95.0	422.9	2.045	0.0130	0.0200	0.789	0.534	1.073
780	186.4	365.9	82.5	448.4	3.270	0.0142	0.0219	0.714	0.571	1.108

For further information, call...

In the United States and Canada: 1-800-447-4369 • FAX: 1-989-832-1465
In Europe: +32 3 450 2240 • FAX: +32 3 450 2815
In the Pacific: +886 22 547 8731 • FAX: +886 22 713 0092
In other Global Areas: 1-989-832-1560 • FAX: 1-989-832-1465

www.dowtherm.com

Published November 2001

NA/LA/Pacific: Form No. 176-01463-1101 AMS
Europe: CH-153-307-E-1101

Appendix B

Data Logger Calibration

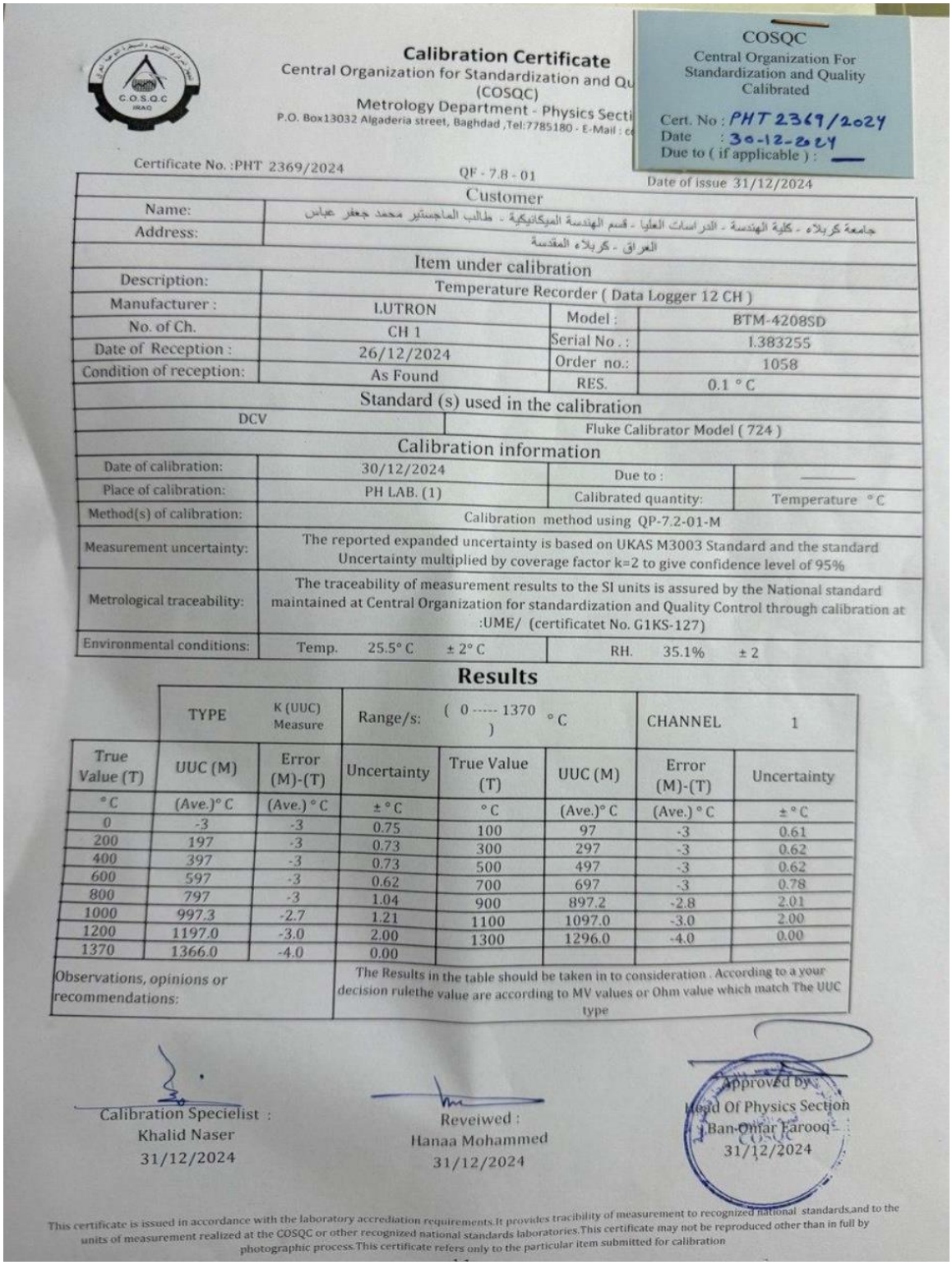

Calibration Certificate

Central Organization for Standardization and Qu
(COSQC)
Metrology Department - Physics Secti
P.O. Box13032 Algaderia street, Baghdad ,Tel:7785180 - E-Mail : c

COSQC
Central Organization For Standardization and Quality Calibrated
Cert. No : PHT 2369/2024
Date : 30-12-2024
Due to (if applicable) :

Certificate No. :PHT 2369/2024 QF - 7.8 - 01 Date of issue 31/12/2024

Customer			
Name:	جامعة كربلاء - كلية الهندسة - الدراسات العليا - قسم الهندسة الميكانيكية - طالب الماجستير محمد جعفر عباس		
Address:	العراق - كربلاء المقدسة		
Item under calibration			
Description:	Temperature Recorder (Data Logger 12 CH)		
Manufacturer :	LUTRON	Model :	BTM-4208SD
No. of Ch.	CH 1	Serial No . :	I.383255
Date of Reception :	26/12/2024	Order no.:	1058
Condition of reception:	As Found	RES.	0.1 ° C
Standard (s) used in the calibration			
DCV		Fluke Calibrator Model (724)	
Calibration information			
Date of calibration:	30/12/2024	Due to :	———
Place of calibration:	PH LAB. (1)	Calibrated quantity:	Temperature °C
Method(s) of calibration:	Calibration method using QP-7.2-01-M		
Measurement uncertainty:	The reported expanded uncertainty is based on UKAS M3003 Standard and the standard Uncertainty multiplied by coverage factor k=2 to give confidence level of 95%		
Metrological traceability:	The traceability of measurement results to the SI units is assured by the National standard maintained at Central Organization for standardization and Quality Control through calibration at :UME/ (certificatet No. G1KS-127)		
Environmental conditions:	Temp. 25.5° C ± 2° C	RH. 35.1% ± 2	

Results

	TYPE	K (UUC) Measure	Range/s: (0 ----- 1370) °C		CHANNEL 1		
True Value (T)	UUC (M)	Error (M)-(T)	Uncertainty	True Value (T)	UUC (M)	Error (M)-(T)	Uncertainty
°C	(Ave.)° C	(Ave.) ° C	± ° C	° C	(Ave.)° C	(Ave.) ° C	± ° C
0	-3	-3	0.75	100	97	-3	0.61
200	197	-3	0.73	300	297	-3	0.62
400	397	-3	0.73	500	497	-3	0.62
600	597	-3	0.62	700	697	-3	0.78
800	797	-3	1.04	900	897.2	-2.8	2.01
1000	997.3	-2.7	1.21	1100	1097.0	-3.0	2.00
1200	1197.0	-3.0	2.00	1300	1296.0	-4.0	0.00
1370	1366.0	-4.0	0.00				

Observations, opinions or recommendations: The Results in the table should be taken in to consideration . According to a your decision rulethe value are according to MV values or Ohm value which match The UUC type

Calibration Specielist : Khalid Naser 31/12/2024

Reveiwed : Hanaa Mohammed 31/12/2024

Approved by : Head Of Physics Section Ban-Omar Farooq 31/12/2024

This certificate is issued in accordance with the laboratory accrediation requirements.It provides tracibility of measurement to recognized national standards,and to the units of measurement realized at the COSQC or other recognized national standards laboratories.This certificate may not be reproduced other than in full by photographic process.This certificate refers only to the particular item submitted for calibration

Appendix C

شهادة استيفاء

Appendix D

Research Papers Accepted

Paper (١)

Numerical Study of the Effect of Filling Ratio in Heat Pipe on the Thermal Performance of Heat Exchanger

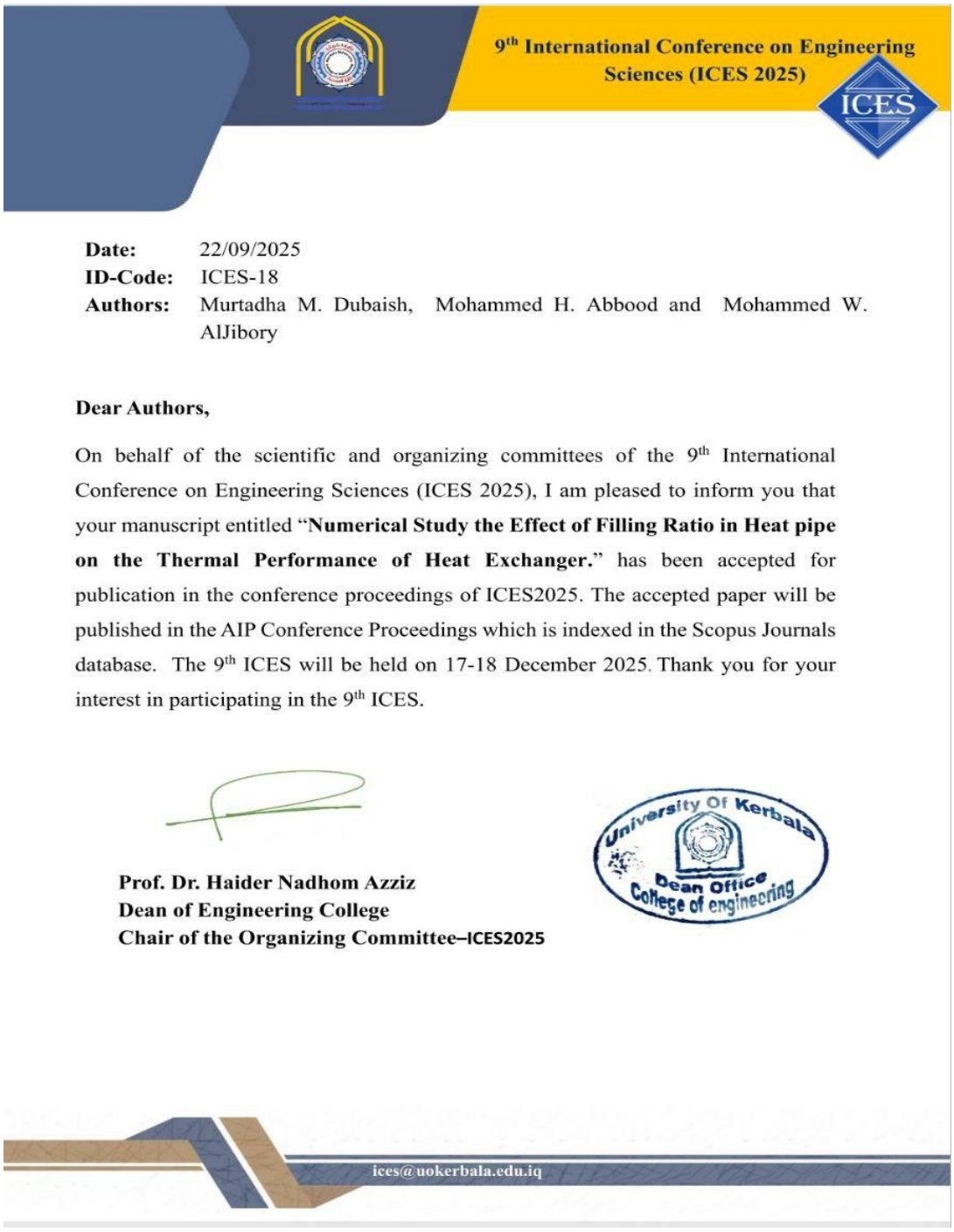

9th International Conference on Engineering Sciences (ICES 2025)

ICES

Date: 22/09/2025
ID-Code: ICES-18
Authors: Murtadha M. Dubaish, Mohammed H. Abbood and Mohammed W. AlJibory

Dear Authors,

On behalf of the scientific and organizing committees of the 9th International Conference on Engineering Sciences (ICES 2025), I am pleased to inform you that your manuscript entitled "**Numerical Study the Effect of Filling Ratio in Heat pipe on the Thermal Performance of Heat Exchanger.**" has been accepted for publication in the conference proceedings of ICES2025. The accepted paper will be published in the AIP Conference Proceedings which is indexed in the Scopus Journals database. The 9th ICES will be held on 17-18 December 2025. Thank you for your interest in participating in the 9th ICES.

University Of Kerbala
Dean Office
College of engineering

Prof. Dr. Haider Nadhom Azziz
Dean of Engineering College
Chair of the Organizing Committee–ICES2025

ices@uokerbala.edu.iq

Paper (٢)

Experimental Investigation of Thermal Performance of Heat Pipe Heat Exchanger for Waste Heat Recovery in Power Plants

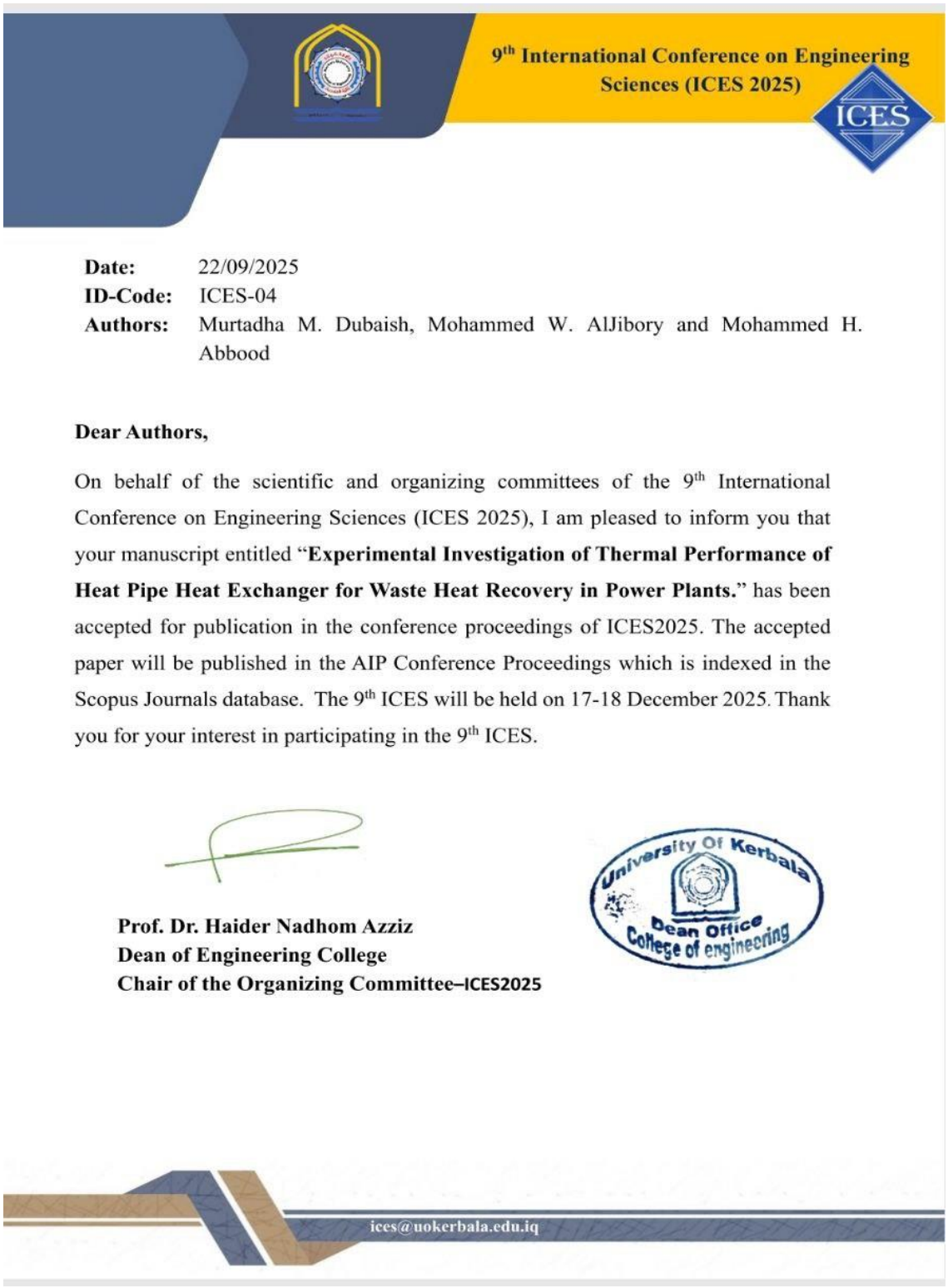

9th International Conference on Engineering Sciences (ICES 2025)

ICES

Date: 22/09/2025
ID-Code: ICES-04
Authors: Murtadha M. Dubaish, Mohammed W. AlJibory and Mohammed H. Abbood

Dear Authors,

On behalf of the scientific and organizing committees of the 9th International Conference on Engineering Sciences (ICES 2025), I am pleased to inform you that your manuscript entitled "**Experimental Investigation of Thermal Performance of Heat Pipe Heat Exchanger for Waste Heat Recovery in Power Plants.**" has been accepted for publication in the conference proceedings of ICES2025. The accepted paper will be published in the AIP Conference Proceedings which is indexed in the Scopus Journals database. The 9th ICES will be held on 17-18 December 2025. Thank you for your interest in participating in the 9th ICES.

University Of Kerbala
Dean Office
College of engineering

Prof. Dr. Haider Nadhom Azziz
Dean of Engineering College
Chair of the Organizing Committee–ICES2025

ices@uokerbala.edu.iq

الخلاصة:

في العديد من التطبيقات، مثل محطات توليد الطاقة، قد تُفقد الطاقة الحرارية الى البيئة المحيطة، لذا من الضروري استخدام أجهزة مثل المبادلات الحرارية ذات الأنابيب الحرارية لاستعادة هذه الطاقة. في هذه الدراسة، تم تصميم وتصنيع مبادل حراري أنبوبي حراري ذو سيفون حراري لهذا الغرض. تم دراسة الأداء الحراري لهذا المبادل عمليًا وعدديًا (باستخدام برنامج ANSYS-Fluent). تم ذلك عند نسب تعبئة مختلفة (٣٥%، ٥٠%، و٧٥%) من سائل التشغيل(DOWTHERM™ A) ، وسرعات هواء (٠.٥، ١، ١.٥، ٢، و٢.٥ متر/ثانية) عند مدخل المكثف، وفي نطاق واسع من درجة حرارة هواء مدخل المبخر (١٦٠ إلى ٣٢٠ درجة مئوية). يتضمن نموذج المبادل المستخدم في هذه الدراسة ٦٠ أنبوبًا حراريًا نحاسيًا بزعانف مربعة من الألومنيوم. يتكون الأنبوب الحراري (بطول إجمالي ١٠٠ سم) من ثلاثة أقسام، وهي: قسم التبخير (بطول ٤٠ سم)، وقسم الأدياباتيك (بطول ٢٠ سم)، وقسم التكثيف (بطول ٤٠ سم). تُظهر النتائج أن نسبة الملء، وسرعة الهواء، ودرجة حرارة هواء المبخر لها تأثير مهم على الأداء الحراري للمبادل الحراري. بشكل عام، القيم المثلى لنسبة الملء، وسرعة الهواء، ودرجة حرارة هواء المبخر، للحصول على أفضل أداء حراري للمبادل الحراري، هي ٥٠%، و٠.٥ متر/ثانية، و٣٢٠ درجة مئوية على التوالي. عند هذه القيم، يتم الحصول على أعلى درجة حرارة لهواء المكثف وأقصى كفاءة للمبادل (٢٤٠ درجة مئوية و٧٤% عدديًا، و٢٥٠ درجة مئوية و٧٧% تجريبيًا). من خلال المقارنة بين النتائج العددية والتجريبية، وُجد توافق ممتاز بينهما، حيث لا تتجاوز نسبة الاختلاف القصوى ٥%.

الكلمات المفتاحية: محطة قدرة بخارية، مبادل حراري لأنبوب حراري، الفعالية الحرارية، درجة الحرارة، نسبة الملء

جمهورية العراق

وزارة التعليم العالي و البحث العلمي

جامعة كربلاء

كلية الهندسة

قسم الهندسة المكانيكية

دراسة العوامل المؤثرة على أداء المبادل الحراري ذي الأنابيب الحرارية ذات فرق درجة حرارة كبير في محطة قدرة بخارية

رسالة مقدمة الى مجلس كلية الهندسة / جامعة كربلاء وهي جزء من متطلبات نيل درجة الماجستير في علوم الهندسة الميكانيكية

مقدمة من قبل الطالب:

مرتضى موسى دبيش

باشراف:

الأستاذ الدكتور محمد وهاب الجبوري

الأستاذ المساعد الدكتور محمد حسن عبود

٢٠٢٥م/ كانون الاول

١٤٤٧ هـ/ رجب